

International Conference
Condensed Matter Research at the IBR-2

Dubna,
Russia

ABSTRACT

O
O
K

Magnetic and Lattice Excitations

Carbon Nanosystems

Functional Materials

Soft Matter

Layered Nanostructures

Computational Studies

Materials for Energy Applications

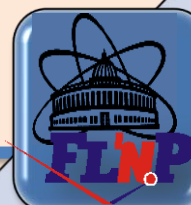
Neutron Imaging and Applied Studies

Instruments and Methods

Magnetic Colloid Nanosystems

CMR @ IBR-2

October 11 - 15,
2015



Joint Institute for Nuclear Research

**CONDENSED MATTER RESEARCH
AT IBR-2 REACTOR**

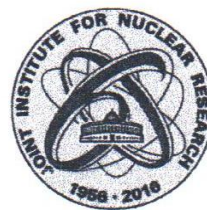
International Conference

Dubna, October 11–15, 2015

Book of Abstracts

Dubna • 2015

УДК 538.9
ББК 22.386
С74



Organized by
the Frank Laboratory of Neutron Physics of the Joint Institute for Nuclear Research

Supported by
the Russian Foundation for Basic Research (grant No. 15-02-20784 Г)

**LOCAL ORGANIZING
COMMITTEE**

Prof. D. P. Kozlenko — Chairman
Dr. M. V. Avdeev
Dr. G. D. Bokuchava
Dr. D. M. Chudoba
Mrs. T. S. Donskova — Secretary
Mrs. Yu. E. Gorshkova — Scientific Secretary
Mr. S. V. Kozenkov
Dr. B. N. Savenko

PROGRAMME COMMITTEE

Prof. V. L. Aksenov (Russia)
Prof. P. A. Alekseev (Russia)
Prof. A. M. Balagurov (Russia)
Prof. P. Balgavý (Slovak Republic)
Prof. A. V. Belushkin (Russia)
Prof. E. Burzo (Romania)
Prof. H. Fuess (Germany)
Prof. V. G. Kantser (Moldova)
Prof. D. Nagy (Hungary)
Prof. W. Nawrocik (Poland)
Prof. V. A. Somenkov (Russia)

Editor *Yu. E. Gorshkova*

The contributions are reproduced directly from the originals
presented by the Organizing Committee.

Condensed Matter Research at IBR-2 Reactor: Book of Abstracts of the International Conference (Dubna, October 11–15, 2015). — Dubna: JINR, 2015. — 146 p.
ISBN 978-5-9530-0428-2

Исследования конденсированных сред на реакторе ИБР-2: Сборник аннотаций международной конференции (Дубна, 11–15 октября 2015 г.). — Дубна: ОИЯИ, 2015. — 146 с.
ISBN 978-5-9530-0428-2

ISBN 978-5-9530-0428-2

© Joint Institute for Nuclear
Research, 2015

PREFACE

Since 2012, the IBR high flux pulsed reactor renewed regular operation at nominal power for scientific research and realization of the User Programme. Neutron scattering research at IBR-2 reactor covers different fields of condensed matter physics, materials science, chemistry, biophysical, geophysical and engineering sciences. At present, 200 experiments per year are performed by scientists from more than 20 countries at IBR-2 instruments in the framework of the User Programme.

The aim of the regular Conferences on Condensed Matter Research at IBR-2 reactor, playing the role of the User Meetings, is to bring together the users of the neutron facility for discussion of recent experimental results, prospects of future research and development of IBR-2 instruments. The previous Conference was held in June 2014 and attracted 105 participants from Azerbaijan, Bulgaria, Czech Republic, Germany, Italy, Moldova, Mongolia, Romania, Russia, Slovak Republic, Ukraine.

The *topics of the Conference* will highlight results of interdisciplinary research and development of neutron instruments and techniques, including:

- Functional and nanostructured materials;
- Magnetic colloid systems;
- Layered magnetic nanostructures;
- Carbon nanostructures;
- Materials under extreme conditions;
- Soft condensed matter:
biological nanosystems,
lipid membranes,
polymers;
- Lattice and molecular dynamics of materials;
- Texture and properties of rocks and minerals;
- Residual stresses in materials and products;
- Neutron imaging;
- Development of IBR-2 instruments;
- Development of neutron scattering techniques;
- Development of neutron detectors.

The present Conference will be dedicated to 100th anniversary of the birth of outstanding Soviet physicist Fyodor L. Shapiro, who provided fundamental contribution to establishment and development of the experimental facilities and basic research areas at the Frank Laboratory of Neutron Physics, Joint Institute for Nuclear Research.

Organizing Committee

F y o d o r
L v o v i c h
S H A P I R O



06.04.1915 - 30.01.1973

- 1941 - graduated from M.V.Lomonosov Moscow State University (MSU)
- 1945-1959 - Physics Institute of the USSR Academy of Sciences, Moscow
- 1959-1973 - LNP JINR, one of the LNP founders, Deputy Director
- 1962 - Doctor of Sciences (Phys. and Math.) defended in ITEP (Moscow)
- 1968 - co-author of the discovery “Phenomenon of retention of slow neutrons”
- 1967 - Professor of M.V.Lomonosov Moscow State University
- 1968 - Corresponding Member of the USSR Academy of Sciences
- 1971 - laureate of the State Prize
- 1977 - laureate of the I.V.Kurchatov Prize of the USSR Academy of Sciences

F.L.Shapiro belonged to the generation that came to the science later than the others did. After his graduation from M.V.Lomonosov Moscow State University in 1941 he, as well as his contemporaries, fought at the war. And only in 1945 he was accepted to the Physics Institute of the USSR Academy of Sciences as a post-graduate student to I.M.Frank with whom he worked closely in all the succeeding years of his life. In 1946 F.L.Shapiro, an assistant of the chair of nuclear physics in MSU headed by I.M.Frank, lectured on neutron physics and organized practical work on nuclear physics. In 1947 F.L.Shapiro was taken on as a junior research assistant to I.M.Frank’s Laboratory and took part in the investigations of subcritical uranium-graphite assemblies using the prism method. In these studies the important data for reactor engineering were obtained and some aspects of reactor physics were specified. In the early 50s Shapiro’s group proceeded to the practical realization of the neutron slowing-down spectrometry in lead. On this spectrometer for the first time the neutron radiation capture cross-sections for more than ten nuclei were measured and a number of effects became a scientific sensation, namely the deviation of cross-sections from the $1/v$ law that had been assumed to be universal for all nuclei. In addition, in the course of work on the “lead cube” (lead slowing-down spectrometer) F.L.Shapiro suggested the method of unsteady-state neutron diffusion in multigroup approximation and developed it with M.V.Kazarnovsky, a theoretician in his

group. These works received wide recognition and F.L.Shapiro presented them at the Geneva Conference on Peaceful Uses of Atomic Energy in 1955.

In 1958 I.M.Frank proposed that F.L.Shapiro combine his job in the Physics Institute with the work in the Laboratory of Neutron Physics (JINR) headed by him, where the construction of a pulsed reactor on fast neutrons was already underway. Feodor Lvovich agreed and rather quickly became deeply involved in the work of the Laboratory.

At the same time F.L.Shapiro together with I.Ya.Barit and M.I.Podgoretskii proposed an experiment using a just discovered Moessbauer effect to verify the consequence of the relativity theory to observe a photon frequency shift in gravitational and inertial fields. In the experiment conducted in LNP, velocity spectra of a narrow gamma-line of Zn67 with a record to the present day relative energy resolution of about 10-15 were obtained, but the effect appeared to be too small and insufficient to be used in a gravitational experiment. Later on American physicists were the first to perform an analogous experiment with another isotope.

In 1960 the IBR reactor was put into operation and the investigations of total and partial neutron-nucleus interaction cross-sections on its beams began. On one of the beams the method of neutron beam polarization suggested by F.L.Shapiro by passing neutrons through a polarized proton target was successfully tested. On this installation the spins of neutron resonances of some nuclei were measured and a set of amplitudes for neutron-deuteron scattering at small energies was determined. Later on the installation was used for other experiments, in particular, the resonant amplification of P-violation effect was discovered on it.

In 1961 F.L.Shapiro suggested that the IBR reactor be used for condensed matter investigations. He proposed the inverse geometry method characterized by higher luminosity that made it possible to study atomic thermal vibrations in solids and to measure the self-diffusion coefficient at a liquid-vapor critical point, which refuted the results of numerous macroscopic experiments that suggested the termination of diffusion at a critical point. F.L.Shapiro together with Polish physicist B.Buras has substantiated the application of the time-of-flight method for diffraction studies of structure of matter. In FLNP with the direct participation of F.L.Shapiro the neutron diffraction method was applied for magnetic structures in strong pulsed fields.

In 1968 F.L.Shapiro proposed a way to test the validity of the time parity conservation law in the experiment on observation of a neutron electric dipole moment. He suggested that this extremely weak effect could be observed only for very slowly moving (ultracold) neutrons. This idea got a skeptical reception from many physicists since a share of UCN in a reactor beam did not exceed one hundred milliardth. The IBR beams were very weak, but nevertheless in the summer of 1968 F.L.Shapiro with his colleagues successfully carried out the experiment on first observation of UCN. Within a few years this result was registered as a discovery. Further studies with UCN were transferred to more powerful stationary reactors.

I.M.Frank used to repeat that he was only a director and the whole “science” in the Laboratory was in charge of F.L.Shapiro. Of course, it was not quite so. I.M.Frank, Academician, the Nobel Prize winner was a very shrewd and far-sighted leader – he saw a powerful generator of ideas in Shapiro, gave him freedom and opportunities for their realization. Shapiro’s ideas underlay the majority of investigations carried out in the Laboratory, not because he was of higher rank, but because among all suggested ideas his idea used to be the best. It was a great piece of luck that such two persons as I.M.Frank and F.L.Shapiro met and successfully supplemented each other.

Original text from FLNP Web site: <http://flnp.jinr.ru>

P R O G R A M M E

	October, 11 Sunday	October, 12 Monday	October, 13 Tuesday	October, 14 Wednesday	October, 15 Thursday	October, 16 Friday
9.00 - 9.30		Registration				Departure
9.30 - 9.50		Opening			Prof. ALEKSEEV, Pavel	
9.50 - 10.10		Dr. SHVETSOV, Valeriy	Dr. KOPCANSKY, Peter	Dr. RAJNAK, Michal	Dr. CLEMENTYEV, Evgeny	
10.10-10.30		Prof. AKSENOV, Victor	Dr. KIRILOV, Andrey Dr. NIKITENKO, Yuri	Dr. NA GORNYI, Anatolii	Dr. BILSKI, Pawel	
10.30 - 10.50			Poster Session 1 &	Poster Session 2 &	Dr. GOREMYCHKIN, Evgeny	
10.50 - 11.10		Coffee break	Coffee break	Coffee break	Coffee break	
11.10 - 11.30		Prof. ANTIPOV, Evgeny	Dr. KOZLENKO, Denis	Prof. VUL, Alexander	Dr. KREZHOV, Kiril	
12.10 - 12.30		Dr. ITKIS, Danil	Dr. KOZHEVNIKOV, Sergey Prof. RAITMAN, Emst	Dr. LEBEDEV, Vasily Dr. KYZYMA, Olena	Dr. MATOVIC, Branko Dr. KURLOV, Alexey	
12.30 - 12.50		Lunch break	Lunch break	Lunch break	Dr. BOBORIKO, Natalia	
12.50 - 13.10					Lunch break	
13.10 - 13.30		Dr. ISTOMIN, Sergey	Mr. ZHAKETOV, Vladimir Ms. RYABUKHINA, Marina Ms. YAKUNINA, Elena	Dr. TROPIN, Timur Dr. EREMIN, Roman Dr. TURCHENKO, Vitalii	Dr. CHUDOBA, Dorota	
13.30 - 15.00		Coffee break	Coffee break	Coffee break	ROUND TABLE & Final remarks	
15.00 - 15.20	Arrival	Dr. IVANISHCHEV, Alexander	Dr. DINCA, Marin	Prof. BALGAVY, Pavol	Meeting closure	
15.20 - 15.40		Dr. DROZHZHIN, Oleg	Mr. PAKHNEVICH, Alexey	Dr. ISAEV-IVANOV, Vladimir	Departure	
15.40 - 16.00		Coffee break	Prof. ZISMAN, Alexander	Mr. KONDELA, Tomas		
16.00 - 16.20			Mr. ZEL, Ivan	Dr. FELDMAN, Tatiana		
16.20 - 16.40						
16.40 - 17.00						
17.00 - 17.20						
17.20 - 17.40						
17.40 - 18.30						
18.30 - 20.30		Hospitality event				

S C I E N T I F I C S E C T I O N S

Opening	Instruments and Methods	Magnetic Colloid nanosystems	Magnetic and lattice excitations
Introductory Session	Layered Nanostructures	Carbon nanosystems	Functional materials
	Neutron Imaging and Applied Studies	Soft Matter	
Materials for energy applications		Computational studies	User programme

I N F O R M A T I O N !

The conference will be held

October 12 in International Conference Hall of the JINR
(*Stroitelej Str. 2*).

October 13 – 15 in Frank Laboratory of Neutron Physics
(*FLNP Conference hall, bild. 42, 3rd floor*)

Hospitality event will take place in the restaurant "Dubna"
(*Vekslera St. 8*)

I N T R O D U C T I O N

Prof. AKSENOV, Victor	Russia Neutron Landscape	14
Dr. SHVETSOV, Valery	Frank Laboratory of Neutron Physics	

ORAL PRESENTATIONS

C A R B O N N A N O S Y S T E M S

Dr. KYZYMA, Olena	On the influence of the nC ₆₀ , nC ₇₀ aggregate structure on the toxicity of aqueous fullerene solutions	16
Dr. LEBEDEV, Vasily	Structure of aqueous gels of nanodiamonds by small-angle neutron scattering	17
Prof. VUL, Alexander	Detonation nanodiamond. Technology, properties and applications	

C O M P U T A T I O N A L S T U D I E S

Dr. EREMIN, Roman	Microstructure of organic solutions of mono-carboxylic acids: Combined study by small-angle neutron scattering and molecular dynamics simulations	19
Dr. TROPIN, Timur	Investigation and theoretical modeling of polystyrene glass transition in a wide range of cooling rates	20
Dr. TURCHENKO, Vitalii	Crystal structure and magnetic properties Sr _{1+x} Ba _{1-x} Fe _{1+x} Mo _{1-x} O ₆ (x= 0 and 0.1)	21

F U N C T I O N A L M A T E R I A L S

Dr. BOBORIKO, Natalia	Structural peculiarities of TiO ₂ :MoO ₃ nanocomposites that ensure their catalytic activity	23
Dr. MATOVIC, Branko	New mesoporous ceria synthesized by templating procedure	24
Prof. KREZHOV, Kiril	Synthesis and characterization of new lead-based perovskites with crystallographic shear planes	25
Dr. KURLOV, Alexey	Microstructure of nanocrystalline nonstoichiometric niobium NbC _{0.93} and vanadium VC _{0.875} carbides	26

I N S T R U M E N T S A N D M E T H O D S

Dr. IOFFE, Alexander	Development of advanced neutron scattering instrumentation for long pulse neutron sources	30
Dr. KIRILOV, Andrey	Sonix+ - основа программного обеспечения комплекса спектрометров реактора ИБР-2	31
Dr. KOZHEVNIKOV, Sergey	System of neutron microbeams from a planar waveguide	32
Dr. KOZLENKO, Denis	Neutron scattering instruments of IBR-2 high flux pulsed reactor for condensed matter research: Current state and recent results	33
Prof. RAITMANS, Ernst	Propagation of neutron spherical waves through a thick, vibrating Ge single crystal	33

L A Y E R E D N A N O S T R U C T U R E S

Dr. GAKOVIĆ, Biljana	Compositional, morphological and accumulation phenomena in laser pulse ablation of nano-layered (Ni/Ti) thin films	34
Dr. NIKITENKO, Yuri	SPIN-ECHO spectrometry in grazing geometry	34
Ms. RYABUKHINA, Marina	Determination of magnetic order in superlattices Fe/Cr/Gd	35
Ms. YAKUNINA, Elena	Investigation of magnetism in multilayer metallic nanostructures Fe/MgO/Fe and Fe/MgO/Cr/MgO/Fe using polarized neutron reflectometry	36
Mr. ZHAKETOV, Vladimir	Magnetism of nanostructures with ferromagnetic and superconducting layers	37

M A G N E T I C A N D L A T T I C E E X C I T A T I O N S

Prof. ALEKSEEV, Pavel	Exotic magnetic ordering in systems with strongly correlated electrons	38
Dr. BILSKI, Paweł	High pressure measurements on the NERA facility	39
Dr. CLEMENTYEV, Evgeny	Direct vs inverted TOF geometry in the studies of magnetic and lattice excitations	40
Dr. GOREMYCHKIN, Evgeny	Spin excitation in the iron based high Tc superconductor FeTe _{1-x} Se _x	41

M A G N E T I C C O L L O I D N A N O S Y S T E M S

Dr. KOPCANSKY, Peter	Ferronematics - the way to magnetovision camera	42
Dr. NAGORNYI, Anatolii	Neutron investigations of water-based ferrofluids synthesized by different methods	43
Dr. RAJNAK, Michal	Electric field driven assembly of ferrofluid magnetic nanoparticles studied by small angle neutron scattering (SANS)	44

M A T E R I A L S F O R E N E R G Y A P P L I C A T I O N S

Prof. ANTIPOV, Evgeny	T _c -enhancement of Fe _{1+δ} Se by electrochemical lithium intercalation	45
Dr. BOBRIKOV, Ivan	Evolution of crystal structure of cathode material LiNi _{0.8} Al _{0.1} Co _{0.1} O ₂ during electrochemical cycling	46
Dr. DROZHZHIN, Oleg	Phase transitions upon Li (de)intercalation in Li _x Fe _{1-y} M _{ny} PO ₄ (0 ≤ x ≤ 1, 0 ≤ y ≤ 0.5)	47
Dr. ISTOMIN, Sergey	Спиновое состояние катионов Co ³⁺ в перовскитоподобных оксидах	
Dr. ITKIS, Daniil	In operando studies of electrochemical interfaces	
Dr. IVANISHCHEV, Alexander	A comparative study of lithium-vanadium phosphate and fluorophosphate: Application of neutron diffraction and electrochemical methods	48
Dr. MINYUKOVA, Tatyana	Distribution of cations in the Cu-containing oxides of a spinel structure and its influence on the catalytic properties in the low-temperature WGS	50

N E U T R O N I M A G I N G A N D A P P L I E D S T U D I E S

Dr. DINCA, Marin	Investigation of an ancient thracian spear fragment with neutrons and X-rays	51
Dr. PAKHNEVICH, Alexey	Опыт исследования палеонтологических объектов с помощью нейтронной томографии на реакторе ИБР-2	52
Mr. ZEL, Ivan	Elastic anisotropy of layered rocks: Crystallographic texture and ultrasonic measurements of plagioclase-biotite gneiss versus effective media modeling	54
Prof. ZISMAN, Alexander	Texture investigation through thickness of rolled high-strength steel by neutron diffraction	55

S O F T M A T T E R

Prof. BALGAVÝ, Pavol	Effects of normal alkanes on bilayer thickness in dioleoylphosphatidylcholine liposomes	56
Dr. FELDMAN, Tatiana	Study of visual pigment rhodopsin supramolecular organization in photoreceptor membrane by small angle neutron scattering method with contrast variation	57
Dr. ISAEV- IVANOV, Vladimir	Фрактальная организация хроматина ядер эукариот по данным МУРН: общие принципы	59
Mr. KONDELA, Tomas	Real-time neutron diffraction from lipid membranes	61

U S E R P O L I C Y

Dr. CHUDOBA, Dorota	FLNP JINR user programme	62
------------------------	--------------------------	----

POSTER PRESENTATIONS October 13 (Tuesday)

F U N C T I O N A L M A T E R I A L S			
Dr. ALEKSEEVA, Olga	Particularities of NaNO ₂ phase state in the ferroelectric composite 0.9NaNO ₂ +0.1BaTiO ₃	T-F 1	64
Ms. BELOZEROVA, Nadezhda	Nanostructured manganites: Neutron diffraction studies at high pressure and low temperature	T-F 2	65
Dr. CRAUS, Mihail Liviu	Influence of chemical compositions and thermal treatments on the structure and mechanical properties of zirconia based thermal coatings	T-F 3	66
Dr. CRAUS, Mihail Liviu	Nanocrystalline stabilized zirconia	T-F 4	67
Dr. DANG, Toan	Influence of Fe doping on structural and electric properties of multiferroics BaTi _{1-x} Fe _x O ₃	T-F 5	69
Dr. DOROSHKEVICH, Alexander	Chemo-voltaic effect in the ZrO ₂ -nanopowder systems	T-F 6	70
Dr. GOLOSOVA, Natalia	Structural, magnetic and vibrational properties of multiferroic GaFeO ₃ at high pressure	T-F 7	71
Ms. GORKOVENKO, Ekaterina	The pressure and temperature induced polymorphic transformations in fluconazole	T-F 8	72
Mrs. ISMAYILOVA, Narmin	Defect formation energy for charge states in TLINS ₂	T-F 9	73
Dr. JABAROV, Sakin	High pressure study on crystal structure of BaTi _{0.99} Fe _{0.01} O ₃	T-F 10	74
Dr. KICHANOV, Sergey	The magnetic and structural modifications in multiferroic YMn ₂ O ₅ at high pressure	T-F 11	75
Ms. ŁUCZYŃSKA, Katarzyna	Experimental (X-ray, ¹³ C CP/MAS NMR, IR, RS, INS, THz) and Solid-State DFT Study on (1:1) Co-Crystal of Bromanilic Acid and 2,6-Dimethylpyrazine	T-F 12	77
Mr. LUSHNIKOV, Stepan	Структура стабильных гидридов ИМС CeNi ₃	T-F 13	78
Mr. NGUYEN, Chi Thang	Structure of optical materials GeO ₂ , In ₂ O ₃ , and SnO ₂ doped Eu ³⁺ studied by means of small angle neutron scattering and neutron diffraction	T-F 14	80
Ms. POPIUK, Tatiana	Molecular orientation in amlodipine besylate	T-F 15	81
Mr. RUTKAUSKAS, Anton	Suppression of the antiferromagnetic state in La _{0.82} Ba _{0.18} CoO ₃ cobaltide at high pressure	T-F 16	82
Dr. SHABANOV, Osman	Neutron diffraction studies of molten salts in nonequilibrium state	T-F 17	83
Dr. SIKOLENKO, Vadim	Antiferromagnetic-ferromagnetic transition in anion deficient cobaltites. Neutron diffraction studies	T-F 18	85
Mr. SUMNIKOV, Sergey	Neutron diffraction study of magnetic and structural phase transitions in nio and mno	T-F 19	86
Dr. TRUKHANOV, Alexey	Investigation of crystal and magnetic structures of barium ferrites doped by diamagnetic ions	T-F 20	87
Ms. VANINA, Polina	Critical scattering in single crystal of uniaxial relaxor Sr _{0.6} Ba _{0.4} Nb ₂ O ₆	T-F 21	88
Mr. VU, Minh Thanh	Crystal and magnetic structure of manganite La _{0.7} Sr _{0.3} Mn _{0.83} Nb _{0.17} O ₃ in wide range of the temperatures and pressures	T-F 22	89

POSTER PRESENTATIONS October 13 (Tuesday)

I N S T R U M E N T S A N D M E T H O D S			
Dr. GAVRILOVS, Viktors	Spatial distribution of diffracted neutron beam in perfect and strained Si crystal	T-I 1	90
Dr. IVANKOV, Oleksandr	SAS program for the preliminary data treatment for the small angle neutron scattering multidetector system on the pulsed source	T-I 2	91
Mr. KRUGLOV, Alexander	Adaptation of the FSS diffractometer at the IBR-2 fast pulsed reactor: current state and prospects of development	T-I 3	92
Dr. KUKLIN, Alexander	Cold and thermal moderator at IBR-2 for SANS spectrometer: Advantages and disadvantages	T-I 4	94
Mr. LUKIN, Evgeny	Neutron Imaging Facility: Current state	T-I 5	95
Ms. SALAMAKHA, Tatsiana	Особенности формирования тонкодисперсных порошков BaI ₂ :Eu для сцинтилляционных детекторов	T-I 6	96
Mr. ZAW LIN, Kyaw	Multilayer neutron monochromator-polarizer on the basis of iron	T-I 7	98

A P P L I E D S T U D I E S			
Dr. BOKUCHAVA, Gizo	High resolution correlation Fourier diffractometry for advanced materials characterization	T-N 1	99
Dr. BOKUCHAVA, Gizo	Neutron diffraction characterization of residual stress and microstructure in reconstituted Charpy specimens	T-N 2	101
Mr. PAPUSHKIN, Igor	Investigation of residual stress in Formula 1 racing car gearwheel welded by electron beam	T-N 3	103
Dr. VASIN, Roman	Crystallographic preferred orientations and elastic anisotropy of sheet silicate bearing rocks	T-N 4	106
Dr. VASIN, Roman	Precise determination of microstructural characteristics from reverse time-of-flight neutron diffraction data	T-N 5	107

POSTER PRESENTATIONS October 14 (Wednesday)

C A R B O N N A N O S Y S T E M S			
Mr. NARMANDAKH, Jargalan	Experimental aspects of investigations of fullerene solutions	W-C 1	108
Mr. TOMCHUK, Oleksandr	Detonation nanodiamonds in aqueous suspensions by SANS	W-C 2	109
C O M P U T A T I O N A L S T U D I E S			
Dr. ANITAS, Eugen	Structural properties of elastomeric membranes based on silicone rubber using small-angle neutron scattering	W-C 3	110
Dr. ANITAS, Eugen	Scattering from surface fractals	W-C 4	110
Prof. FILAROWSKI, Aleksander	To the question of conformational equilibrium and polymorph's states in the solid state and under the matrix conditions	W-C 5	111
L A Y E R E D N A N O S T R U C T U R E S			
Dr. BAYEV, Vadim	Structural and phase characterization of porous Co/Pd multilayered thin films	W-L 1	112
Dr. BALASOIU, Maria	Titanium based composites deposited by thermionic vacuum arc method investigated by means of SANS	W-L 2	114
Mr. ZHAKETOV, Vladimir	Neutron depolarization investigations of spring exchange interaction nanocomposites	W-L 3	115
M A G N E T I C A N D L A T T I C E E X C I T A T I O N S			
Dr. CRAUS, Mihaíl Liviu	Transition from spin glass to ferromagnetic state: Influence on transport phenomena in some Cr doped manganites	W-M 1	116
Dr. HETMANCZYK, Joanna	Phase transition, structural changes and H ₂ O reorientational motion in [Ca(H ₂ O) ₂](ReO ₄) ₂ studied by neutron scattering methods	W-M 2	117
Mrs. ORDON, Magdalena	Spectroscopic and thermal analysis of lithocholic acid	W-M 3	119
Dr. SAVENKO, Boris	Pressure effects on crystal structure and vibration spectra of an antiferroelectric NaNbO ₃	W-M 4	120
Dr. SMIRNOV, Lev	Dynamics of (NH ₄) ₂ MeO ₂ F ₄ (Me=W, Mo) compounds by the inelastic incoherent neutron scattering	W-M 5	121
M A G N E T I C C O L L O I D N A N O S Y S T E M S			
Dr. BALASOIU, Maria	Structural comparison of several water based ferrofluids by means of TEM and SANS methods	W-N 6	122
Dr. BALASOIU, Maria	On the silicone rubber elastomer microstructure by means of SANS	W-N 7	123
Dr. BALASOIU, Maria	Hydrophilic versus hydrophobic oleate coated magnetic particles	W-N 8	125
Dr. MELNÍKOVÁ, Lucia	Structure of magnetoferritin in aqueous solution	W-N 9	126
Mr. HAPON, Ihor	Structure of magnetic fluids at interface with silicon investigated by neutron and X-ray reflectometry	W-N 10	127

POSTER PRESENTATIONS October 14 (Wednesday)

M A T E R I A L S F O R E N E R G Y A P P L I C A T I O N S

Dr. BOBRIKOV, Ivan	Structural and electrochemical properties of doped 5 V spinel cathode materials $\text{LiNi}_{0.5-x}\text{Mn}_{1.5-y}\text{M}_{x+y}\text{O}_4$ (M = Co, Cr, Ti; $x+y=0.05$) prepared by mechanochemical way	W-E 1	128
Dr. IVANISHCHEV, Alexander	Investigation of electrochemically stimulated structural transformations in $\text{Li}_3\text{V}_2(\text{PO}_4)_3$ electrode using neutron diffraction method	W-E 2	129
Mr. SUMANOV, Vasily	Hydro- and solvothermal synthesis of complex lithium and d-metals phosphates as cathode materials for Li-ion batteries	W-E 3	131
Mr. TERESHCHENKO, Ivan	Hydrothermal synthesis of sodium and transition metals fluorophosphates as cathode materials for lithium- and sodium-ion batteries	W-E 4	132
Mr. USHAKOV, Arseni	Neutron diffraction and electrochemical study of lithium intercalation in the system $\text{Li}_4\text{Ti}_5\text{O}_{12}$ - $\text{Li}_7\text{Ti}_5\text{O}_{12}$	W-E 5	133

S O F T M A T T E R

Ms. ANGHEL, Lilia	Influence of tetrasodium ethylenediaminetetraacetate on binding capacity of human lactoferrin	W-S 1	134
Mr. ARTYKULNYI, Oleksandr	Combined surface tension and small-angle neutron scattering investigations of aqueous micelle solutions of dodecylbenzene sulfonic acid	W-S 2	136
Ms. GORSHKOVA, Yulia	Small angle neutron investigation of the lithocholic acid derivative in the dimethyl sulfoxide presence: Morphology and phase transitions	W-S 3	137
Ms. GORSHKOVA, Yulia	Effect of ions and polar solvents on the structure and phase transitions of phospholipid membranes	W-S 4	139
Dr. RAJEWSKA, Aldona	Structure of mixed micellar solutions study by small angle neutron scattering method	W-S 5	141
Mr. RYZHYKAU, Yury	Investigation of phase transition in nanodiscs by small-angle scattering method	W-S 6	142
Dr. SIPOSOVA, Katarina	Bicelles: New nanosystem for studying mitochondrial membrane proteins	W-S 7	144
Mr. VLASOV, Alexey	Multi-methodical investigation and SAXS/SANS data analysis of apoferritin behavior in water solutions	W-S 8	146

GADALINSKA, Elzbieta	Micromechanical properties of a Al/SiCp metal matrix composite determined using TOF neutron diffraction using <i>in situ</i> tensile test		147
Dr. SCHEFFZUEK, Christian	The neutron time-of-flight diffractometer EPSILON for strain analysis on geological samples under uniaxial and triaxial load conditions		148

I N T R O D U C T I O N

RUSSIA NEUTRON LANDSCAPE

V.L.Aksenov

*Petersburg Nuclear Physics Institute NRC “Kurchatov Institute” (Gatchina),
Frank Laboratory of Neutron Physics JINR (Dubna)*

Review of modern trends in neutron physics and present state and perspectives of neutron sources in Russia is presented.

The discovery of Higgs boson initiated more activities in researches beyond of Standard Model. First of all it concerns with measurements of the neutron electric dipole moment. New possibilities were appeared in investigations of basic problems in quantum theory: paradoxes of “Schrödinger and Cheshire Cats”. In these investigations ultracold neutrons (UCN) are used. New concept of UCN sources were proposed by JINR-ILL group. Modern problems in nuclear physics and structural biology are discussed.

Perspectives of research with the use of beam neutrons in Russia are related mostly with reactors IBR-2 and PIK. Other neutron sources in Europe and Russia are discussed. Proposals of a new neutron source on the base of IBR-2 reactor after 2037 are discussed. The running state in the construction of the reactor PIK is reported.

ORAL PRESENTATIONS

C A R B O N N A N O S Y S T E M S

ON THE INFLUENCE OF THE NC_{60} , NC_{70} AGGREGATE STRUCTURE ON THE TOXICITY OF AQUEOUS FULLERENE SOLUTIONS

O.A. Kyzyma^{1,2}, A.A. Tomchuk¹, M.V. Avdeev¹, V.I. Petrenko^{1,2}, L. Almasy³, M.V. Korobov⁴, D.S. Volkov⁴, I.V. Mikheev⁴, I.V. Koshlan⁵, N.A. Koshlan⁵, P. Blaha^{5,6}, V.F. Korolovych^{2,7}, V.L. Aksenov^{8,1}, L.A. Bulavin^{2,9}

¹*Frank Laboratory of Neutron Physics, Joint Institute for Nuclear Research, Joliot-Curie St. 6, 141980 Dubna, Moscow Reg., Russia*

²*Taras Shevchenko Kyiv National University, Volodymyrska St. 64, 01601 Kyiv, Ukraine.*

³*Research Institute for Solid State Physics and Optics, Wigner Research Centre for Physics, Hungarian Academy of Sciences, Budapest, H_1525 Hungary*

⁴*Faculty of Chemistry, Moscow State University, Moscow, 119991 Russia*

⁵*Laboratory of Radiation Biology, Joint Institute for Nuclear Research, Dubna, Moscow reg., 141980 Russia*

⁶*Faculty of Nuclear Sciences and Physical Engineering, Czech Technical University in Prague, Prague, 166 36 Czech Republic*

⁷*Saratov State University, Astrakhanskaya Street 83, 410012 Saratov, Russia.*

⁸*National Research Center "Kurchatov Institute", Academician Kurchatov Sq. 1, 123182 Moscow, Russia*

⁹*Institute for Safety Problems of Nuclear Power Plants, National Academy of Sciences of Ukraine, Chornobyl', Ukraine*

The aim of the work is to clarify the correlation between structure and toxicity and also biological activity of the fullerene aqueous solutions, which will lead to the rapid development of biomedical applications of such systems.

The given report presents results of complex structural characterization, toxicity and efficiency in antitumor therapy for various types of fullerenes C_{60} and C_{70} aqueous solutions, and also their complexes with anticancer drugs. Correlation of structure with biological properties of studied fullerenes systems is analyzed.

STRUCTURE OF AQUEOUS GELS OF NANODIAMONDS BY SMALL-ANGLE NEUTRON SCATTERING

V.T.Lebedev¹, Yu.V.Kulvelis¹, M.V. Avdeev², A.I.Kuklin², A.Ya.Vul³

¹*Petersburg Nuclear Physics Institute, NRC Kurchatov Institute, Gatchina, Leningrad distr., Russia*

²*Joint Institute for Nuclear Research, Dubna, Russia*

³*A.F.Ioffe Physical-Technical Institute of RAS, Saint-Petersburg, Russia*

Recent results of structural studies of first prepared aqueous gels of nanodiamonds with charged surface are presented. The obtained SANS-data (YuMO-facility) allowed observe a short-range order in the ensembles of carbon particles (size $D \sim 6$ nm) associated into fractal clusters interpenetrating and forming a network at scale ~ 100 nm. These structures are stable in the concentration range of diamonds $C \sim 1-5$ wt. % at ambient temperature according to neutron scattering results.

The pattern in Fig.1 illustrates the behavior of the scattering cross section $\sigma(q)$ (per unit solid angle and for 1 cm^3 of sample volume) as a function of momentum transfer for the gel with 5.05 % wt. of carbon component. Spectrum profile demonstrates a kink at $q \sim q^* = 2\pi/D \approx 1.5 \text{ nm}^{-1}$ the position of which is defined by a characteristic particle size. Thus, at $q > q^*$ scattering from single particles dominates, $\sigma(q) \sim 1/q^{4.18}$, where the exponent indicates their slightly diffusive borders. On the other hand, at $q < q^*$ a gain of cross section $\sigma(q) \sim 1/q^{df}$ at low q -values is determined by the interference in scattering when the particles are organized into large-scale clusters having fractal dimension $df \approx 2.33$.

In the first approach the scattering spectra (Fig.1a) for this gel as well as for diluted systems are described by the function being the sum of partial scattering functions for spherical particles having radii R . The related distribution of their volume parts $C_V(R)$ has a main peak with maximum position $R_{m1} \sim 3 \text{ nm} \sim D/2$ corresponding to characteristic radius of diamond particles (Fig.1b).

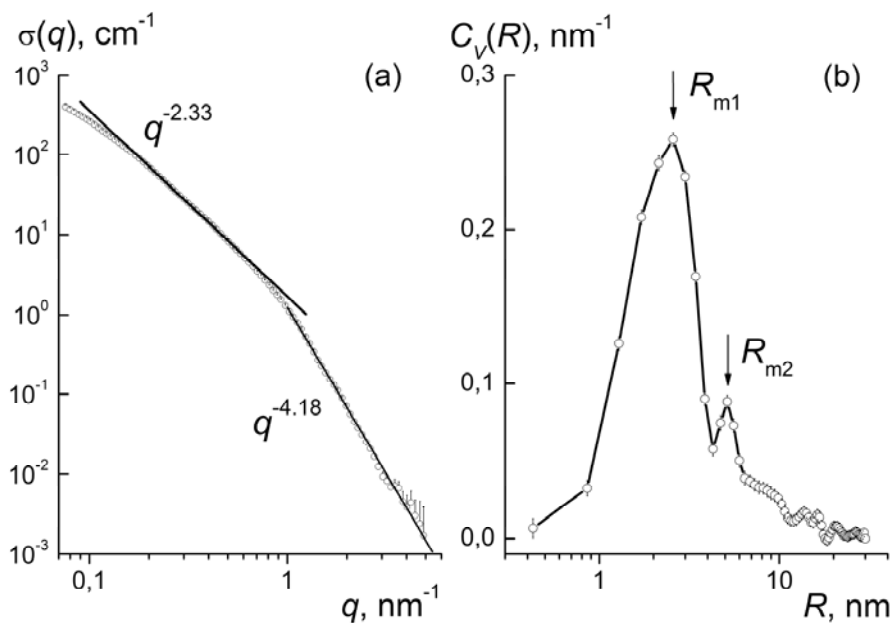


Fig.1. (a) Cross section $\sigma(q)$ of gel (5.05 % wt.) vs. momentum transfer. Lines show the intervals with characteristic exponential behaviors. (b) Restored volume part $C_V(R)$ of scattering objects with the radii R .

While the second peak at $R_{m2} \sim 7$ nm should be attributed to the correlations of neighboring particles near any chosen particle (first coordination sphere), it is revealed in scattering as a contribution of clusters with diameter $\sim 2R_{m2} \sim 14$ nm.

Along with this, more extended formations are visible in spectrum at the radii $R \sim 10$ -20 nm. These structures having the size ≤ 40 nm are characterized by fractal scattering law $\sigma(q) \sim 1/q^{df}$. The interpenetration of clusters creates a gel network where a size of cells ~ 40 nm $\sim 2\pi/q^{**}$ can be estimated from the value of $q^{**} \sim 0.015$ nm below which scattering is depressed due to structure factor in concentrated system of cells (Fig.1a).

In general, the discussed peculiarities in scattering are qualitatively of the same kind as a short-range order in concentrated diamond dispersions where the correlations of particles are detected at the distances ~ 20 -30 nm related to the maximum of structure factor [1-3]. In both cases the mechanism of diffusion limited aggregation leads to the integration of particles. However, the role of electrostatic forces in gel arisen from charged facets of particles is more pronounced when the particles are covered by massive hydration shells which serve as the links between particles, and it makes the system being solid-like.

[1] M.V.Avdeev, N.N.Rozhkova, V.L.Aksenov, V.M.Garamus, R.Willumeit, E.Osawa, *J.Phys. Chem. C*, (2009) 113, 9473.

[2] O.V.Tomchuk, L.A.Bulavin, V.L.Aksenov, V.M.Garamus, O.I.Ivankov, A.Ya.Vul', A.T.Dideikin, M.V.Avdeev, *J. Appl. Cryst.* (2014) 47, 642.

[3] O.V.Tomchuk, D.S.Volkov, L.A.Bulavin, A.V.Rogachev, M.A.Proskurnin, *Chem. C* (2015) 119, 794.

C O M P U T A T I O N A L S T U D I E S

MICROSTRUCTURE OF ORGANIC SOLUTIONS OF MONO-CARBOXYLIC ACIDS: COMBINED STUDY BY SMALL-ANGLE NEUTRON SCATTERING AND MOLECULAR DYNAMICS SIMULATIONS

R. Eremin¹, V. Petrenko¹, L. Rosta², Kh. Kholmurodov¹, M. Avdeev¹

¹ *Joint Institute for Nuclear Research, Dubna, Russia*

² *Wigner Research Centre for Physics, Hungarian Academy of Sciences, Budapest, Hungary*

E-mail: era@jinr.ru

The problem of the experimental small-angle neutron scattering (SANS) data structural interpretation for diluted organic solutions of saturated monocarboxylic (namely, myristic and stearic) acids in deuterated (d-) benzene and decalin is considered. Despite the fact acid molecules size is enough to obtain reliable SANS signal it is demonstrated that Guinier approximation is not applicable within the structural data interpretation for the both mentioned solvent simultaneously [1] according to the residual incoherent background (bkg) values. This observation is mainly caused by a specific short-range solvent ordering in the vicinity of the acid molecules and its inhomogeneous effect on the scattering that is greater for decalin-based solutions.

In the first instance, we used the method of classical molecular dynamics (MD) simulations to obtain the atomic number density distributions, and, as a consequence, the scattering length density (SLD) spatial distribution in the solute – solvent interface area (about 2 nm around the acid molecules), assuming the acid molecules rigid (all-trans) conformation and non-associated state in d-decalin [1]. Basing on the cylindrical symmetry of the acid molecules a number approximations to the simulated SLD distributions were probed to achieve the best consistency with the experimental SANS curves by varying of the bkg parameter only.

The following modelling of SANS from MD calculations for stearic acid in d-benzene [2] was carried out and no sufficient deviations of the obtained SANS signal from the Guinier-predicted ones were expected. However, the indications of the overestimated bkg value in Guinier approach were obtained. That fact demonstrated a necessity of other structural properties of fatty acids organic solutions accounting. In addition to the solvation shell formation the acid molecule dimerization and alkyl chains trans/gauche isomerization are the main intrinsic particularities of studied systems. In particular, the degree of dimerization was found from the FTIR measurements and scattering model was modified. In result, the effective characteristic sizes of the acids in solutions comprising the information about the molecule trans/gauche isomerization were obtained and an agreement with the experiment was achieved for the both studied solvents.

For decalin-based solutions the increase in solvent excluded volume in comparison with benzene-based ones was observed repeating the results of acid limiting molar volumes calculations [3]. Finally, the SANS data for concentrated solutions showed a partial self-assembling of the acids within the nematic transition. The differences in this effect for the two solvents can be explained by the acid lyophobic peculiarities revealed in the analysis of diluted solutions in the scope of the scattering model plotted in the frame of the current research.

[1] R.A. Eremin et al., *J. Appl. Cryst.* 46 (2013) 372-378.

[2] R.A. Eremin et al., *Phys. Sol. State* 56 (2014) 81-85.

[3] R.A. Eremin et al., *Rus. J. Phys. Chem. A* 87 (2013) 745-751.

INVESTIGATION AND THEORETICAL MODELING OF POLYSTYRENE GLASS TRANSITION IN A WIDE RANGE OF COOLING RATES

T.V. Tropin¹, G.Schulz², J.W.P. Schmelzer^{2,1}, C. Schick²

¹Joint Institute for Nuclear Research, Dubna, Russia

²Institut für Physik der Universität Rostock, Rostock, Germany

E-mail: ttv@jinr.ru

The formulation of a comprehensive theory of the glassy state and of the glass transition remains one of the challenges for modern physics [1]. This is one of the reasons of the continuing interest in analysis of these problems. In addition, also from a practical viewpoint, experimental study and theoretical description of glass transition are very important topics, due to the wide distribution of modern technological applications of glasses as well as their frequent occurrences in everyday life.

Polymers are known to be good glass formers, allowing one to study glass transition effects as well as to verify the applicability of various theoretical models [2]. In the presented work experimental and theoretical investigations of glass transition of atactic polystyrene (PS) in a broad range of cooling rates ($5 \cdot 10^{-6}$ -2 K/s) were performed [3]. The capability of commonly employed theoretical techniques for C_p modeling to describe the obtained data is considered. It is shown that the extended Tool-Narayanaswamy-Moynihan (TNM) model with Vogel-Fulcher-Tammann-Hesse (VFTH) or Adam-Gibbs (AG) expressions for relaxation time with the common single set of parameters do not fit the experimental data well. Moreover, the values of parameters required to produce an adequate fit of the whole set of heating curves are quite different from their estimates obtained from independent additional experiments. An additional expression for relaxation time is proposed within the Gutzow-Schmelzer (GS) approach for describing the kinetics of glass transition leading to results of similar precision. The obtained results reconfirm the general conclusion that the considered models of glass transition require parameter readjusting for different cooling or heating rates in order to adequately describe the experimental data.

A perspective of neutron measurements of the structural (bulk and surface) features of the PS glass transition at various cooling rates at the YuMO and GRAINS spectrometers of the IBR-2M reactor is briefly discussed.

- [1] A. Cavagna, "Supercooled liquids for pedestrians," *Phys. Rep.*, vol. 476, no. 4–6, pp. 51–124, Jun. 2009.
- [2] A. D. Drozdov, "Kinetics of enthalpy relaxation in polymeric glasses," *Polym. Bull.*, vol. 45, no. 3, pp. 303–310, Nov. 2000.
- [3] T. V. Tropin, G. Schulz, J. W. P. Schmelzer, and C. Schick, "Heat capacity measurements and modeling of polystyrene glass transition in a wide range of cooling rates," *J. Non. Cryst. Solids*, vol. 409, pp. 63–75, Feb. 2015.

CRYSTAL STRUCTURE AND MAGNETIC PROPERTIES $\text{Sr}_{1+x}\text{Ba}_{1-x}\text{Fe}_{1+x}\text{Mo}_{1-x}\text{O}_6$ ($X=0$ AND 0.1)

V.A. Turchenko^{1,2}, N.A. Kalanda³, L.V. Kovalev³, Simkin V.G.¹

¹ Frank Laboratory of Neutron Physics of Joint Institute for Nuclear Research, 141980, Dubna, 6 Joliot-Curie Street Russia;

² Donetsk Institute of Physics and Technology named after O. O. Galkin of the NASU, 83114 Donetsk, 72 R. Luxemburg str., Ukraine.

³ SSPA “Scientific and practical materials research center of NAS of Belarus” 19 Brovki Str., 220072, Minsk, Republic of Belarus.

E-mail: vitalja-turchenko@rambler.ru

The ideal crystal structure of double perovskites with molar formula $\text{AA}'\text{BB}'\text{O}_6$ (where A and $\text{A}'=\text{Ca}$, Sr, La et al., $\text{B}=\text{Fe}$, Cr... and $\text{B}'=\text{Mo}$, W, Re...) [1] is built up by ordering perovskite blocks in a rock salt superlattice [2]. The renewed attention to research of these materials is motivated by the recent report that $\text{Sr}_2\text{FeMoO}_6$ is a half-metallic ferro-magnet with a relatively high Curie temperature (about 410–450 K) [3]. However, the degree of polarization of these materials is significantly depends versus quality of the surface as well as presence of defects and temperature factor. For instance, the value of spin polarization decreases near the room temperature and become insignificant [4]. Therefore, the increase of the Curie temperature of these ferromagnets (ferrimagnets) is the important condition for practical application of semiconductor properties of these materials in the field of the room temperature. It can be achieved by variation of chemical composition [5] or through control of crystal structure disorder [6, 7].

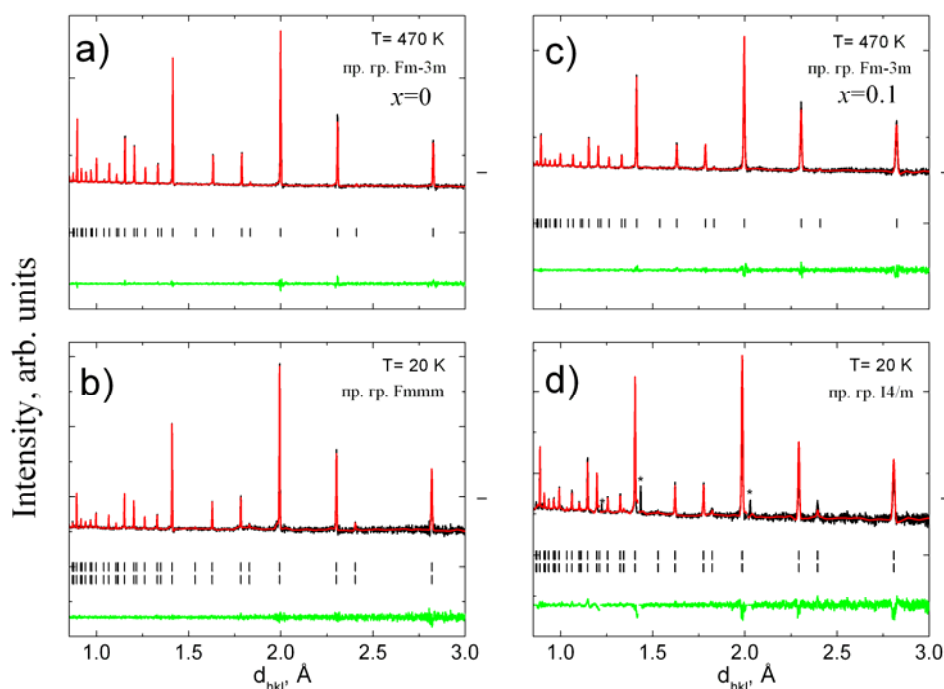


Fig. 1.

The main aim of the work is definition of substitution influence of barium and molybdenum by strontium and iron ions, consequently, onto structural features and magnetic properties of double perovskites: $\text{Ba}_{1-x}\text{Sr}_{1+x}\text{Mo}_{1-x}\text{Fe}_{1-x}\text{O}_6$ ($x = 0$ and 0.1) in a wide temperature range. All samples were prepared by solid-state method at temperature 1200°C in a continuous stream H_2/Ar during 10 h. The crystal and magnetic structures were investigated at the High Resolution Fourier Diffractometer HRFD) [8] at the IBR-2 pulsed nuclear reactor in Dubna. According to neutron diffraction (Fig.1, a-d), all investigated samples are homogeneous in a wide temperature range.

Diffraction patterns of the $\text{Ba}_{1-x}\text{Sr}_{1+x}\text{Mo}_{1-x}\text{Fe}_{1-x}\text{O}_6$ ($x = 0$ and 0.1) samples were measured at different temperatures and treated with Rietveld method. The experimental points, calculated profile and difference curve are shown at Fig.1. The difference is weighted by the mean-squares deviation for each point. Ticks below the graph indicate the calculated peak positions for nuclear and magnetic phases of double perovskites. The sign (*) marks diffraction peaks of copper sample holder. The increase of substitution leads to decrease of unit cell volume. Temperature dependences of refined unit cell volumes of the $\text{Ba}_{1-x}\text{Sr}_{1+x}\text{Mo}_{1-x}\text{Fe}_{1-x}\text{O}_6$ ($x = 0$ and 0.1) samples versus temperature are shown at Fig.2.

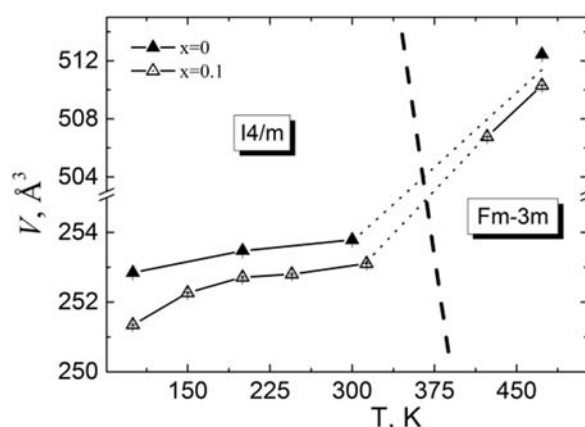


Fig. 2.

The Curie temperature increases from 350 to 380 K and values of microstresses increases in two times as the concentration x is changed. The crystal structures for compounds were calculated for both tetragonal and orthorhombic models. The decrease of the unit cell volume with increasing of substitution of Ba and Mo by Sr and Fe ions was explained by different value of their ionic radii. The increase of microstresses in the $\text{Ba}_{1-x}\text{Sr}_{1+x}\text{Mo}_{1-x}\text{Fe}_{1-x}\text{O}_6$ ($x = 0$ and 0.1) samples as the temperature decreases was explained by influence of magnetostrictive effect.

- [1] Serrate D., 22 . V.19. P.023201.
- [2] J. M. Longo, R. Ward // J. Am. Chem. Soc. 1961. **V.83**. P.1088.
- [3] K.-I. Kobayashi; T. Kimura; H. Sawada; K. Terakura; Y. Tokura, Nature 1998. 395. P.677.
- [4] Gupta A and Sun J Z J. Magn. Mater. 1999. **200** P.24
- [5] C. Ritter, M. R. Ibarra, L. Morellon, J. Blasco, J. Garcí'a, and J. M. De Teresa, J. Phys.: Condens. Matter 2000. **V.12**. P.8295.
- [6] O. Nganba Meetei, Onur Erten, Anamitra Mukherjee, Mohit Randeria, Nandini Trivedi, and Patrick Woodward // Phys. Rev. 2013. **B 87**, 165104.
- [7] Onur Erten, O. Nganba Meetei, Anamitra Mukherjee, Mohit Randeria, Nandini Trivedi, and Patrick Woodward // Phys. Rev. 2013. **B 87**, P.165105.
- [8] A. M. Balagurov // Neutron News 2005. **V.16**. P.8.

F U N C T I O N A L M A T E R I A L S

STRUCTURAL PECULIARITIES OF TiO₂:MoO₃ NANOCOMPOSITES THAT ENSURE THEIR CATALYTIC ACTIVITY

N. Boboriko¹, I. Bobrikov²

¹ *Belarusian State University*

² *Joint Institute for Nuclear Research, Dubna, Russia*

E-mail: natchem@tut.by

Precise structural parameters of TiO₂:MoO₃ nanocomposites synthesized by sol-gel method with MoO₃ content in the range of 0.1-10 mol % were investigated by neutron diffraction employing the High-Resolution Fourier Diffractometer at IBR-2 pulsed reactor. TiO₂:MoO₃ composites find practical application as catalysts in heterogeneous oxidation processes and as gas sensing materials for detection of such burning gases as H₂, CO, C₂H₅OH. Structural peculiarities of TiO₂:MoO₃ oxide systems that ensure catalytic properties in the reaction of hydrogen oxidation were revealed.

It was established that in TiO₂:MoO₃ nanocomposites thermostimulated tetragonal distortions in [MoO₆] octahedra, which are the base units in MoO₃, take place after heating at 850 °C. In the issue of these distortions alteration of the Mo-O bond distance was observed. Moreover neutron diffraction data allowed calculating the mean particle size of TiO₂ and MoO₃ in the composites. The magnitude of the tetragonal distortions and the mean particle size of the oxides appeared to be dependent on the TiO₂:MoO₃ ratio in the composite. It was revealed that the catalytic activity of TiO₂:MoO₃ nanocomposite increases with the decrease of the mean size of the particles in the composite and with the increase of the Mo-O bond distance.

NEW MESOPOROUS CERIA SYNTHESIZED BY TEMPLATING PROCEDURE

B. Matovic, M. Momcilovic, J. Pantic, B. Babic

Vinca Institute of Nuclear Sciences, Belgrade, Serbia

The new mesoporous CeO₂ were obtained by templating procedure using ordered mesoporous carbon (OMC) as a matrix. The Ce/C mass ratio was varied in the range of 0.1 to 0.25. All obtained samples have mesoporous structure with specific surface of about 60 m²/g. X-Ray diffraction revealed that all patterns possess fluorite structure. Raman spectroscopy showed that the main F2g mode is shifted to higher energies at 459 cm⁻¹ and the oxygen vacancy mode is situated at 600 cm⁻¹. It is found that the morphology of CeO₂ replica is a function of Ce/C mass ratio.

SYNTHESIS AND CHARACTERIZATION OF NEW LEAD-BASED PEROVSKITES WITH CRYSTALLOGRAPHIC SHEAR PLANES

P. Tzvetkov¹, D. Kovacheva¹, B. Blagoev² and K.Krezhov³

¹ *Institute of General and Inorganic Chemistry, Bulgarian Academy of Sciences, 1113 Sofia, Acad. Georgi Bonchev str. bld.11*

² *Institute of Solid State Physics, Bulgarian Academy of Sciences, 1784 Sofia, 72 Tzarigradsko chaussee Blvd.*

³ *Institute for Nuclear Research and Nuclear Energy, Bulgarian Academy of Sciences, 1784 Sofia, 72 Tzarigradsko chaussee Blvd.*

E-mail: krezhov@inrne.bas.bg

Recently, the structural details and properties of the new $A_nB_nO_{3n-2}$ ($n = 4$) homologous series ($A=Pb, Sr, Ba, Bi$; $B=Fe, Ti, Co, Sn$) of oxygen deficient perovskite-related compounds with fragmentation of the perovskite matrix by periodical translational interfaces (crystallographic shear planes) have attracted considerable attention [1-3]. The shear planes can contribute to frustrated magnetic couplings between the edge- and the corner-sharing metal-oxygen polyhedra in the perovskite blocks and a range of unusual physical properties might result from substitution of transition-metal B cations.

We will report on our recent results on several polycrystalline single phase materials with general formula $PbBaFeMeO_5$ ($Me=Co, Mn$) and $PbSrFe_{1.25}Cr_{0.75}O_5$. In principle, cations of p elements with lone pair electrons as Pb^{2+} or Bi^{3+} create irregular oxygen coordination environment of the cations and to stabilize the phases often requires the use of high pressure or specific soft chemistry. We have synthesized the phases by solid state reaction or solution-combustion technique and studied their structure and some properties through x-ray (XRD), electron microscopy (TEM, SEM, SAED), magnetometry and Mössbauer spectroscopy. The synthesized oxide compositions are isostructural with $Pb_{1.33}Sr_{0.67}Fe_2O_5$ [4]. Part of the experimental evidence accumulated and the crystal structure parameters in particular have been published previously [5-7]. The room temperature Mossbauer spectra of $PbBaFeCoO_5$ reveal magnetic ordering through presence of well resolved two sextets [5]. On the other hand, $PbBaFeMnO_5$ and $PbSrFe_{1.25}Cr_{0.75}O_5$ are paramagnetic at room temperature and the magnetic ordering sets in below 150 K as shown by Mossbauer data [5] and magnetization (ZFC, FC curves). A compound of chemical composition $Pb_2Mn_2O_5$ with very close structure was recently reported [8]. The proposed structural model by Hadermann et al. shares many features, like the observed by us Jahn-Teller distortion of the MnO_6 octahedra.

[1] A. Abakumov et al., *Inorg. Chem.* 49 (2010) pp. 9508-9516.

[2] M. Batuk et al., *Inorg. Chem.* 53 (2014) pp. 2171-2180.

[3] I. Nikolaev et al., *Phys. Rev. B* 78 2 (2008) 024426.

[4] V. Raynova-Schwarten, W. Massa, D. Babel, *Z. Anorg. Allg. Chem.* 623 (1997) pp. 1048-1058.

[5] P. Tzvetkov, D. Kovacheva, D. Nihtianova, T. Ruskov, *Bulg. Chem. Comm.*, 43, (2011) 339-345.

[6] P. Tzvetkov, D. Kovacheva, D. Nihtianova, T. Ruskov, *Z. Kristallogr. Proc.*, 1, (2011) 397-402.

[7] P. Tzvetkov, D. Kovacheva, D. Nihtianova, N. Velichkova, T. Ruskov, *Bulg. Chem. Comm.*, 44, (2012) 137-145.

[8] J. Hadermann et al., *J. Solid State Chem.* 183, (2010) 2190-2195.

MICROSTRUCTURE OF NANOCRYSTALLINE NONSTOICHIOMETRIC NIOBIUM $\text{NbC}_{0.93}$ AND VANADIUM $\text{VC}_{0.875}$ CARBIDES

A. Kurlov¹, A. Balagurov², I. Bobrikov², A. Gusev¹

¹ *Institute of Solid State Chemistry of the Ural Branch of the Russian Academy of Sciences, Ekaterinburg, Russia*

² *Joint Institute for Nuclear Research, Dubna, Russia*

E-mail: kurlov@ihim.uran.ru

Evolution of the microstructure of nonstoichiometric niobium $\text{NbC}_{0.93}$ and vanadium $\text{VC}_{0.875}$ carbide powders subjected to high-energy ball milling is investigated by neutron diffraction. It is established that milling produces a non-uniform powders, in which two distinct fractions with differing microstructure can be identified. It is shown that TOF (time-of-flight) neutron diffraction technique is promising for studying of microstructure of strongly deformed nonstoichiometric carbides and for quantitative determination of the anisotropy of microstrains.

All previous studies of nanocrystalline nonstoichiometric compounds were performed only using standard X-ray or neutron diffraction method. This work is the first experimental study of microstructure of nanocrystalline nonstoichiometric carbides by the TOF (time-of-flight) neutron diffraction technique. As objects of the study, we used coarse-grained and nanocrystalline powders of nonstoichiometric niobium and vanadium carbides.

The initial $\text{NbC}_{0.93}$ niobium carbide powder contains large-sized particles of more than 1 μm and also many particles of $\sim 0.5 \mu\text{m}$ or smaller (Fig. 1). However, these smallest particles are connected among themselves and form the large branched agglomerates with a size about 2-5 μm .

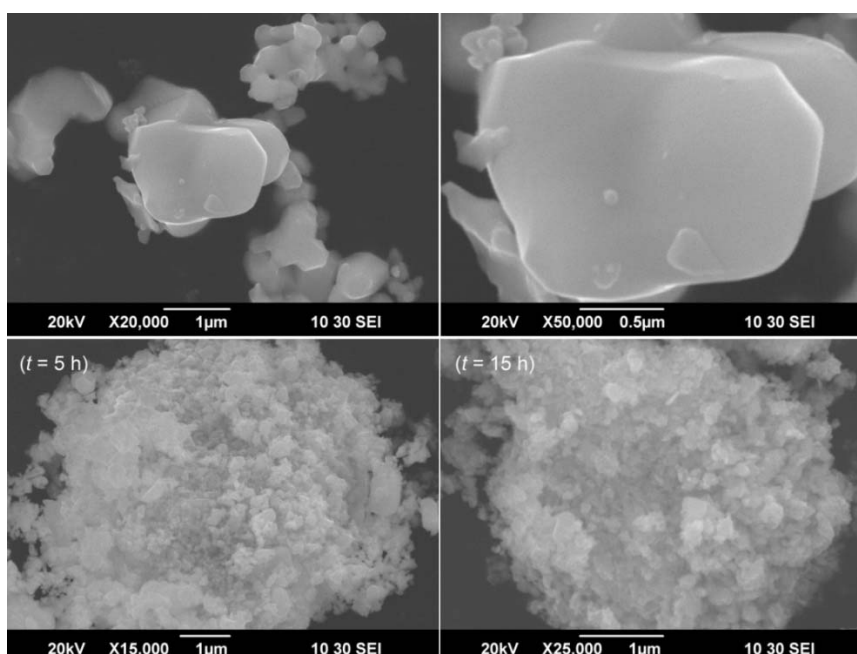


Fig. 1. SEM images of the initial coarse-grained $\text{NbC}_{0.93}$ powder at different magnifications and of $\text{NbC}_{0.93}$ nanocrystalline powders produced by high-energy ball milling during 5 h and 15 h.

The initial $\sim\text{V}_8\text{C}_7$ ($\text{VC}_{0.875}$) ordered vanadium carbide powder contains large agglomerated particles which are a set of a large number of very small particles. Small particles look like an open flower (Fig. 2). The observed crystallites have the shape of curved leaves or petals. As a first approximation, the crystallites can be simulated by a disk with a diameter of 6000-8000 Å and a thickness of approximately 200-400 Å. The formation of such microstructure of ordered vanadium carbide is caused by the disorder-order structural phase transition $\text{VC}_{0.875} - \text{V}_8\text{C}_7$. The lattice constant a_{ord} of perfect cubic V_8C_7 superstructure is equal to the doubled lattice constant a_{B1} of a disordered basic phase $\text{VC}_{0.875}$, i.e. $a_{\text{ord}} = 2a_{\text{B1}}$.

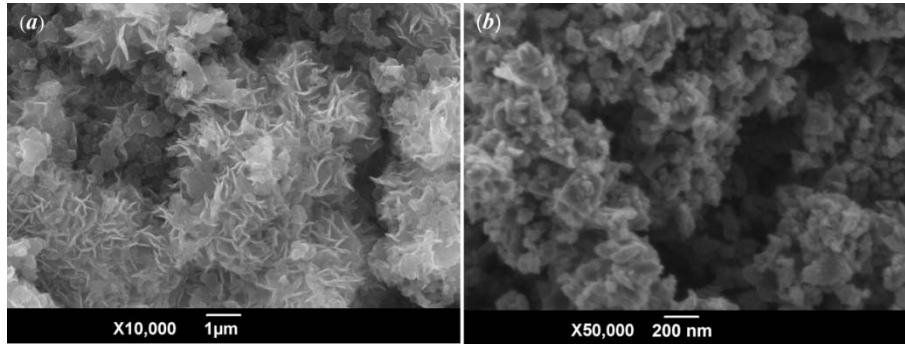


Fig. 2. SEM images of (a) initial coarse-grained $\text{VC}_{0.875}$ powder and (b) nanocrystalline $\text{VC}_{0.875}$ powder produced by high-energy ball milling during 10 h.

The nanocrystalline $\text{NbC}_{0.93}$ powders were prepared by high-energy milling of the initial coarse-grained powder on a PM-200 Retsch planetary ball mill for 1, 5, 10, and 15 h. $\text{VC}_{0.875}$ nanopowder was prepared by milling of initial powder during 10 h.

After milling of initial $\text{NbC}_{0.93}$ powder during 1, 5, 10, and 15 h, average particle size in prepared nanopowders was equal to ~ 1000 , ~ 470 , ~ 450 , and ~ 180 Å, respectively. Average particle size in $\sim\text{V}_8\text{C}_7$ ($\text{VC}_{0.875}$) nanopowder produced by ball milling during 10 h was equal to ~ 200 Å.

All neutron diffraction patterns were measured on the high-resolution Fourier diffractometer (HRFD) installed at the long-pulse IBR-2 reactor in Dubna.

The diffraction patterns of the $\text{NbC}_{0.93}$ powders, normalized by the effective neutron spectrum, are shown in Fig. 3. These patterns demonstrate a notable increase in peak broadening due to the mechanical work and an increase in the incoherent background arising probably from a non-crystalline component or diffuse effects. The diffraction patterns of the $\sim\text{V}_8\text{C}_7$ ($\text{VC}_{0.875}$) powders are shown in Fig. 4. The small particle size and microstrains are responsible for the broadening of diffraction reflections of $\sim\text{V}_8\text{C}_7$ ($\text{VC}_{0.875}$) nanopowder.

A comprehensive analysis of the neutron diffraction data for the $\text{NbC}_{0.93}$ nanopowders revealed that the diffraction reflection profiles should be modeled by two independent fractions of powder.

Judging by the dependence of lattice constant on the NbC_y composition, the finest $F1$ fraction of niobium carbide nanopowders has a compositions $\text{NbC}_{0.87}$, $\text{NbC}_{0.84}$, $\text{NbC}_{0.82}$, and $\text{NbC}_{0.80}$ for the nanopowders produced by milling during 1, 5, 10, and 15 h, respectively. On the contrary, the $F2$ fraction of niobium carbide shows an almost constant composition $\text{NbC}_{0.95}$ (Fig. 5).

Results on particle size D and microstrain ε_{hkl} found from the neutron diffraction measurements are in good agreement with analogous data obtained by the X-ray diffraction and with the D value estimated from the specific surface of nanopowders (Fig. 6a). Figure 6b shows the anisotropic distribution of the microstrains ε_{hkl} over the directions $[hkl]$ in the $\text{NbC}_{0.93}$ nanopowder prepared by 10 h milling. The radius of the sphere is proportional to the microstrain $\varepsilon_{\text{aver}}$ averaged over all crystallographic directions.

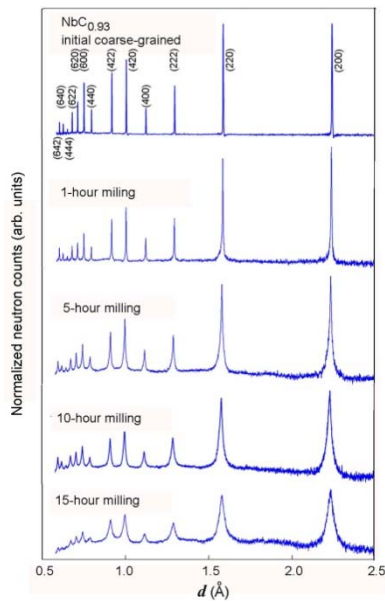


Fig. 3. Normalized HRFD neutron diffraction patterns of the initial coarse-grained $\text{NbC}_{0.93}$ powder and $\text{NbC}_{0.93}$ nanopowders prepared from it by milling for 1, 5, 10, and 15 h. As the milling time increases, the peak widths and the incoherent background increase as well. Miller indices of the diffraction reflections are indicated.

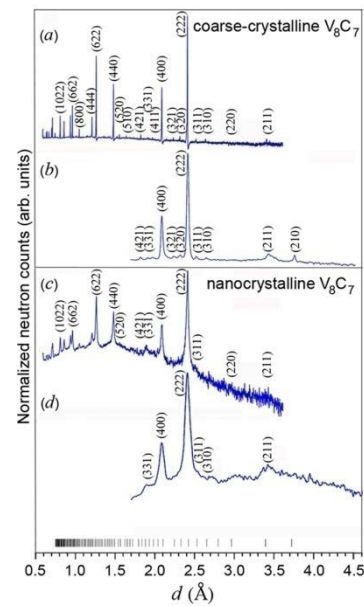


Fig. 4. Normalized diffraction patterns of coarse-grained (a,b) and nanocrystalline (c,d) $\sim\text{V}_8\text{C}_7$ ($\sim\text{VC}_{0.875}$) powders measured with HRFD: (a) and (b) high-resolution measurements with DOR and DPR detectors, respectively; (c) high-resolution measurement with DOR detector; (d) low-resolution measurement with DPR detector. The vertical ticks correspond to the diffraction reflections of V_8C_7 cubic superstructure. Miller indices of the diffraction reflections are indicated.

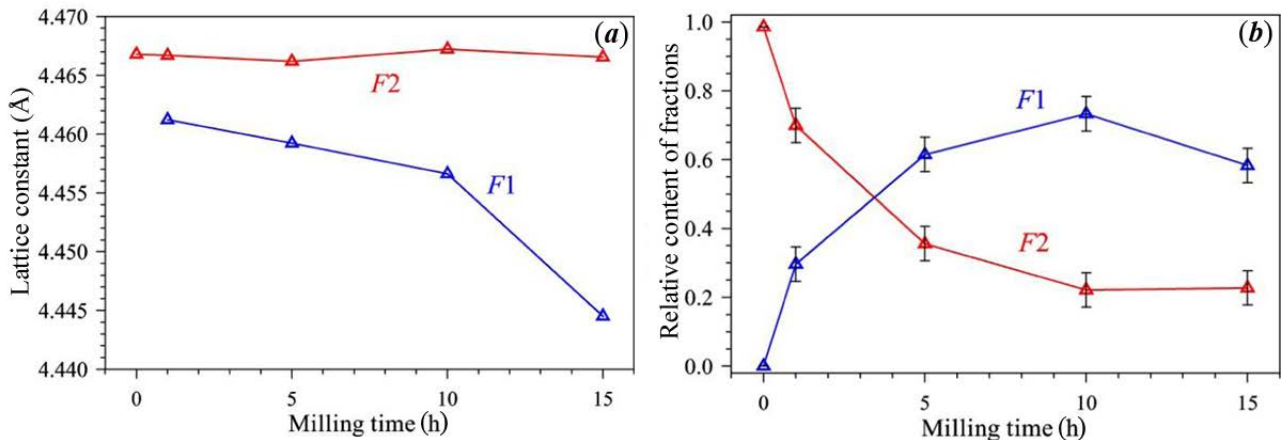


Fig. 5. Dependence of the lattice constant (a) of F1 (blue triangles) and F2 (red triangles) fractions and the volume ratio (b) of these fractions in niobium carbide nanopowders on the milling time.

The neutron diffraction patterns of vanadium carbide powders (Fig. 4) have the following peculiarity. Shoulders are observed to the left of the diffraction peaks. These shoulders are caused by presence of disordered $\text{VC}_{0.875}$ phase along with main ordered V_8C_7 phase. For real disordered and ordered vanadium carbide phases the lattice constant $a_{B1} < a_{\text{ord}}/2$. Therefore Rietveld analysis of the neutron diffraction data for the $\text{VC}_{0.875}$ powders was performed in two-phase model considering presence of main ordered phase V_8C_7 and disordered phase $\text{VC}_{0.875}$ (Fig. 7).

The found real superstructure V_8C_7 is characterized by noticeable displacements of vanadium atoms and small displacements of carbon atoms from the positions of the ideal superstructure. Vanadium atoms constituting the octahedral environment of vacant sites of the carbon sublattice are displaced toward the vacancy.

A significant feature of the real V_8C_7 superstructure is a lowered occupancy of 4(a) sites of the unit cell by carbon atoms which is equal to ~ 0.97 . This means that the nanostructured ordered phase has a composition of $\sim V_8C_{6.97}$. It means that ordered V_8C_7 phase has a very narrow homogeneity interval.

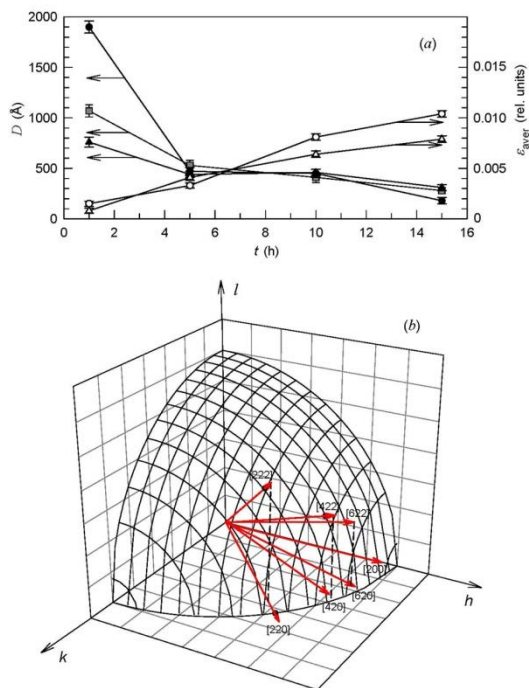


Fig. 6. Size of particles and microstrains in nanopowders of the nonstoichiometric niobium carbide $NbC_{0.93}$: (a) average size D of particles and the average value of microstrains ϵ_{aver} in $NbC_{0.93}$ nanopowders versus the milling duration t measured using (closed and open triangles) X-ray and (closed and open circles) neutron diffraction and (squares) by the BET method; (b) distribution of microstrains ϵ_{hkl} over the nonequivalent $[hkl]$ directions in the $NbC_{0.93}$ nanopowder prepared by 10 h milling.

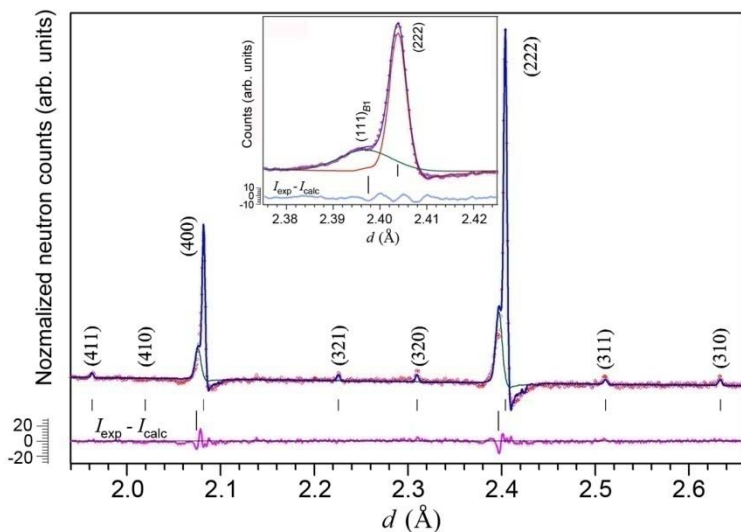


Fig. 7. Part of neutron diffraction pattern of $\sim V_8C_7$ powder. Along with the reflections of basic ordered phase V_8C_7 there are weak broadened reflections of a disordered V_8C_7 phase with $B1$ structure. Experimental diffraction pattern is shown by points, theoretical diffraction pattern and contributions of the ordered and disordered phases to the theoretical spectrum are shown by solid lines. Inset represents description of profiles of (222) reflection of ordered phase $\sim V_8C_7$ and (111)_{B1} reflection of disordered phase $VC_{0.875}$. Short and long ticks correspond to the diffraction reflections of V_8C_7 cubic superstructure and of disordered $VC_{0.875}$ phase.

Investigation of niobium carbide powders are financially supported by the Russian Foundation for Basic Research within the project No. 14-29-04091_ofi_m. Investigation of nonstoichiometric vanadium carbide nanopowder is financially supported by the Russian Science Foundation (Grant 14-23-00025) through the Institute of Solid State Chemistry of the Ural Branch of the RAS.

I N S T R U M E N T S A N D M E T H O D S

DEVELOPMENT OF ADVANCED NEUTRON SCATTERING INSTRUMENTATION FOR LONG PULSE NEUTRON SOURCES

A. Ioffe

*Jülich Centre for Neutron Science (JCNS), Forschungszentrum Jülich GmbH
Outstation at MLZ, 85747 Garching, Germany*

The next high flux neutron source to become operative at 2019 - the European Spallation Source (ESS) – will be the 5MW long pulse source with the pulse duration of 2.8ms and the repetition rate of 14Hz. A number of concepts of advanced neutron instrumentation have been developed to profit from the long pulse structure of the neutron beam and in many cases allow to achieve outstanding instrument parameters exceeding the present-day state-of-the-art by orders of magnitude.

In this talk some of these concepts – for high-resolution powder diffraction, small-angle neutron scattering (SANS), reflectometry and grazing incidence small-angle neutron scattering (GISANS) - will be considered.

SONIX+ - ОСНОВА ПРОГРАММНОГО ОБЕСПЕЧЕНИЯ КОМПЛЕКСА СПЕКТРОМЕТРОВ РЕАКТОРА ИБР-2

А.С.Кирилов, С.М. Мурашкевич, Т.Б. Петухова, И.А. Морковников

ОИЯИ, Дубна, Россия

Начиная с 1995 года программный инструментальный комплекс Sonix+ (Sonix) используется спектрометрах реактор ИБР-2 для управления экспериментом. Изначально это была инсталляция на единственном инструменте НСВР. Постепенно год за годом комплекс переносился на новые спектрометры, развиваясь и совершенствуясь в ходе этого процесса. В настоящее время комплекс используется на около 20 установках в ЛНФ и в ряде других российских центров. На наш взгляд причинами этого успеха послужили два обстоятельства. Во-первых, был сделан правильный выбор решений, положенных в основу комплекса. Это был компромиссный выбор, учитывающий как мировые тенденции развития в данной области, так и традиции, а также принятую в ЛНФ практику. Во-вторых, важно отметить плодотворное сотрудничество с пользователями, некоторые из которых внесли существенный вклад, как в выбор концепции, так в разнообразие реализованных возможностей.

В докладе предполагается рассмотреть историю развития комплекса Sonix, его современное состояние и перспективы развития в ближайшие годы.

SYSTEM OF NEUTRON MICROBEAMS FROM A PLANAR WAVEGUIDE

S. Kozhevnikov¹, V. Ignatovich¹, Yu. Nikitenko¹, F. Ott², A. Petrenko¹

¹ *JINR, Dubna, Russia*

² *LLB, CEA/CNRS, Saclay, France*

E-mail: kozhevn@nf.jinr.ru

Results of experimental investigations of space, angular and wavelength distribution in neutron microbeams obtained for the first time with the help of a resonant planar neutron waveguide at the time-of-flight reflectometer of the IBR-2 pulsed reactor are reported and comparison with theoretical calculations is presented. Possible application of microbeams in physical experiments is discussed.

We have observed the system of the neutron microbeams emitted from the planar waveguide. The microbeams are produced because of resonant enhancement of the neutron wave function density inside the waveguiding layer. The microbeams angular divergence is found to coincide with that predicted by Fraunhofer diffraction theory. Experiment was carried out at the time-of flight neutron reflectometer of the pulsed IBR-2 reactor. Several microbeams with different wavelength and space distribution were produced simultaneously and studied separately. It is a new result, which shows that microbeams can be effectively obtained at pulsed sources and used in applications. In this experiment we used nonpolarized neutrons and nonmagnetic sample. There are no limitation for production of polarized neutron microbeams, which can be used for the investigations of one-dimensional magnetic systems like magnetic microwires, domains, lithographic gratings, and vortices in superconductors.

Contrary to the fixed wavelength method at steady state sources, the time-of-flight technique allows to change the wavelength of the neutron microbeam by changing grazing angle of the incident beam. In this way one can produce microbeams with long wavelength. Here with the help of the cold neutron source we were able to produce microbeams with wavelength 5.25 Å, but there are no limitations for production of microbeams with even longer wavelength.

NEUTRON SCATTERING INSTRUMENTS OF IBR-2 HIGH FLUX PULSED REACTOR FOR CONDENSED MATTER RESEARCH: CURRENT STATE AND RECENT RESULTS

D.P. Kozlenko

Frank Laboratory of Neutron Physics, Joint Institute for Nuclear Research, 141980 Dubna Moscow Reg., Russia

Since the re-start of the regular operation of the IBR-2 high flux pulsed reactor after full-scale modernization in 2012, the complex of neutron scattering instruments installed at the reactor was substantially upgraded. It contains in total 14 instruments, including diffractometers, small angle scattering spectrometer, reflectometers, inelastic neutron scattering spectrometers. New instruments – DN-6 diffractometer for studies of microsamples under extreme conditions, GRAINS multifunctional reflectometer, neutron imaging facility were put into operation. A number of existing spectrometers was also modernized to improve technical parameters. An overview of the recently obtained scientific results and prospects for interdisciplinary research in the fields of condensed matter physics, materials science, chemistry, biophysical and geophysical sciences at IBR-2 neutron scattering instruments is presented.

PROPAGATION OF NEUTRON SPHERICAL WAVES THROUGH A THICK, VIBRATING GE SINGLE CRYSTAL

E. Raitmans¹, V. Gavrilov¹, D. Mjasishchev¹, A. Hoser², O. Seidel² and J. Stanh³

¹ *Institute of Physical Energetics, Riga, Latvia,*

² *Helmholtz-Zentrum, BENSC, Berlin, Germany,*

³ *Paul Scherrer Institute, Villigen, Switzerland*

E-mail: eraitmans@apollo.lv

The results of experimental and theoretical studies into the influence of ultrasound on the propagation of neutron waves in a thick Ge crystal are presented. The neutron intensity profiles were measured for the case of Laue diffraction inside the Borrmann fan. At low amplitudes of ultrasonic waves interference effects (diffraction intensity beatings) were observed. The observations were possible because of the uniform acoustic-field distribution through the whole bulk of the crystal. As distinct from the classical Shull experiments, wide analysing slits or position-sensitive detectors were used. To explain the results obtained, a modified theory for the spatial distribution of neutron diffraction intensities in the presence of acoustic excitation of the crystal is proposed. A good agreement between experiment and theory is obtained. At high amplitudes of ultrasonic waves the transition to kinematic scattering was not observed, despite the large strains in the crystalline lattice created by ultrasound. This could be connected with the formation of a superlattice having a standing wave period. A strong rise in the diffraction intensity and a sharp constriction of the neutron beam at the centre of the Borrmann fan were observed. This new effect could be used for the creation of ultrasound-controlled monochromators.

L A Y E R E D N A N O S T R U C T U R E S

COMPOSITIONAL, MORPHOLOGICAL AND ACCUMULATION PHENOMENA IN LASER PULSE ABLATION OF NANO-LAYERED (NI/TI) THIN FILMS

Biljana Gaković, Suzana Petrović, Milan Trtica

Institute of Nuclear Science Vinča, University of Belgrade, POB 522, 11001 Belgrade, Serbia

E-mail: biljagak@vinca.rs

Laser surface modification technique is one non-contact surface engineering tool in processing of thin films which can alter them on the micro- and nanoscale. The interaction of a laser, operating at 1540 nm wavelength and pulse duration of 40 ns, with Ni/Ti thin films has been studied. Laser ablation was performed at fluences of 6.4 and 8.8 Jcm⁻². As samples a nano-layered (Ni/Ti) thin film were used. Five (Ni/Ti) bilayers were deposited by direct current (DC) ion sputtering on Si(100) wafers to a total thickness of about 180 nm. Single and multi-pulse laser irradiation was done at normal incidence in air. The composition and surface morphology were monitored by particle-induced x-ray emission (PIXE), Rutherford backscattering spectrometry (RBS), scanning electron microscopy (SEM) and profilometry. Most of the absorbed laser energy was rapidly transformed into heat, producing intensive modifications of composition and morphology on the target surface. The results show an increase in surface roughness, formation of parallel periodic surface structures, appearance of hydrodynamic features and ablation of surface material. Compositional analysis revealed that laser modification induced inter-mixing between the components of individual Ni and Ti layers, with indications of the formation of NiTi intermetallic compounds.

SPIN-ECHO SPECTROMETRY IN GRAZING GEOMETRY

Yu.V. Nikitenko

FLNP, JINR, Dubna, Russia

Two neutron magnetic mirrors placed in perpendicular directed magnetic field are a neutron spin-interferometer. The neutron spin-interferometer can be used in scheme of a spin-echo spectrometer in grazing geometry. In spin-echo spectrometer are accessible the measurements with ultrasmall values of transfer neutron wave vectors 10^{-7} \AA^{-1} and transfer energy 1 peV. It allows to investigate in medium and at surface a low frequency dynamic and nuclear structure with micron correlation length.

DETERMINATION OF MAGNETIC ORDER IN SUPERLATTICES FE/CR/GD

M. V. Ryabukhina¹, E. A. Kravtsov^{1,2}, Yu. V. Nikitenko³, V. V. Proglyado¹, Yu. N. Khaydukov⁴

¹*Institute of Metal Physics, Ural Branch, Russian Academy of Sciences, Yekaterinburg, 620041 Russia*

²*Ural Federal University, Yekaterinburg, 620002 Russia*

³*Joint Institute for Nuclear Research, Dubna, 141980 Russia*

⁴*Max Planck Institute for Solid State Research, Stuttgart, D 70569 Germany*

E-mail: ryabykhina@imp.uran.ru

Ferromagnetic 4f rare-earth/ 3d transition metal (RE/TM) multilayers are popular model systems showing a rich variety of magnetic phases in applied field. In particular, complex magnetic order in Fe/Gd multilayers is governed by several competing mechanisms: enhancement and temperature-independence of Gd magnetic moment in the interfacial region near Fe, strong RE-TM antiferromagnetic coupling at interfaces, and Zeeman interaction with external fields.

It was recently shown that RE/Cr/TM multilayers, where RE-TM exchange is mediated by antiferromagnetic Cr, display a number of novel magnetic phases, including switching an otherwise AFM Gd-Fe coupling to ferromagnetic coupling, together with a dominant biquadratic RE-TM exchange coupling over bilinear coupling at certain Cr thicknesses near where the oscillatory interlayer coupling (with Cr thickness) changes sign. The latter should lead to non-collinear ordering. Cr layer thickness in the samples was chosen in order to cover 3 different types of magnetic ordering in the system: ferromagnetic, antiferromagnetic and non-collinear.

Polarized neutron reflectometry are the most powerful technique to probe magnetization depth profiles in multilayered nanostructures. In order to understand and utilize the physical mechanism responsible for novel properties of magnetic of magnetic heterostructures, it is important to precisely resolve inhomogeneous magnetization density depth profiles, which are typical in the Fe/Cr/Gd structures. It was also known that the magnetization density profile inside Gd layers becomes no uniform at high temperatures, with the Gd magnetic moment enhanced at the Fe/Gd interfaces and reduced in the core of the Gd layers.

In our work, we are studying magnetic multilayers [Fe(31.5 Å)/Cr(t Å)/Gd(45 Å) /Cr(t Å)]₁₂, t= 4 -20 Å, we focused on the reduced magnetic coupling near interfaces. In this work we performed polarized neutron reflectometry measurements, followed by simultaneous refinement of the experimental spectra within a unified parametrized model. This procedure allows us to obtain depth-resolved and element-specific magnetization profiles in magnetically inhomogeneous Fe/Cr/Gd heterostructures.

This work was partially supported by the Russian Foundation for Basic Research, project nos. 14-22-01063 and 15-32-50494_mol_nr.

INVESTIGATION OF MAGNETISM IN MULTILAYER METALLIC NANOSTRUCTURES FE/MGO/FE AND FE/MGO/CR/MGO/FE USING POLARIZED NEUTRON REFLECTOMETRY

E. M. Yakunina¹, V. I. Bodnarchuk², V. V. Proglyado¹, E. A. Kravtsov¹

¹*Institute of Metal Physics, Ural Division of the Russian Academy of Science
620990 Yekaterinburg, Russia*

²*Joint Institute for Nuclear Research 141980 Dubna, Russia*

E-mail:eyakuninaart@gmail.com

Giant magnetoresistance (GMR) observed in Fe/Cr superlattices are of great interest due to their technological importance as elements of spintronic devices [1, 2]. Drastic change in resistance under applied magnetic field makes investigation of GMR systems a hot direction in condensed matter physics. Another interesting system is a Fe/MgO/Fe multilayer in which the effect giant tunneling magnetoresistance (GTMR) is observed. This phenomenon is due to the tunneling of electrons between the Fe layers through the insulating layer of MgO [3]. GTMR occurs in Fe/MgO/Fe systems when the magnetic ordering changes from antiparallel to parallel.

This work is aimed to study Fe/MgO/Fe and Fe/MgO/Cr/MgO/Fe multilayers, specifically the exchange interaction that occurs between Fe and Cr layers after adding an MgO spacer. Fe/MgO/Cr/MgO/Cr system is certainly interesting in that there is a combination of both GMR and GTMR effects may be observed. In our research we investigate the series of samples Fe(200Å)/MgO(tÅ)/Fe(50Å)/Ta(50Å) and Fe(100Å)/MgO(tÅ)/Cr(nÅ)/MgO(tÅ)/Fe(70Å)/Ta (50Å), that was grown on a high-vacuum magnetron sputtering setting. The structure was deposited on a MgO substrates and annealed during the growth process. MgO layer thickness (t) varies in the range of 0-25Å and Cr layer thickness (n) was 9-18Å. Practically, it is very important to understand microscopic picture of magnetization reversal in these systems depending on MgO tunnel barrier properties.

The best of our knowledge, the structures in which an insulator is added to the Fe/Cr interface is poorly studied for today, although it is of great interest. It's unknown, how the Fe layers will interact with Cr through a thin MgO spacer and what other effects this will be followed. Practically, it is very important to understand microscopic picture of magnetization reversal in these systems depending on spacer properties.

The work was partially supported by the Russian Foundation for Basic Research (grants nos. 14-22-01063 ofi_m and 15-32-50570 mol_nr, and 14-02-00013).

[1] Fert, A. The origin, development and future of spintronics. Nobel lecture, 2007

[2] Grunberg, P. From spinwaves to giant magnetoresistance (GMR) and beyond. Nobel lecture, 2007

[3] Parkin, S.S.P., et al. Giant tunneling magnetoresistance at room temperature with MgO (100) tunnel barriers. Nature Materials, vol. 3, p. 862-867, 2004

MAGNETISM OF NANOSTRUCTURES WITH FERROMAGNETIC AND SUPERCONDUCTING LAYERS

V. Zhaketov

Joint Institute for Nuclear Research, Dubna, Russia

E-mail: zhaketov@nf.jinr.ru

Magnetic properties of superconductor are antagonistic to the ferromagnetic ones. So in layered structures ferromagnetic/superconductor, where thickness of layers are order of the correlation length of superconducting or magnetic order parameters, arise different nontrivial effects. One of such effects is cryptoferromagnetic state of ferromagnetic contacting with superconductor. It appear as a formation of a special domain structure in ferromagnetic, which characteristic size is order of superconducting correlation length in the ferromagnetic or correlation length in the superconductor. Such state was predicted in the theoretical works, and it hasn't been discovered by experiment yet. In this work were made attempts to find such state.

MAGNETIC AND LATTICE EXCITATIONS

EXOTIC MAGNETIC ORDERING IN SYSTEMS WITH STRONGLY CORRELATED ELECTRONS

P.A. Alekseev

NRC “Kurchatov Institute” Moscow, Russia

NRNU “MEPI” Moscow, Russia

E-mail: pavel_alekseev-r@mail.ru

Rare earth based strongly correlated electron systems (SCES) demonstrate a wide range of different types of a ground state. Its started from trivial paramagnetic one originating from crystal field splitting of f-electron multiplet and arrived at highly exotic ones. The latter, for instance, could be as Kondo-insulator with combination of charge-, spin-gap with valence instability; or long range magnetic ordered state in initially singlet ground state system; or some combination of long range magnetic order with superconductivity and valence instability; etc. Physical background for these features inherent to electron subsystem may be elucidated by detailed neutron scattering experiments, first of all by magnetic neutron scattering spectroscopy and diffraction.

Specific features of such unusual ground states are analyzed on the base of the results of the extended experimental studies. The report displays previous and recent results in the field for a number of representative rare earth intermetallic compounds. The number of the examples is presented, in particular: the systems with induced long range ordering for crystal field defined singlet ground state metals; Kondo-insulators with possibility for formation of long range magnetic order below metal to insulator transition; systems with coexistence of long range magnetic order with intermediate valence state or heavy fermion state.

This work is partially supported by the RFBR grant 14-22-01002 and grant 14-02 00272.

HIGH PRESSURE MEASUREMENTS ON THE NERA FACILITY

P. Bilski^{1,2}, D. Chudoba^{1,2}, I Sashin¹

¹*Frank Laboratory of Neutron Physics, Joint Institute for Nuclear Research, Dubna, Russia*

²*Faculty of Physics, Adam Mickiewicz University, Poznan, Poland*

E-mail: bilski@amu.edu.pl

The aim of the most projects realize on the NERA spectrometer is to establish molecular dynamics of different polymorphous of substances in particular phases, determine their p-T diagrams and identify the molecular mechanisms of the phase transitions. The knowledge of molecular dynamics permits drawing conclusions on inter- and intramolecular interactions in particular phases of the systems studied and helps establish the molecular mechanism of phase transitions. Results of the study are expected to provide the information on possible changes in the character of phase transitions induced by high hydrostatic pressure and a possibility of new pressure-induced phases appearance.

Measurements of neutron scattering as a function of temperature and pressure, performed with the use of the NERA spectrometer and a compressor U11 400 MPa, supplemented with the dielectric spectroscopy and magnetic nuclear resonance study, permit construction of p-T phase diagrams which would considerably improve characterisation of novel materials. The results will be of cognitive value and of great application interest.

DIRECT VS INVERTED TOF GEOMETRY IN THE STUDIES OF MAGNETIC AND LATTICE EXCITATIONS

E. Clementyev¹, P. Alekseev², I. Sashin³

¹ *I. Kant Baltic Federal University, Kaliningrad, Russia*

² *NRC "Kurchatov institute, Moscow, Russia*

³ *JINR, Dubna, Russia*

E-mail: clement@inr.ru

Time-of-flight (TOF) neutron spectrometers are indispensable experimental tools to study in detail magnetic and structural excitations in condensed matter. For about 55 years these instruments provide valuable information in the 4-dimensional Q-E space on the dynamics of solids, liquids and soft matter. Nowadays TOF instruments based on the pulsed neutron sources are getting to prevail as the most efficient “excitation scanners” compared to other spectrometers like triple-axis instruments (TAS) designed to study limited regions in the Q-E space. Two main principles are widely known to build TOF spectrometers: to fix the energy of the incoming neutrons (the so-called direct TOF geometry) or to fix the final neutron energy (inverted TOF geometry). Choppers and monochromators are typical for the direct geometry spectrometers while crystal analyzers and filters in addition to choppers are typical components in the inverted geometry case. The direct geometry principle dominates in the world, however many leading neutron facilities were building the inverted TOF instruments. TOF instruments of both types were in operation in Dubna at the neutron source IBR-2. This fact provides good local experience in dealing with both types and also in the analysis of the experimental data originating from either direct or inverted TOF. We report on the studies of the magnetic and lattice dynamics in many systems on the TOF spectrometers of different types. The objects of studies included strongly correlated electron systems, rare-earth-based intermetallics, superconductors, magnetic materials with spin density waves and singlet ground states. Powder samples as well as single crystals were used in the measurements. The scientific cases and most beneficial areas for the direct and inverted geometry TOF spectrometers are different. The accessible domains in the Q-E space along with the energy and Q-resolution issues are discussed. A few sources of artefacts and spurious contribution to the scattering are shown on the basis of our practical experience. Advantages and weak sides of both types are clearly visible in the diagrams and in the collected neutron spectra. The direct and inverted geometry TOF instruments are in fact good complementary spectroscopic tools on the pulsed neutron sources. These instruments are also complementary to TAS spectrometers widely used in the case of continuous neutron sources. The IBR-2 neutron source has a good potential for TOF neutron spectroscopy which is of high demand.

SPIN EXCITATION IN THE IRON BASED HIGH T_C SUPERCONDUCTOR $\text{FeTe}_{1-x}\text{Se}_x$

E.A. Goremychkin¹, M.D. Lumsden², A.D. Christianson²

¹ *FLNP, JINR, Dubna, Moscow Region, 141980, Russia*

² *QCMD, ORNL, Oak Ridge, Tennessee 37831, USA*

We use inelastic neutron scattering to study spin dynamics of superconducting and non-superconducting $\text{FeTe}_{1-x}\text{Se}_x$. Our results indicate a spin fluctuation spectrum dominated by two-dimensional incommensurate excitations extending to energies greater than 250meV. Most importantly, the spin excitations in $\text{FeTe}_{1-x}\text{Se}_x$ have four-fold symmetry about the (1, 0) wavevector. Moreover, the excitations are described by the identical wavevector and can be characterized by the same model as the normal-state spin excitations in the high- T_c cuprates. These results demonstrate commonality between the magnetism in these classes of materials, which perhaps extends to a common origin for superconductivity.

MAGNETIC COLLOID NANOSYSTEMS

FERRONEMATICS - THE WAY TO MAGNETOVISION CAMERA

P. Kopcansky^a, N. Tomasovicova^a, M. Timko^a, V. Gdovinova^a, N. Eber^b, T.-T.-Katona^b, Ch.-K. Hu^c, Sh. Hayryan^c, V. M. Haramus^d, V. Petrenko^e, M. Avdeev^e

^a *Institute of Experimental Physics SAS, Watsonova 47, 04001 Košice, Slovakia*

^b *Institute for Solid State Physics and Optics, Wigner Research Centre for Physics, Hungarian Academy of Sciences, H-1525 Budapest, P.O.Box 49, Hungary*

^c *Institute of Physics, Academia Sinica, 128 Sec.2, Academia Rd., Nankang, Taipei, Taiwan*

^d *Helmholtz- Zentrum Geesthacht Outstation at EMBL/DESY, Notkestrasse 85, Hamburg, Germany*

^e *Joint Institute for Nuclear Research, Joliot-Curie 6, 141980 Dubna, Moscow region, Russia*

Liquid crystals (LCs), due to their large dielectric anisotropy, respond very sensitively to application of an external electric field, whereas they are only weakly sensitive to the magnetic field. A possible way of improving that sensitivity is doping LCs with magnetic nanoparticles (MNPs). As a result, stable colloidal suspensions of LCs with relatively low concentrations of MNPs, called ferronematics, can be produced. These suspensions are considered to be extremely promising materials, in which the properties of LCs are modified by doping. As a representative example, the presence of the magnetic admixture enhances the magnetic susceptibility of ferronematics in comparison to that of the undoped nematic LCs and allows controlling their orientation with much lower magnetic fields [1]. We will demonstrate that even very low magnetic fields ($B < 0.1$ T) may induce a significant magnetic response in ferronematics. We will also show the possibility to alter the nematic-isotropic transition temperature with an external field in the thermotropic calamitic doped with rodlike MNPs [2]. Our results have proven that ferronematics can be just as effective in demonstrating the magnetic field induced isotropic-nematic phase transition as pure bent-core nematics [3]. Recently a consistent mean-field model was developed for the field-induced shift of the temperature of isotropic–nematic phase transition in ferronematics [4]. It will show that depending on the anchoring conditions on the particle surface, the particles might either enhance or decrease the clearing temperature of the suspension [5].

An important feature of lyotropic LCs is the self-assembly of the amphiphilic molecules as supermolecular structures. We will present the formation of nematic LC phase in solutions containing lysozyme amyloid fibrils and MNPs. Interaction and adsorption ability of MNPs on lysozyme amyloid fibrils were studied by SAXS and TEM. Visualization of the fibrils by TEM also indicates that MNPs adsorb on the fibril surface. This fact provides possible ordering of the fibrils applying to the nematic phase.

This work was supported by project VEGA 0045, the Slovak Research and Development Agency under the contract No. APVV-0171-10 and APVV-2013-0009, Ministry of Education Agency for Structural Funds of EU in frame of projects 26110230097, and M-era.Net project MACOSYS.

[1] N. Tomasovicova, M. Timko, Z. Mitroova, M. Koneracka, M. Rajnak, N. Eber, T. Toth-Katona, X. Cahud, J. Jadzyn, P. Kopcansky, *Phys. Rev E* 87, 014501 (2013).

[2] P. Kopcansky, N. Tomasovicova, M. Koneracka, V. Zavisova, M. Timko, M. Hnatic, N. Eber, T. Toth-Katona, J. Jadzyn, J. Honkonen, E. Beaugnon, X. Chaud, *IEEE Trans. Magn.* 47, 4409 (2011).

[3] T. Ostapenko, D.B.Wiant, S.N.Sprunt, A. Jakli, J.T.Gleeson, *Phys. Rev. Lett.* 101, 247801 (2008)

[4] Y.L. Raikher, V.I.Stepanov, A.N.Zakhlevnykh, *Soft Matter* 9, 177 (2013)

[5] N. Tomasovicova, M. Timko, N. Eber, T. Toth-Katona, K. Fodor-Csorba, A. Vajda, V. Gdovinova, X. Chaud, P. Kopcansky, *Liquid Crystals* DOI: 0.1080/02678292.2015.1010618 (2015)

NEUTRON INVESTIGATIONS OF WATER-BASED FERROFLUIDS SYNTHESIZED BY DIFFERENT METHODS

A.V.Nagorny^{1,2}, V.I.Petrenko^{1,2}, M.V.Avdeev¹, O.I.Ivankov^{1,2}, L.A.Bulavin², S.O.Solopan³, O.V.Yelenich³, A.G.Belous³

¹ *Joint Institute for Nuclear Research, Dubna, Russia*

² *Taras Shevchenko National University of Kyiv, Kyiv, Ukraine*

³ *Institute of General and Inorganic Chemistry, Kyiv, Ukraine*

Investigation of colloidal systems of magnetic nanoparticles dispersed into a liquid medium constitutes a specific trend in condensed matter science by enabling the use of magnetic particles in a wide range of technical applications and especially in medicine [1,2]. For medical destinations the particles have to meet special requirements, like being nanosized, nontoxic and having stability to aggregation, etc. Prospects of using magnetic NPs in particular hyperthermia treatment of cancer impose an additional requirement: the ensemble of particles has to demonstrate high heating efficiency under alternating magnetic field.

Manufacturing of new ferrofluids with the specified properties for biomedical purposes involves the development of new methods of synthesis of magnetic nanoparticles. The first basic requirement to ferrocolloid in this case is biocompatibility of the liquid medium.

Water based agarose gel due to haptic behaviour compared to biological material [3] is often used as a model of biological tissue in biomedical experiments with magnetic nanoparticles [4-6]. For this reason, a mixture of agarose (polysaccharide, C₁₂H₁₈O₉) in a water is selected as liquid carrier of magnetite contained ferrofluids.

Samples of the magnetic liquids prepared by three different methods of magnetite nanoparticles synthesis [7,8] were studied in frameworks of Small-Angle Neutron and Synchrotron Scattering methods. Obtained experimental data allowed to make some conclusions about the structure of considered ferrofluids. All samples demonstrated the separation of liquids on a precipitate and a supernatant fractions. Small-angle experimental measurements were performed on the corresponding supernatant fractions.

It is shown that two kinds of ferrofluids have a similar microstructure: monomers of magnetite with Guinier radius of 2.8-2.9 nm are resolved by SANS and aggregation with 2.6-2.8 fractal dimension is presented in the systems. The magnetic liquid prepared using microemulsion differs from previous ones by its complex aggregation.

[1] *Belous A., Solopan S., Yelenich O., Osinsky S., Bubnovskaya L., Bovkun L. // IEEE ELNANO 2014, Kyiv, 2014, P. 245–249.*

[2] *Kopcansky P., Timko M., Kovac J., Vaclavikova M., Odenbach S. Journal of Physics: Condensed Matter. 20(20), 200301 (2008).*

[3] *Rahn H., Odenbach S. // Proc. Appl. Math. Mech. 2010, V.10, P. 87- 88.*

[4] *Basak S., Brogan D., Dietrich H., et al. // Int. J. Nanomedicine. 2009, V. 4, P.9–26.*

[5] *Holligan D. L., et al. // Nanotechnology. 2003, V. 14, P. 661-666.*

[6] *Salloum M., et al. // Int. J.of Hyperthermia. 2008, V.24, No.4 , P. 337-345.*

[7] *Yelenich O.V., et al. // Solid State Phenomena 2013, V. 200, P. 149–155.*

[8] *Yelenich O. V., et al. // Russian Journal of Inorganic Chemistry 2013, V. 58, №. 8, P. 901–905.*

ELECTRIC FIELD DRIVEN ASSEMBLY OF FERROFLUID MAGNETIC NANOPARTICLES STUDIED BY SMALL ANGLE NEUTRON SCATTERING (SANS)

M. Rajnak^a, M. Timko^a, P. Kopcansky^a, V. Petrenko^{b,c}, M. Avdeev^b, O. Ivankov^b, A. Feoktystov^d

^a*Institute of Experimental Physics SAS, Watsonova 47, 04001 Košice, Slovakia*

^b*Joint Institute for Nuclear Research, Joliot-Curie 6, 141980 Dubna, Moscow region, Russia*

^c*Kyiv Taras Shevchenko National University, Volodymyrska Street 64, Kyiv, 01033 Ukraine*

^d*Jülich Centre for Neutron Science (JCNS), Forschungszentrum Jülich GmbH, Outstation at MLZ, Lichtenbergstrasse 1, 85747 Garching, Germany*

Ferrofluids are remarkable suspensions of magnetic nanoparticles in conventional base fluids such as water, oils, or glycols [1]. In this presentation we focus on a transformer oil-based ferrofluid (TOFF) containing magnetite nanoparticles covered with oleic acid. TOFF are of great scientific interest due to the enhanced cooling effect and fascinating dielectric properties, especially the increased electrical breakdown field strength [2, 3]. This phenomenon is paradoxical and still not fully understood. Within this context we have therefore undertaken investigations into structural behavior of the nanoparticles exposed to electric fields far below the sample breakdown. For that purpose, *in situ* Small Angle Neutron Scattering experiments were conducted on a sample placed in a standard quartz cuvette equipped with two tubular electrodes inside. It has been found that DC electric field induces remarkable aggregation processes in the sample, dependent on the applied field strength. Moreover, anisotropic alignment of the elongated clusters in the direction of the applied field has been revealed. On the other hand, no changes in SANS profiles in the investigated q -range were observed when AC electric field with the power line and higher frequencies was applied. However, at 6kV/cm, the frequency of 800 mHz has been found as the critical one, at which the particles are initiated to form the aggregates. The analyses of the structural changes in the ferrofluid can make essential steps towards solving the paradoxically higher breakdown field strength of ferrofluids in comparison to pure transformer oils. As the response of magnetic nanoparticles in ferrofluids to electric fields was not expected and often neglected, the presented study may open a new avenue of research on magnetic colloidal systems.

This work is supported by NMI3 to perform the neutron scattering measurements at the Heinz Maier-Leibnitz Zentrum (MLZ), Garching, Germany, Slovak Academy of Sciences and Ministry of Education in the framework of projects VEGA No. 2/0043/12, 2/0045/13, 1/0311/15, Ministry of Education Agency for structural funds of EU in frame of projects Nos. 26110230061, 26220120046, 26220120055 and 26220220182, Slovak Research and Development Agency in project APVV 0171-10, and COST RADIOMAG TD 1402.

[1] R. E. Rosensweig, *Ferrohydrodynamics*. Courier Dover Publications, 1997.

[2] V. Segal, A. Hjortsberg, A. Rabinovich, D. Nattrass, and K. Raj, "AC (60 Hz) and impulse breakdown strength of a colloidal fluid based on transformer oil and magnetite nanoparticles," in *Conference Record of the 1998 IEEE International Symposium on Electrical Insulation, 1998*, 1998, vol. 2, pp. 619–622 vol.2.

[3] M. Rajnak, J. Kurimsky, B. Dolnik, K. Marton, L. Tomco, M. Molcan, P. Kopcansky, and M. Timko, "Influence of Magnetic Field on Dielectric Breakdown in Transformer Oil Based Ferrofluids," *Acta Phys. Pol. A*, vol. 126, no. 1, pp. 248–249, Jul. 2014.

MATERIALS FOR ENERGY APPLICATIONS

T_c -ENHANCEMENT OF $\text{Fe}_{1+\delta}\text{Se}$ BY ELECTROCHEMICAL LITHIUM INTERCALATION

A. M. Alekseeva^{1,2}, O. A. Drozhzhin^{1,2}, K. V. Zakharov³, O. S. Volkova³, D. A. Chareev⁴, A. N. Vasiliev³, C. Koz⁵, Yu. Grin⁵ and E.V. Antipov¹

¹*Department of Chemistry, Lomonosov Moscow State University, 119991 Moscow, Russia*

²*MPG-MSU Partner Group, Department of Chemistry, Lomonosov Moscow State University, 119991 Moscow, Russia*

³*Department of Physics, Lomonosov Moscow State University, 119991 Moscow, Russia*

⁴*Institute of Experimental Mineralogy, Russian Academy of Sciences, 142432 Chernogolovka, Russia*

⁵*Max-Planck-Institut für Chemische Physik fester Stoffe, 01187 Dresden, Germany*

The superconducting transition temperature (T_c) of tetragonal $\text{Fe}_{1+\delta}\text{Se}$ can be enhanced from 8.5 K to 44 K by chemical structure modification resulting in significant increase of $[\text{Fe}_2\text{Se}_2]$ -interlayer separation: from 5.5 Å in native $\text{Fe}_{1+\delta}\text{Se}$ to > 7 Å in $\text{K}_x\text{Fe}_{1-y}\text{Se}$ and to > 9 Å in $\text{Li}_{1-x}\text{Fe}_x(\text{OH})\text{Fe}_{1-y}\text{Se}$. Structure modification is achieved by the shift of the $[\text{Fe}_2\text{Se}_2]$ -slabs and filling the interlayer space by solvated lithium and iron cations or by large alkaline cations like K. We firstly report the application of electrochemical approach to modification of $\text{Fe}_{1+\delta}\text{Se}$ superconducting properties. In contrast to chemical way the electrochemical approach allows to insert small amount of non-solvated Li^+ into $\text{Fe}_{1+\delta}\text{Se}$ structure keeping the native structure and $[\text{Fe}_2\text{Se}_2]$ -layers arrangement. The amount of intercalated lithium is extremely small (about 0.07 Li^+ per f.u), however, caused slight change of carrier concentration results in enhancement of T_c up to ~ 44 K. The obtained results provide the opportunity to better understand the mechanism of superconductivity in Fe-based superconductors and open new possibilities for T_c -enhancement.

This work was supported by Russian Scientific Foundation grant No. 14-13-00738.

EVOLUTION OF CRYSTAL STRUCTURE OF CATHODE MATERIAL $\text{LiNi}_{0.8}\text{Al}_{0.1}\text{Co}_{0.1}\text{O}_2$ DURING ELECTROCHEMICAL CYCLING

I.A. Bobrikov, N.Yu. Samoylova, A.I. Beskrovny, A.M. Balagurov

Joint Institute for Nuclear Research, Dubna, Russia

The evolution of crystal structure of cathode material $\text{LiNi}_{0.8}\text{Co}_{0.1}\text{Al}_{0.1}\text{O}_2$ during electrochemical cycling has been studied using neutron diffraction at RTD (Real-Time-Diffractometer) at the IBR-2 pulsed reactor (FLNP JINR, Dubna).

$\text{LiNi}_x\text{M}_y\text{Co}_{1-x-y}\text{O}_2$ -type of material has just only begun to be used as a cathode material in lithium-ion battery manufacturing instead of widely used lithium cobaltite. Investigation of this type compounds in real time during electrochemical cycling have been carried out until now only in special model electrochemical cells using X-ray diffraction ([1]). Neutron diffraction allows one to investigate a crystal alteration in the electrode materials not only in a tailor-made electrochemical cell, but also in the real lithium-ion devices, and to exclude thus such a factor as a difference between constructions of model cells and real batteries.

The real lithium-ion battery Panasonic with cylinder 18650-type has been studied in this work. Graphite is used as a negative electrode, material with composition $\text{LiNi}_x\text{Al}_y\text{Co}_{1-x-y}\text{O}_2$ with $x \approx 0.8$ and $y \approx 0.1$ (x, y were refined from neutron diffraction data) is used as a positive electrode. Crystal structure of $\text{LiNi}_{0.8}\text{Al}_{0.1}\text{Co}_{0.1}\text{O}_2$ in a fully charged state corresponds to space group $R\bar{3}m$ with cell parameters $a = b = 2.8645(1) \text{ \AA}$ and $c = 14.2099(2) \text{ \AA}$.

Analysis of experimental data collected during several charge-discharge cycles at different cycling rate ($C/3$ and $C/10$, C - full battery capacity) has shown that intercalation of lithium into graphite accompanies by a formation of several LiC_n phases (Fig.1). The formation of final LiC_6 phase is clear detected as an abrupt appearance of diffraction peak at $d \approx 3.67 \text{ \AA}$. We have obtained no such phase separation in cathode material $\text{LiNi}_{0.8}\text{Al}_{0.1}\text{Co}_{0.1}\text{O}_2$ as, for instance, in $\text{LiNi}_{0.8}\text{Co}_{0.15}\text{Al}_{0.05}\text{O}_2$ [1]. In the meanwhile, the unit cell parameters of these two compounds change during charge equally, expansion and subsequent compression of unit cell is anisotropic. When charging, first, the unit cell expands along hexagonal c -axis and somewhat compresses in a basal plane (a and b axes). Then, near full charge state, there are a drastic compression of unit cell along c -axis and somewhat its expansion along a and b axes.

Authors I.A. Bobrikov, N.Yu. Samoylova, A.M. Balagurov thank Russian Science Foundation for financial support of this research (project 14-12-00896).

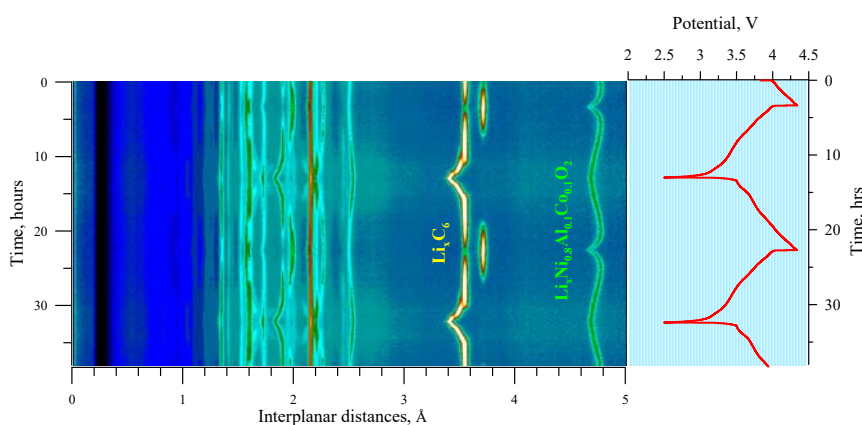


Fig.1. Evolution of neutron diffraction patterns of $\text{LiNi}_{0.8}\text{Al}_{0.1}\text{Co}_{0.1}\text{O}_2$ -based lithium-ion battery in the course of charge-discharge cycles at the rate of $0.1C$. Exposition time for every diffraction pattern is 150 seconds.

[1] Won-Sub Yoon et al., *Electrochemistry Communications* 8 (2006) 1257–1262.

PHASE TRANSITIONS UPON LI (DE) INTERCALATION IN $\text{Li}_x\text{Fe}_{1-y}\text{Mn}_y\text{PO}_4$ ($0 \leq x \leq 1$, $0 \leq y \leq 0.5$)

O.A. Drozhzhin¹, V.D. Sumanov¹, A.N. Baranov¹, E.V. Antipov¹

¹Chemistry department of Lomonosov Moscow State University, Moscow, Russia

Complex phosphates $\text{LiFe}_{1-y}\text{Mn}_y\text{PO}_4$ became an object of a great interest as cathode materials for Li-ion batteries. Partial substitution of Fe by Mn in LiFePO_4 allows to increase specific energy density of the cathode material because of higher electrochemical potential $\text{Mn}^{2+}/\text{Mn}^{3+}$, keeping proper stability and low degradation rate during galvanostatic cycling. Two-phase mechanism of Li^+ deintercalation-intercalation is typical for LiFePO_4 , but for Mn-substituted olivines extraction and insertion of Li^+ occurs via single phase in broad ranges of composition [1], [2]. Phase transformations in $\text{Li}_x\text{Fe}_{1-y}\text{Mn}_y\text{PO}_4$ were studied in a number of works with *in situ* and *ex situ* diffraction methods, but X-ray diffraction data provides only one-sided notion about the processes which occur during Li^+ (de)intercalation in these compounds. The aim of the present work is detailed study of phase transformations in $\text{Li}_x\text{Fe}_{1-y}\text{Mn}_y\text{PO}_4$ ($0 \leq x \leq 1$, $0 \leq y \leq 0.5$) by means of *in situ* X-ray powder diffraction (XRPD) and potentiostatic intermittent titration technique (PITT).

Single-phase samples of $\text{LiFe}_{1-y}\text{Mn}_y\text{PO}_4$ ($0 \leq y \leq 0.5$) were obtained by hydrothermal method. Phase transformations during Li^+ extraction/insertion in $\text{Li}_x\text{Fe}_{1-y}\text{Mn}_y\text{PO}_4$ ($0 \leq x \leq 1$, $0 \leq y \leq 0.5$) were studied using *in situ* XRD and – independently – by corresponding treatment of PITT data, described in [3]. Using this method, we calculated contribution of single-phase mechanism (parameter f , where $f = 0$ means complete two-phase reaction, and $f = 1$ regards to ideal solid solution) into total process of Li^+ (de)intercalation. Results obtained by these two methods are in a good agreement with each other (Fig. 1). Three different types of phase transformations may be observed for the compositions LiFePO_4 , $\text{LiFe}_{0.9}\text{Mn}_{0.1}\text{PO}_4$ and $\text{LiFe}_{0.5}\text{Mn}_{0.5}\text{PO}_4$; also different behavior may be seen for $\text{LiFe}_{0.5}\text{Mn}_{0.5}\text{PO}_4$ during charge and discharge. Explanation for the observed phenomena is proposed basing on crystal chemistry parameters of lithiated and delithiated phases.

The work was supported with the RFBR grants (14-03-31473, 14-29-04064).

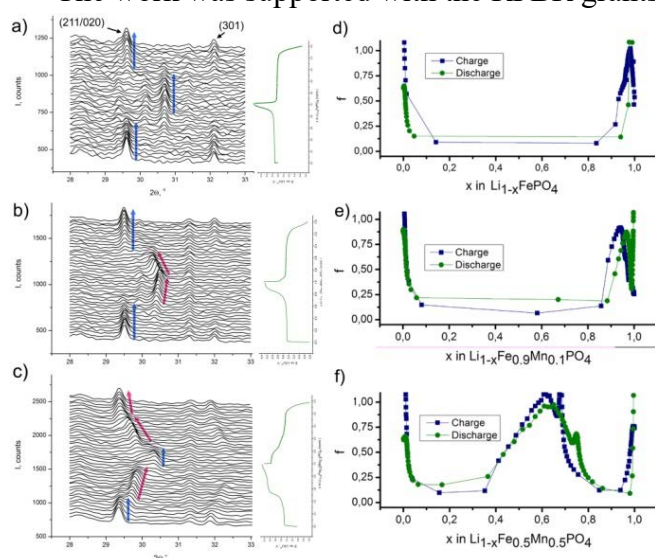


Fig. 1. Selected region of *in situ* X-ray diffraction patterns for Li_xFePO_4 (a), $\text{Li}_x\text{Fe}_{0.9}\text{Mn}_{0.1}\text{PO}_4$ (b) and $\text{Li}_x\text{Fe}_{0.5}\text{Mn}_{0.5}\text{PO}_4$ (c), and corresponding f - x dependence obtained with PITT (d-f).

- [1] A. Yamada et al., J. Electrochem. Soc., 148 (2001) A960;
- [2] D. B. Ravnsbaek et al., Nano Lett., 14 (2014) 1484–1491;
- [3] N. Meethong et al., Chem. Mater., 22 (2010) 1088–1097.

A COMPARATIVE STUDY OF LITHIUM-VANADIUM PHOSPHATE AND FLUOROPHOSPHATE: APPLICATION OF NEUTRON DIFFRACTION AND ELECTROCHEMICAL METHODS

A.V. Ivanishchev¹, A.V. Churikov¹, I.A. Bobrikov², O.Yu. Ivanshina², A.V. Ushakov¹, I.M. Gamayunova¹

¹*Institute of Chemistry, Saratov State University named after N.G. Chernyshevsky, Astrakhanskaya str. 83, Saratov, Russian Federation, 410012*

²*Frank Laboratory of Neutron Physics, Joint Institute for Nuclear Research, Joliot-Curie str. 6, Dubna, Moscow reg., Russia, 141980*

E-mail: ivanischevav@inbox.ru

The need of modern devices for reliable and energy-intensive autonomous power sources stimulates the progress of lithium-ion batteries (LIB). Expansion of large-scale LIBs for electric vehicles (EV) and energy storage systems (ESS) puts to the fore the safety of power sources. In Fig.2. Structural and electrochemicetals have a distinct advantage over the layered oxides, traditionally used as LIB's cathode materials. Examples of such compounds include lithium-vanadium phosphate ($\text{Li}_3\text{V}_2(\text{PO}_4)_3$) and fluorophosphate (LiVPO_4F). $\text{Li}_3\text{V}_2(\text{PO}_4)_3$, related to the NASICON-type compounds can be modified by introduction of substituent atoms into the cation and anion sublattice. Usually this leads to a change in parameters of the crystal structure and energy state of lithium therein, which in turn is reflected as an increase of electrode potential and conductive properties of such compounds. However, in the case of the anionic substitution by fluorine the compound of another structural type is formed – tavorite (LiVPO_4F). The electrochemical behavior of these two lithium intercalation compounds differs considerably. Charge-discharge characteristics of lithium-vanadium phosphate at a constant current in the potential range of 3.6-4.7 V are of asymmetric shape (Fig.1a): delithiation curve has a multi-step shape, lithiation curve, in opposite, is of sloping, smoothed shape. Lithium-vanadium fluorophosphate has symmetrical flat charge-discharge characteristics (Fig.1b) similar to curves of well known LiFePO_4 , but at a higher potential of 4.2 V.

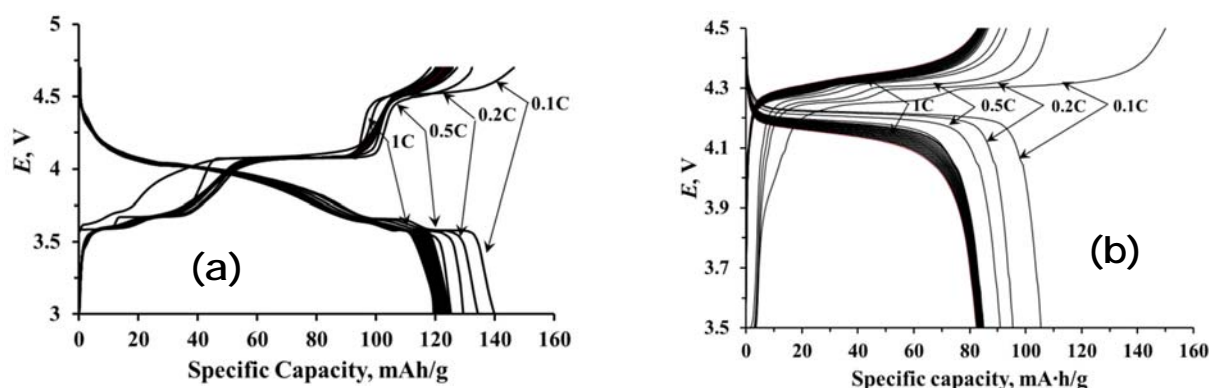


Fig.1. Galvanostatic charge-discharge curves for (a) $\text{Li}_3\text{V}_2(\text{PO}_4)_3$ and (b) LiVPO_4F -electrodes at different currents.

By the theoretical specific capacity $\text{Li}_3\text{V}_2(\text{PO}_4)_3$ looks like more advantageous with 197 mAh/g vs. 156 mAh/g for LiVPO_4F . However, each of these compounds has a number of advantages over the opponent, which allows to separate the fields of their application. Common to both of them is

inherent to all phosphate materials low electronic conductivity, coexisting with high ionic conductivity, which makes it necessary to obtain these compounds in the form of a special composite wherein the electroactive compound particles are dispersed in a matrix of conductive carbon materials. Further improvement of these materials is possible by the structural and morphological modification, as well as selection of a composition and content of electrically conductive matrix of such composite. These tasks can be solved provided detailed knowledge of the structural and electrochemical properties of $\text{Li}_3\text{V}_2(\text{PO}_4)_3$ and LiVPO_4F .

The main tool for structural studies in this work is the method of neutron diffraction. The measurements were performed using HRFD-diffractometer at high resolution. The exposure time was 12 hours for each sample. The neutron diffraction pattern of $\text{Li}_3\text{V}_2(\text{PO}_4)_3$ processed by the Rietveld method is shown in Fig.2a. Processing was performed using the FullProf software package. Coordinates of atoms and the unit cell parameters were refined, in some cases population of atomic positions were determined (as it turned out, the occupancies were filled nominally, so at the final stage of refinement, they were fixed).

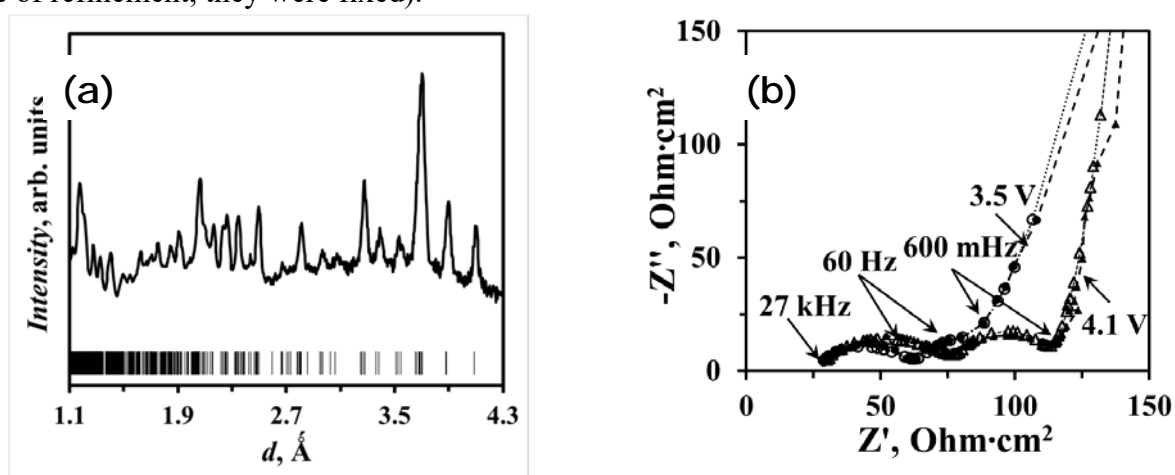


Fig.2. Structural and electrochemical investigation of $\text{Li}_3\text{V}_2(\text{PO}_4)_3$ -electrode: (a) – neutron diffraction pattern for Rietveld refinement and (b) electrochemical impedance spectra of the fully lithiated (3.5 V) and delithiated (4.1 V) states of the electrode.

The electrochemical properties of the materials were studied by the complex of methods: galvanostatic charge-discharge, cyclic voltammetry (CV), pulsed chronoampero- and chronopotentiometry (PITT and GITT, relatively), electrochemical impedance spectroscopy (EIS). The theoretical bases of methods in the application to lithium-vanadium-phosphate and fluorophosphate electrodes were developed in our studies [1,2]. Using the EIS method different stages of the electrochemical process (transfer through the boundary particle, diffusion in the bulk) were identified and their parameters (lithium diffusion coefficient (D), resistance and geometric capacitance of surface layer, intercalation capacitance) were determined. The results of different methods are in good agreement.

The neutron diffraction study of the electrode materials is supported by Russian Science Foundation (project 15-13-10006), and synthesis and electrochemical study of the materials are supported by Russian Foundation for Basic Research (project 14-29-04005).

[1] A.V. Ivanishchev, A.V. Churikov, A.V. Ushakov, *Electrochim. Acta.* 2014 (122) 187.

[2] A.V. Churikov, A.V. Ivanishchev, A.V. Ushakov, V.O. Romanova, *J. Solid State Electrochem.* 18 (2014) 1425.

DISTRIBUTION OF CATIONS IN THE CU-CONTAINING OXIDES OF A SPINEL STRUCTURE AND ITS INFLUENCE ON THE CATALYTIC PROPERTIES IN THE LOW-TEMPERATURE WGSR

L.M. Plyasova¹, I.A. Bobrikov², T.P. Minyukova¹, T.M. Yurieva¹, A.M. Balagurov²

¹ *Boreshkov Institute of Catalysis, Novosibirsk, Russia*

² *Joint Institute for Nuclear Research, Dubna, Russia*

E-mail: pls@catalysis.ru

Oxide catalysts of the spinel type structure attract a great attention in recent years because of their high activity and high resistance to adverse factors of the reaction medium - high temperatures and high water content. Although the study of these catalysts are held for a long time, it is unclear the impact of the chemical composition and the ratio of trivalent cations on the distribution of copper cations in the oxide and its catalytic properties. Therefore, in this paper on the example of mixed oxides $\text{CuAl}_x\text{Cr}_{2-x}\text{O}_4$ and $\text{CuAl}_x\text{Fe}_{2-x}\text{O}_4$ ($x = 0\div 2$) we investigated the influence of chemical composition on the structural features and catalytic properties in low temperature WGSR.

The samples were obtained by thermal decomposition at 900°C of mixed CuAlCr and CuAlFe hydroxocompounds at Boreshkov Institute of Catalysis.

Structural study was performed by neutron diffraction technique. Experimental data were obtained with High Resolution Fourier Diffractometer at the IBR-2 pulsed reactor in Dubna. Analysis of diffraction patterns was carried out using MRIA and FullProf packages.

It is shown that depending on the Al/Cr ratio spinel phase exists in two modifications - the cubic and tetragonal distorted cubic. Crystallographic analyzes of the connection between cubic and tetragonal distorted spinel phase was done. It is shown that the distribution of cations on crystallographic positions, nature and extent of tetragonal distortion of the spinel $\text{CuAl}_x\text{Cr}_{2-x}\text{O}_4$ depends on the Al/Cr ratio. The real cation distribution in them was determined by the Rietveld refinement of neutron diffraction data.

For $\text{CuAl}_x\text{Fe}_{2-x}\text{O}_4$ spinels the structure is cubic and partly inverted for all Al/Fe ratios.

The correlation of distribution of copper ions on the octahedral and tetrahedral positions and the activation energy of the low-temperature WGSR, occurring at active Cu-centers, was found.

The study was supported by RFBR Projects № 13-03-00469 «a» and № 14-29-04091 ofi_m.

The authors are grateful to I.Yu Molina and M.P. Demeshkina (BIC, Novosibirsk) and V.G. Simkin (JINR, Dubna) for their help.

NEUTRON IMAGING AND APPLIED STUDIES

INVESTIGATION OF AN ANCIENT THRACIAN SPEAR FRAGMENT WITH NEUTRONS AND X-RAYS

M. Dinca¹, M. Mihalache¹, M.G.Stanciulescu¹, D.Mandescu², O.Culicov³, D.P. Kozlenko³, G. Bokuchava³, S.E. Kichanov³, A. Rutkauskas³

¹*Institute for Nuclear Research (INR), Mioveni, Romania*

²*Arges County History Museum, Pitesti, Romania*

³*Joint Institute for Nuclear Research, Dubna, Russian Federation*

E-mail: marin.dinca@nuclear.ro

An ancient Thracian spear fragment was discovered in September 2014 close to INR near Argesel river in a tomb with remains after dead body incineration. The tomb was over over 2500-2600 years old and the spear fragment is from late Hallstatt iron age from Thracian culture, type Ferns III. The fragment was made in forging iron with a tubular conical form for wood handle of the spear. This fragment has the size of about 12 cm length, 2.2 cm maximum diameter and 0.3 cm thickness of the wall and was borrowed from Arges County History Museum (ACHM). There are presented the activities and their results with investigations on spear fragment made by neutron imaging in INR and JINR Dubna, neutron diffraction and NAA in JINR Dubna, XRF and SEM-EDS in INR. The collaboration among INR, JINR Dubna and ACHM was done within a research contract with IAEA with title “The neutron and gamma imaging method combined with neutron-based analytical methods for cultural heritage research” that helps curators to reveal the internal structure and composition of the objects. This is a good beginning for the dissemination of the investigation methods based on neutrons and X-rays for cultural heritage and beyond this area.

ОПЫТ ИССЛЕДОВАНИЯ ПАЛЕОНТОЛОГИЧЕСКИХ ОБЪЕКТОВ С ПОМОЩЬЮ НЕЙТРОННОЙ ТОМОГРАФИИ НА РЕАКТОРЕ ИБР-2

А.В. Пахневич¹, Д.П. Козленко², С.Е. Кичанов²

¹ *Палеонтологический институт им. А.А. Борисяка РАН, Москва*

² *Объединенный институт ядерных исследований, Дубна*

В настоящее время в палеонтологии используются различные направления неразрушающего метода – томографии, например, рентгеновская томография, микротомография, нанотомография. Нейтронная томография только начинает занимать свое место, и первые результаты ее применения уже известны. Тем не менее, до сих пор она остается недостаточно востребованной, хотя имеет свои особенности в сравнении с рентгеновским методом.

Исследование палеонтологических объектов на установке реактора ИБР-2, Объединенного института ядерных исследований началось больше года назад. Первые пробные исследования были выполнены на материале Палеонтологического института им. А.А. Борисяка РАН при участии НИЦ «Курчатовский институт». Они были выполнены на примере раковин юрского аммонита и брахиоподы *Kaninospirifer kaninensis* пермского периода (п-ов Канин). В настоящее время, как результат сотрудничества, вырисовались следующие направления, отражающие преимущества метода и особенности установки для нейтронной радиографии и томографии на реакторе ИБР-2.

1. На установке для нейтронной радиографии и томографии на реакторе ИБР-2 существует возможность исследования больших объектов с пространственным разрешением до 300 мкм и величиной пикселя – 87 мкм. Для палеонтологии всегда существовала необходимость томографии крупных объектов. В Палеонтологическом институте она начиналась с исследования черепов панцирных динозавров рода *Tarchia* на медицинском томографе. Поэтому востребованность нейтронной томографии в области неразрушающего исследования крупных объектов очевидна. В настоящий момент совместно с В.В. Булановым (ПИН РАН) исследуются два черепа пермских земноводных, один из которых является голотипом вида.

2. Ряд химических элементов имеют высокие коэффициенты поглощения нейтронов. Среди них можно отметить В, Rh, Cd, Hg, Ir, Н и другие. Для палеонтологии может иметь значение водород, элемент формирующий контрастность некоторых структур в палеонтологических объектах. Один из таких случаев это сохранившееся органическое вещество в окаменевших объектах. В редких случаях палеонтологи сталкиваются с сохранившимся органическим веществом, например, его обнаруживают в уникальных местонахождениях, где сохраняются мягкие ткани живых организмов – лагерштеттах, в костях животных, возраст которых составляет несколько сотен и тысяч лет. Больших успехов достигла четвертичная палеонтология и палеоантропология в расшифровке ДНК шерстистого мамонта и некоторых древних людей. Нейтронная томография может оказаться хорошим подспорьем для подобных исследований. В нашем случае мы начали совместно с А.Б. Соколовой (ПИН РАН) анализ распространения органического вещества в растительных объектах – шишках хвойных растений. Выяснилось, что все ископаемое вещество шишек насыщено органическими соединениями. В связи с этим ископаемые растения можно считать перспективным объектом для данных исследований.

3. В некоторых случаях водородсодержащей может быть вмещающая порода, например, глина. Это влияет на контрастность содержащихся в ней ископаемых объектов, также она может заполнять полости разрушенных структур ископаемого объекта, создавая его слепок (в палеонтологии - ядро). Или же она заполняет пустоты от нор и каналов, проделанных животными. Эти следы жизнедеятельности можно рассмотреть внутри породы с помощью нейтронной томографии. В том числе и построить трехмерную модель их распространения в горной породе. Подобные исследования проводятся на примере следов жизнедеятельности совместно с В.Б. Кушлиной (ПИН РАН) и А.В. Дроновым (ГИН РАН).

4. Используя различные методы, совмещая их с нейтронной томографией, мы можем получить дополнительные результаты, которые позволяют всесторонне изучить исследуемый объект. С помощью рентгеновской микротомографии и нейтронной томографии мы начали изучение современных строматолитов щелочного озера Петуховского (Алтайский край), совместно с О.С. Самылиной (ИНМИ РАН) и Л.В. Зайцевой (ПИН РАН). Это исследование поможет понять процессы образования ископаемых строматолитов. В дополнении к томографическим методам применялась ИК-Фурье спектроскопия. Рентгеновская микротомография позволит выявить элементы микроструктуры строматолита, распределение слоев с кальцитом и песком, слоев обогащенных стронцием. Задача нейтронной томографии определить локализацию органического вещества в слоях строматолита.

Таким образом, используя возможности нейтронной томографии, мы можем получить новые результаты в изучении палеонтологических объектов, которые невозможно получить с помощью другой техники и методов.

ELASTIC ANISOTROPY OF LAYERED ROCKS: CRYSTALLOGRAPHIC TEXTURE AND ULTRASONIC MEASUREMENTS OF PLAGIOCLASE-BIOTITE GNEISS VERSUS EFFECTIVE MEDIA MODELING

Ivan Zel¹, Tatiana Ivankina¹, Tomáš Lokajíček²

¹ Frank Laboratory of Neutron Physics, Joint Institute for Nuclear Research, 141980 Dubna, Russia

² Institute of Geology, Academy of Sciences of the Czech Republic, 165 00 Prague 6, Czech Republic

Elastic anisotropy is an important property of Earth's crustal and upper mantle rocks. This study investigates the contribution of structural fabrics (layering, shape preferred orientations (SPO) and mineral lattice preferred orientations (LPO) to the bulk elastic properties of a strongly anisotropic plagioclase-biotite gneiss, using neutron diffraction texture analysis and ultrasonic measurements. Mineral LPOs measurements were done by the time-of-flight (TOF) texture diffractometer SKAT in Dubna, Russia. The spatial distributions of P -wave ray velocities were obtained on a spherical sample at different hydrostatic pressures up to 400 MPa. The inversion procedure was then applied to recalculate specific elastic moduli and phase velocities of P -waves. The nonlinear approximation of velocity-pressure relationship

$$\rho V^2(P) = \rho_0 V_0^2 + B \cdot P - D \exp(-k \cdot P)$$

was used to estimate the influence of flat cracks at low pressures (by D value distribution) and mineral skeleton properties ($\rho_0 V_0^2 + B \cdot P$) at high pressures on the elastic anisotropy of bulk rock sample. Modeling of the effective properties of gneiss was based on the texture data and included different averaging procedures (Voigt, Reuss, Geomean, Geomixself, Backus). A major contribution to the bulk anisotropy is from biotite and muscovite CPOs. Moreover, intercrystalline and intracrystalline cracks are closely linked to the morphologic sheet plane (001) of the biotite and muscovite minerals, leading to very high anisotropy of bulk sample at low pressures. Above about 150 MPa the effect of cracks is almost eliminated, due to progressive closure of flat microcracks. Comparison of the LPO-based calculated anisotropy with the intrinsic anisotropy obtained by the nonlinear approximation (at 0.1 MPa) gives hints for a major contribution of micas LPO rather than SPO to the overall elastic properties of the rock sample.

TEXTURE INVESTIGATION THROUGH THICKNESS OF ROLLED HIGH-STRENGTH STEEL BY NEUTRON DIFFRACTION

A.A. Zisman¹, T.A. Lychagina², D.I. Nikolayev², N.F. Drozdova¹, S.N. Panpurin³

¹Central Research Institute of Structural Materials "Prometey", St.Petersburg, Russia

²Joint Institute for Nuclear Research, Dubna, Russia

³St.-Petersburg State Polytechnic University, St.Petersburg, Russia

E-mail crism_ru@yahoo.co.uk

Structure of hot rolled steels commonly has a macroscopic non-uniformity that appears first in crystallization and then evolves because of temperature and strain inhomogeneity across the billet thickness. The strain inhomogeneity, in turn, results in a corresponding deformation texture of high-temperature γ -phase (austenite). Although the latter texture is eventually replaced by the texture of low-temperature α -phase (bainite) because of the phase transformation in quenching, a characteristic non-uniformity of structure and properties is retained due to the pronounced "crystallographic memory" peculiar to bainitic and martensitic steels. However, to study *macroscopic* non-uniformity with the conventional XRD or other local techniques is hardly possible because of extremely small thickness of diffracting layers. Meanwhile, owing to very high penetration ability of neutrons, the neutron diffraction from *macroscopic* samples is easily recorded thus allowing one to tell between different parts of the processed steel through its thickness.

In this work the crystallographic texture for a set of steel samples cut from the primary steel slab (crystallized semi-product) has been measured by neutron diffraction. These samples correspond to different parts through the slab thickness. Besides, two rolled sheets underwent different deformation degree by rolling have been investigated. The texture measurements were carried out by neutron diffraction using time-of-flight technique at SKAT diffractometer situated at IBR-2 reactor (Dubna, Russia). The high SKAT resolution allows to have non-overlapped diffraction peaks for α -Fe phase of the steel. The three complete pole figures (110), (200), (211) of α -Fe in $5^\circ \times 5^\circ$ grid have been extracted from a set of 1368 spectra measured for each sample. It was used the local peak fit procedure for the pole figures extraction.

It was concluded that both the crystallization texture and, accordingly, its inhomogeneity is weak. At the same time, the rolling texture is distinct and sharpens with deformation degree; besides it is accompanied by the grain refinement. The transformation texture of rolled sheets can be described by two components

$$\{112\} \langle 1\bar{1}0 \rangle \quad (\alpha = 90^\circ, \beta = 35.26^\circ, \gamma = 45^\circ)$$

and

$$\{111\} \langle 11\bar{2} \rangle \quad (\alpha = 0^\circ, \beta = 54.74^\circ, \gamma = 45^\circ)$$

S O F T M A T T E R

EFFECTS OF NORMAL ALKANES ON BILAYER THICKNESS IN DIOLEOYLPHOSPHATIDYLCHOLINE LIPOSOMES

P. Balgavý¹, A Islamov²; D. Uhríková¹; N. Kučerka^{1,2}

¹Faculty of Pharmacy, Comenius University, 832 32 Bratislava, Slovakia

²Frank Laboratory of Neutron Physics, JINR, 141980 Dubna, Moscow Region, Russia

It is known that the composition and the thickness of the lipid bilayer play an important role in controlling the function of membrane proteins. It is therefore important to fully understand the factors that affect bilayer thickness. In particular, for experiments that use artificial bilayers to understand membrane protein function, a precise characterization of bilayer thickness is vital. Artificial bilayer black lipid membranes (BLMs) formed on a small hole (0.8–2.5 mm) in a Teflon cup immersed in larger glass compartment filled by electrolyte have been used extensively to characterize bilayer thickness. From the BLM capacitance, its thickness is calculated supposing that BLM is a parallel plate capacitor with a hydrophobic interior with the relative dielectric permittivity $\epsilon \approx 2.1$. Using this approach, it has been found in case of normal alkanes (C_n, n is number of carbons) as admixtures in BLMs prepared from DOPC (dioleoylphosphatidylcholine) that the thickness decreases with increasing the length n of the alkane C_n [1-3]. We have found just the opposite using small-angle neutron scattering on bilayers in unilamellar DOPC vesicles (ULVs).

ULVs were prepared from DOPC and C_n using the cholate (CH) dilution technique. Weighed DOPC, C_n and CH amounts were mixed in needed molar ratios in the CHCl₃+CH₃OH solvent. After solvent evaporation in a vacuum, mixed DOPC+C_n+CH micelles were prepared by adding an appropriate amount of D₂O. The mixed micelles were transferred to small dialysis packs and CH was removed from micelles by placing packs in a rigorously stirred large volume of D₂O at room temperature. SANS measurements were performed on the YuMO spectrometer with ULVs thus prepared. The scattering curves were evaluated using the model of hollow polydisperse spheres with the bilayer having the homogeneous neutron scattering length density. At the molar ratio C_n:DOPC=0.4 and at 25°C, the bilayer thickness d, the ULVs mean radius R and the half-width σ of Gaussian distribution of ULVs obtained from fitting of SANS curves are following:

ULVs	d [nm]	R [nm]	σ [nm]
DOPC	3.19	28.3	5.4
DOPC+C6	3.24	29.2	5.7
DOPC+C8	3.22	17.4	4.0
DOPC+C10	3.38	12.5	3.8
DOPC+C12	3.53	12.0	3.2
DOPC+C14	3.60	12.3	3.1
DOPC+C16	3.59	13.6	3.4

This work was supported by the VEGA grant 1/1224/12 and by the JINR 04-4-1121-2015 project.

[1] R. Benz, K. Janko: Biochim. Biophys. Acta 455 (1976) 721

[2] T. Hianik: Acta Physica Slovaca 56 (2006) 687

[3] L.C.M. Gross, A.J. Heron, S.C. Baca, M.I. Wallace: Langmuir 27 (2011) 14335

STUDY OF VISUAL PIGMENT RHODOPSIN SUPRAMOLECULAR ORGANIZATION IN PHOTORECEPTOR MEMBRANE BY SMALL ANGLE NEUTRON SCATTERING METHOD WITH CONTRAST VARIATION

T.B. Feldman^{1,2,3}, A.I. Ivankov^{4,5,6}, T.N. Murugova^{4,5}, A.I. Kuklin^{4,5}, P.V. Shelyakin², M.A. Yakovleva², V.I. Gordeliy^{5,7,8}, A.V. Belushkin⁴, M.A. Ostrovsky^{1,2,3}

¹ *Department of Molecular Physiology, Biological Faculty Lomonosov Moscow State University, Leninskie Gory1, Moscow, 119991, Russia*

² *Emanuel Institute of Biochemical Physics Russian Academy of Sciences Kosygin st.4, Moscow, 119334, Russia*

³ *Laboratory of Radiation Biology, Joint Institute for Nuclear Research, Dubna, Russia*

⁴ *Frank Laboratory of Neutron Physics, Joint Institute for Nuclear Research, Dubna, Russia*

⁵ *Moscow Institute of Physics and Technology, Institutsky per. 9, Dolgoprudny, Moscow Region, 141700, Russia*

⁶ *Taras Shevchenko National University of Kyiv, Kiev, Ukraine*

⁷ *Institut de Biologie Structurale, Grenoble, France*

⁸ *Research Center Juelich, Juelich, Germany*

The visual pigment rhodopsin is a prototypical member of a large G-protein-coupled receptor (GPCR) family, which plays a key role in all regulatory processes of living organisms [1]. Like many other membrane receptors, GPCRs are known to form dimers and high-order oligomers in membranes. However, the supramolecular organization of rhodopsin in photoreceptor membranes is discussed. Atomic force microscopy images of the native rod outer segment disk membranes showing the rows of rhodopsin dimers provide a striking demonstration of their possible supramolecular organization [2]. At the same time there are a number of works, which present the evidence of a rhodopsin monomeric state in the photoreceptor membranes [3, 4].

We have investigated the rhodopsin supramolecular organization in the photoreceptor membranes in the solution by small angle neutron scattering method (SANS). SANS experiments were performed with the various parts of heavy water in the solution (contrast variation method) to obtain the information about the lipid and the protein components separately (Fig 1). It was shown that the packing density of the rhodopsin molecules in the photoreceptor membrane is unusually high. The distance between the centers of the molecules is approximately 56 Å. The probability of the monomeric state of rhodopsin molecules in the photoreceptor membrane, according to our data, is rather high.

Ivankov O.I., Murugova T.N., Kuklin A.I. and Gordeliy V.I. are greatly acknowledging the “5Top100” program.

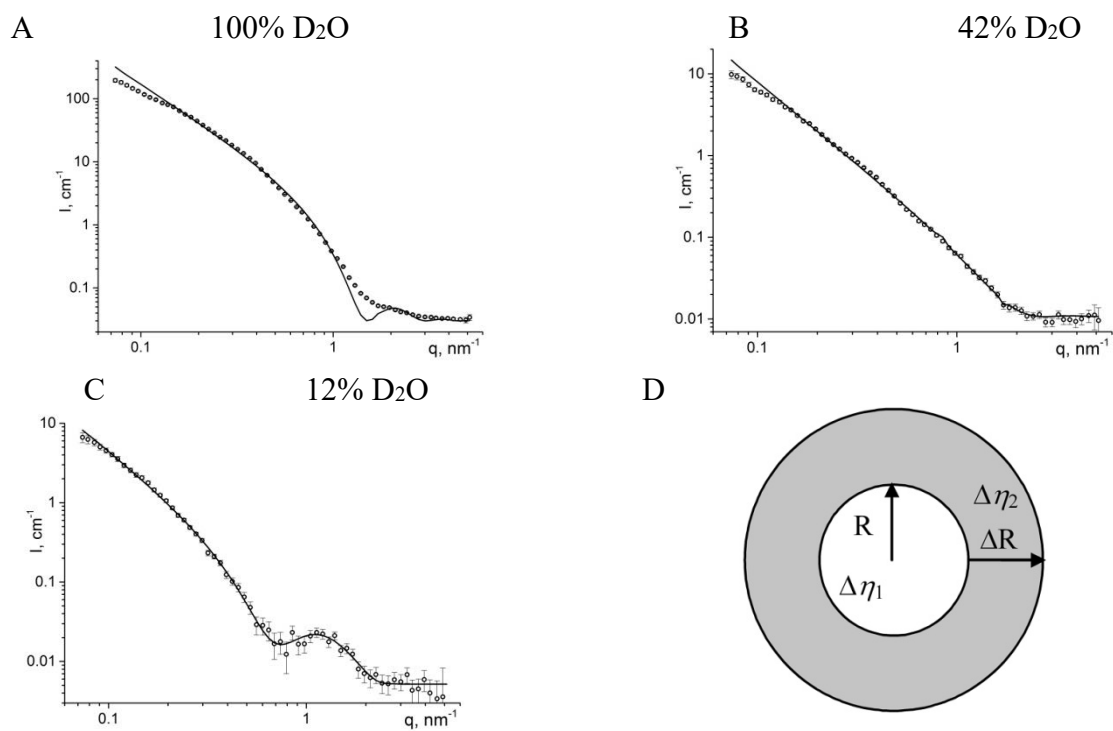


Fig 1. Small-angle neutron scattering curves for the photoreceptor membranes suspension with the various parts of heavy water in the solution: A – 100% D_2O , B – 42% D_2O , C – 12% D_2O . D – a spherical shell model for the photoreceptor membranes in a buffer solution. Each curve is approximated by a spherical shell model (solid line).

- [1] Mirzadegan, T., et al. *Biochemistry*, 2003. **42**(10): p. 2759-2767.
- [2] Fotiadis, D., et al. *Nature*, 2003. **421**(6919): p. 127-128.
- [3] Edrington, T.C.t., et al. *Biophysical Journal*, 2008. **95**(6): p. 2859-2866.
- [4] Yasuda, S., et al. *Biochem. Biophys. Res. Com.*, 2012. **425**(2): p. 134-137.
- [5] Kuklin, A.I., et al. *Neutron News*, 2005. **16**: p. 16-18.
- [6] Kuklin, A.I., et al. *Surface*, 2006. **6**: p. 73-84.

ФРАКТАЛЬНАЯ ОРГАНИЗАЦИЯ ХРОМАТИНА ЯДЕР ЭУКАРИОТ ПО ДАННЫМ МУРН: ОБЩИЕ ПРИНЦИПЫ

Д.В. Лебедев¹, М.М. Филатов¹, А.Ю. Конев¹, Р.А. Пантина¹, Н.В. Белякова¹,
Е.Ю. Варфоломеева¹, В. Пипич³, А.В. Онуфриев², В.В. Исаев-Иванов¹

¹ФГБУ «Петербургский институт ядерной физики им. Б.П. Константинова» НИЦ «Курчатовский институт», 188300, Орлова роща, Гатчина, Россия

²Departments of Computer Science and Physics, Virginia Tech 2050 Torgersen Hall (0106), Blacksburg, Virginia 24061, USA

³Juelich Centre for Neutron Science, Outstation at FRM II, Lichtenbergstraße 1, Garching 85747, Germany

Одна из моделей упаковки ДНК в хроматине интерфазных ядер клеток высших, которая дискутируется в последние годы, предполагает фрактальную организацию наднуклеосомной структуры двойной спирали. Применение методов конфокальной микроскопии, малоуглового нейтронного рассеяния и техники Hi-C, позволяет сделать предположение о том, что фрактальная организация хроматина имеет, по крайней мере, два режима упаковки, которые отличаются размерностью.

В этой работе приведены экспериментальные данные полученные методом МУРН на клеточных ядрах эритроцитов кур (Hen), которые находятся в фазе G₀ клеточного цикла, ядрах клеток лимфоцитов крыс (RatL), карциномы шейки матки человека (HeLa), глиомы крысы (RatC6) и эмбрионов дрозофилы (DE), которые находятся в фазе G₁ клеточного цикла. Во всех исследованных ядрах после их выделения хроматин был фиксирован глутаровым альдегидом.

Представляемые экспериментальные данные, полученные на различных установках МУРН (IBR-2 Дубна, Россия; D11 Гренобль, Франция; KWS2 и KWS3 Мюнхен, Германия) есть результат многолетних измерений. Максимальный диапазон рассеянных векторов, в котором получены кривые рассеяния, составил $Q = 0.00029 - 0.25 \text{ \AA}^{-1}$, что соответствует диапазону линейных размеров рассеивателя $l = 2.5 \text{ нм} - 2.17 \text{ мкм}$ и перекрывает практически всю иерархию структур хромосом хроматина. Измерения кривых рассеяния проводилось при двух значениях содержания D₂O в H₂O - 99% и 40%. Кривые рассеяния, полученные при 40% D₂O, характеризуют структуру нуклеиновой компоненты хроматина (DNA+RNA).

Для всех исследуемых ядер форма этих кривых имеет общую качественную черту: кривые, в координатах log-log, имеют два линейных участка и точку их кроссовера. Такую форму кривой рассеяния в методе МУРН имеют фрактальные структуры.

Количественно анализ кривых показал, что наклоны линейных участков кривых рассеяния справа от точки кроссовера (большие углы) близки по своим значениям для ядер Hen, RatL, HeLa и RatC6 и среднее значение этой величины составляет $D_m = 2.4 \pm 0.1$ и $D_m = 2.25 \pm 0.1$ при регистрации в 99% и 40% D₂O соответственно. Слева от точки кроссовера (малые углы) наклоны кривых рассеяния ядер Hen, RatL, HeLa, RatC6 и DE составили величины > 3 , что соответствует структурам поверхностного фрактала. При этом значения величины размерности составляют $D_s = 2.5 \pm 0.3$ и $D_s = 2.3 \pm 0.3$ в 99% и 40% D₂O соответственно

Точки кроссовера линейных участков:

$Q_{\text{HeH}}=0.0022\text{\AA}^{-1}$ ($300\pm 70\text{nm}$), $Q_{\text{RatL}}=0.0025\text{\AA}^{-1}$ ($260\pm 20\text{nm}$), $Q_{\text{RatC6}}=0.0035\text{\AA}^{-1}$ ($180\pm 20\text{nm}$), $Q_{\text{HeLa}}=0.005\text{\AA}^{-1}$ ($130\pm 30\text{nm}$), и DE $Q_{\text{DE}}=0.012\text{\AA}^{-1}$ (52nm) в 40% D₂O.

Таким образом, из приведенных данных МУРН следует:

Упаковка хроматина исследованных интерфазных ядер высших независимо от фазы клеточного деления и степени пролиферативности консервативна и в наднуклеосомных порядках упаковки представляет собой фрактальную структуру, которая из масс-фрактала в более низких порядках упаковки переходит в структуру поверхностного фрактала в более высоких порядках упаковки хроматина. При этом размерности фрактальных структур по своим величинам также близки. Существенные отличия наблюдаются в величинах определяющих точку кроссовера двух фрактальных режимов. У ядер, выделенных из пролиферирующих клеток, точка кроссовера сдвинута вправо на кривой рассеяния, то есть в сторону меньших линейных размеров. Другими словами в делящихся клетках область масс-фрактальной структуры имеет меньшие линейные размеры.

REAL-TIME NEUTRON DIFFRACTION FROM LIPID MEMBRANES

T. Kondela¹, S.G. Sheverev², A.I. Beskrovnyi², N. Kučerka^{1,2}

¹ Faculty of Pharmacy, Comenius University, 832 32, Bratislava Slovakia

² Joint Institute for Nuclear Research, 141980, Dubna, Russia

E-mail: kondela@fpharm.uniba.sk

We have studied structural changes in lipid membranes as a function of hydration and isotopic exchange of D₂O for H₂O. The data were collected at the DN-2 time-of-flight diffractometer at the IBR-2 pulsed reactor (Joint Institute for Nuclear research, Dubna, Russia) utilizing 2D position sensitive detector. The combination of time-of-flight scattering mode and 2D detector allowed for a recent upgrade of this diffractometer into a real-time-diffraction (RTD) instrument. The standard measurement now covers a large range of scattering data even in short exposure times. Our experimental setup for example, provided for at least 4 simultaneously measured diffraction peaks, analysis of which resulted into lipid bilayer structural parameters. RTD measurements then allowed us to trace the evolution of lipid bilayer profiles during the hydration and dehydration processes. Additional hydration kinetics was studied utilizing the isotopic exchange of D₂O for H₂O in the case of fully hydrated multilayer membranes aligned on a silicon substrate.

Acknowledgement: This work was supported by Dubna JINR 04-4-1121-2015/2017 project.

USER POLICY

FLNP JINR USER PROGRAMME

Chudoba D.M., Gorshkova Yu.E., Zinicovskaia I.

Joint Institute for Nuclear Research, Dubna, Russia

E-mail: Scientific_Secretary@nf.jinr.ru

Since 2012, the IBR high flux pulsed reactor (Dubna, Russia) [1] renewed regular operation at nominal power for scientific research. Neutron scattering investigations at IBR-2 reactor cover an extensive field of research in condensed matter physics, materials science, chemistry, biophysical, geophysical and engineering sciences (Fig.1).

The IBR-2 reactor is operated according to the User Policy Programme[2]. Calls for proposals are issued twice a year. The proposals are peer-reviewed and rated and beam time for experiments is allocated on the basis of the reviews by Expert Committees. At present, 200 experiments per year are performed by scientists from more than 20 countries (Fig.1) at IBR-2 instruments in the framework of the User Programme.

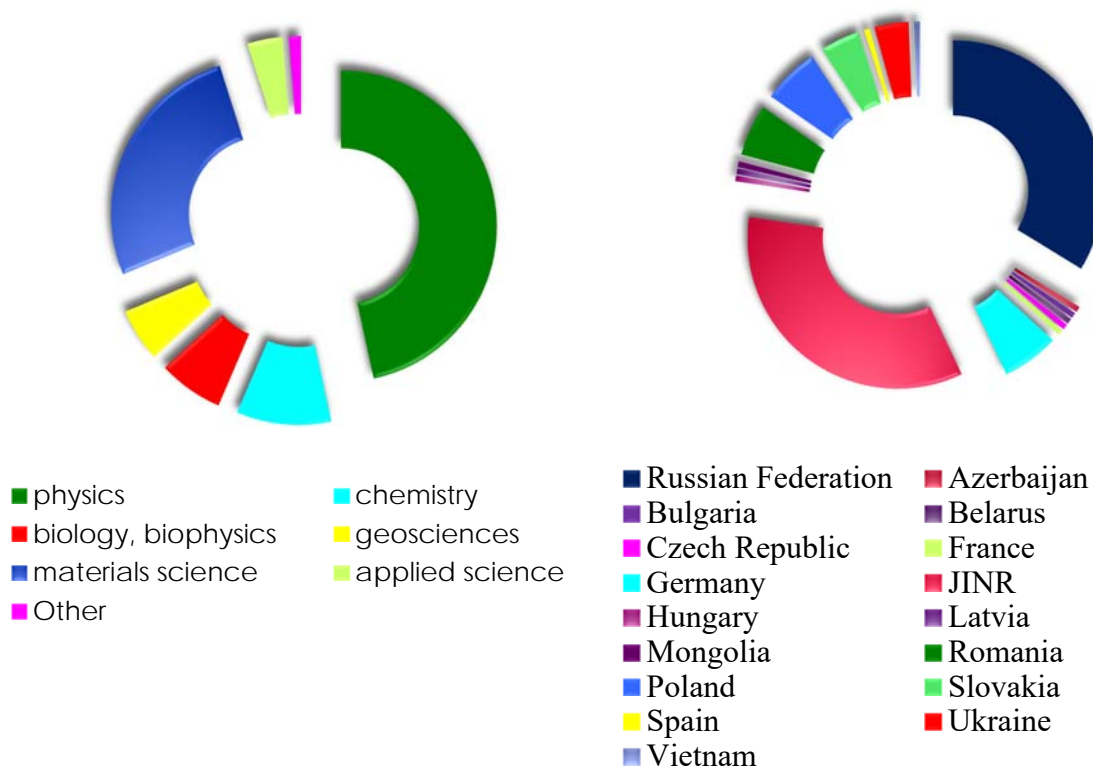


Fig.1. Proposal distribution by science (left) and by applicant's affiliation (right) in 2014. Data are adopted from IBR-2 User Club site [2].

We would like to discuss a present state and plan of development of a User Programme at Frank Laboratory of Neutron Physics, JINR.

[1] <http://flnp.jinr.ru/34/> - IBR-2 Pulsed Reactor

[2] <http://ibr-2.jinr.ru/> - IBR-2 User Club

POSTER

PRESENTATIONS

F U N C T I O N A L M A T E R I A L S

PARTICULARITIES OF NaNO_2 PHASE STATE IN THE FERROELECTRIC COMPOSITE $0,9\text{NaNO}_2+0,1\text{BaTiO}_3$

O. Alekseeva¹, A. Naberezhnov^{1,2}, E. Stukova³, S. Borisov², V. Simkin⁴

¹ Peter the Great St.-Petersburg Polytechnic University, 195251, St.-Petersburg, Polytechnicheskaya 29, Russia

² Ioffe Institute, 194021, St.-Petersburg, Polytechnicheskaya 26, Russia

³ Amur State University, 675027, Amur region, Blagoveshchensk, Ignat`evskoe road, 21, Russia.

⁴ JINR, 141980, Dubna, Joliot-Curie 6, Moscow region, Russia

The results of studies of BaTiO_3 admixture effect on temperature range, where NaNO_2 incommensurate phase exists, in the $(1-x)\text{NaNO}_2+(x)\text{BaTiO}_3$ composite at $x=0,1$ are reported.

Previous dielectric spectroscopy measurements of $(1-x)\text{NaNO}_2+(x)\text{BaTiO}_3$ with different BaTiO_3 particles concentration and size [1] have shown that dielectric permittivity temperature dependences of these composites have two maxima. One of them is observed at 437 K corresponding to the phase transition in NaNO_2 , the other is observed at $T \approx 420$ K and its maximum value differs significantly on heating or cooling. It has been supposed that this maximum is attributed to the incommensurate-ferroelectric phase transition in NaNO_2 . Thus temperature range where NaNO_2 incommensurate phase exists significantly broadens in $(1-x)\text{NaNO}_2+(x)\text{BaTiO}_3$ composites (≈ 18 K) in comparison with the pure NaNO_2 (≈ 1 K). We have performed the temperature evolution studies of $0,9\text{NaNO}_2+0,1\text{BaTiO}_3$ composite structure by neutron diffraction using the high resolution Fourier-diffractometer in JINR(Dubna).

It has been established that the dielectric response anomaly at 420 K isn't caused by phase transition in BaTiO_3 particles. The temperature dependences of NaNO_2 order parameter in the composite and the pure NaNO_2 have been obtained. It has been found that BaTiO_3 admixture leads to decrease of the order parameter in the composite in comparison with pure NaNO_2 in the temperature range of $\approx 360-433$ K. This fact permits us to suppose that the incommensurate and ferroelectric phases coexist in this temperature range. From the obtained order parameter temperature dependences the fraction of incommensurate phase has been evaluated at different temperatures. The dielectric anomaly at $T=420$ K has been revealed to relate with the maximal fraction of the NaNO_2 incommensurate phase in the composite $0,9\text{NaNO}_2+0,1\text{BaTiO}_3$.

[1] Stukova E.V., Koroleva E.Yu., Truchan T.A., Baryshnikov S.V. Changing of incommensurate phase existence region in ferroelectric composite $(1-x)\text{NaNO}_2+(x)\text{BaTiO}_3$. St. Petersburg State Polytechnical University Journal. Physics and Mathematics. Issue 2(146), 2012, p.23

NANOSTRUCTURED MANGANITES: NEUTRON DIFFRACTION STUDIES AT HIGH PRESSURE AND LOW TEMPERATURE

N.M. Belozerova¹, S.E. Kichanov¹, E.V. Lukin¹, D.P. Kozlenko¹, Z. Jirak², B.N. Savenko¹

¹*Frank Laboratory of Neutron Physics, Joint Institute for Nuclear Research, 141980 Dubna, Moscow Region, Russia*

²*Institute of Physics, AS CR, Cukrovarnická 10, 162 00 Praha 6, Czech Republic*

E-mail: NMBelozerova@mail.ru

Apart from potential application, the complex manganites are attractive for great number of scientific research. The knowledge of relationship between magnetic and crystal structure of nanostructured manganites $\text{La}_{1-x}\text{Sr}_x\text{MnO}_3$, which can be obtained from high-pressure investigations, is very essential for understanding the nature and mechanism of physical phenomena observed in these nanostructured compounds.

Also recently it has been discovered that nanostructured manganites $\text{La}_{1-x}\text{Sr}_x\text{MnO}_3$ (near $x \sim 0.33$) have a rhombohedral structure both in the corresponding bulk samples. However, the magnetic state of these compounds, in contrast to powder samples that exhibit ferromagnetic metallic state, characterized by coexistence of ferromagnetic (FM) and antiferromagnetic (AFM) phase A-type.

The crystal and magnetic structure of nanostructured manganites $\text{La}_{1-x}\text{Sr}_x\text{MnO}_3$ with doping level $x = 0,28$ и $0,37$ has been studied by means of a neutron diffraction method on diffractometer DN-6 of IBR-2 high-flux pulsed reactor (Frank Laboratory of Neutron Physics, JINR, Dubna) using high pressure chambers with sapphire anvils under pressure up to 5,7 GPa.

In both samples the FM ordering is formed close the room temperature and at cooling below $T < 270$ K the ferromagnetic FM phase coexists with an A-type antiferromagnetic AFM phase. At high pressures the volume fraction of AFM phase increases while FM is gradually suppressed. The structural aspects of the magnetic phase separation and pressure effects on the studied nanostructured manganites are discussed.

Pressure dependences of unit cell parameters and volume, magnetic moments of ferromagnetic (FM) phase and antiferromagnetic (AFM) phase, Curie and Neel temperature were calculated.

The work was supported by the RFBR grant No. 15-32-20358-mol-a-ved.

INFLUENCE OF CHEMICAL COMPOSITIONS AND THERMAL TREATMENTS ON THE STRUCTURE AND MECHANICAL PROPERTIES OF ZIRCONIA BASED THERMAL COATINGS

M. L. Craus^{1,2}, V. Turchenko², A. Savin¹, A. Doroshkevith¹

¹ *National Institute for Research and Development for Technical Physics, Iasi, Romania*

² *Joint Institute for Nuclear Research, Dubna, Russia*

E-mail: mihailiviu@yahoo.com

Present day TBCs generally consist of a yttria-stabilized zirconia (YSZ) coating deposited onto an oxidation-resistant bond-coat alloy that is first applied to a nickel-based superalloy component. In diesel engine applications where the temperatures are usually lower, the YSZ coating is generally applied directly onto the alloy. Two main types of coating are in use. For relatively small components such as blades and vanes in aerospace turbines, the coatings can be applied by electron-beam physical vapour deposition (EB-PVD). For larger components such as the combustion chambers and the blades and vanes of power generation, stationary turbines, the coatings are usually applied by plasma-spraying (PS). In many respects, the choice of materials and their production represent a mature materials technology. While improvements in their capabilities continue, there is a growing realization that new TBC systems will be required for the next generation turbines presently being designed.

The hydrothermal synthesis of doped ZrO₂ powders was conducted starting from ZrOCl₂·8H₂O (0.5M) aqueous solutions. Yttrium was added as nitrate salt in order to prepare the doped samples. Both solutions were neutralized with NaOH. The suspensions were then treated in a Teflon-lined vessel at a maximum pressure of 25 atm, at 300°C. The reaction vessel was connected to a pressure transducer that monitors and controls the pressure during synthesis. Our aim is to obtain better mechanical properties of the coatings using various chemical compositions and thermal treatments.

Specimens were manufactured from 316 stainless steel. Conventional NiFe + ZrO₂-8 wt.%Y₂O₃ thermal barrier coatings were deposited by atmospheric spraying at Frank Laboratory for Neutron Physics, JINR, Dubna, Russia. Before spraying, all specimens were processed with sandpaper. This operation, which is employed to achieve a better mechanical interlocking with the bond coat, induced a compressive residual stresses in the substrate and caused a surface roughening. The average thickness of the bond coat and the top coat was approximately 210 μm and 190 μm respectively, with the local thickness varying on the order of tens microns. Several of coated specimens were isothermally oxidized in air at 1050 °C for 200 h in a furnace and cooled to ambient air temperature after the removal from the furnace. The microstructure was observed using an optical microscope EQ-MM500T-USB. The substrate was typical of a cast nickel-base stainless steel. We used intermediate thermal treatments to decrease the concentrations of defects. A partial oxidation of metallic NiFe powder takes place due to thermal treatment, accompanied by a change in the concentration of defects and phase composition. The structural modification of the TBC with thermal treatment was investigated by x-ray diffraction. The microhardness values were obtained using a PMT II microhardness tester. It is proposed the use of an electromagnetic method for evaluation of zirconia doped with yttria coating on some stainless steels using a new sensor and comparison of the results with those obtained by complementary methods. The electrical conductivity of ZrO₂ layer

structure with and without stabilizers deposited on austenitic steels (AISI 316L) is significant decreasing at the appearance of the fatigue phenomenon, in the stage of pre-cracking. After this stage, when fatigue cracks appear, the electrical resistance of structure increase due their presence.

Summary

We investigated the structural modification of the TBC induced by thermal treatment, using X-ray diffraction and measuring some mechanical properties of the samples (microhardness). An electromagnetic method for evaluation of zirconia doped with yttria coating on some stainless steels was applied using a new sensor. It was observed a decrease of the electrical conductivity of ZrO₂ layer structure at the appearance of the fatigue phenomenon.

NANOCRYSTALLINE STABILIZED ZIRCONIA

A. Savin¹, M. L. Craus^{1,2}, V. Turchenko², A. Bruma³, T. Konstantinova⁴

¹ *National Institute for Research and Development for Technical Physics, Iasi, Romania*

² *Joint Institute for Nuclear Research*

³ *University of Texas at San Antonio, One UTSA Circle, San Antonio, Texas, 78249, USA*

⁴ *Donetsk Institute of Physics and Technology named after O.O.Galkin, Donetsk, Ukraine*

E-mail: mihailiviu@yahoo.com

Recent developments in advanced dental materials, solid-oxide fuel-cell design to oxygen detection, nuclear waste confinement, optics, medical prosthesis, and catalytic technologies have drawn attention towards the remarkable structural properties of zirconia (ZrO₂) - based ceramics. In all the current technological applications, ZrO₂-based ceramics are preferred due to their advanced mechanical properties such as high-fracture toughness and bulk modulus, corrosion resistance, chemical inertness, low chemical conductivity and biocompatibility. It is well known that three polymorphic forms of pure ZrO₂ can be found: the monoclinic state, P21/c, stable at temperatures below 11700C, the tetragonal phase, P42/nmc stable in the temperature range between 1170-23700C and the cubic, Fm-3m phase, appearing at a temperature above 23700C. The remarkable mechanical properties of these ceramics, already exploited in a variety of applications are mainly due to the tetragonal (t) monoclinic (m) phase transition which takes place at normal temperatures and can be induced by external stress, such as grinding, cooling or impact. The main method used for the stabilization of the ZrO₂ tetragonal phase is the introduction of stabilization components in the zirconia lattice, such as Mg, Ce, Fe, Y, etc. At nanoscale level, the metastable phase formation in ZrO₂ can be induced by including in the oxide structure some vacancy defects.¹¹ Although, the stabilization effect of the oxygen vacancies in tetragonal ZrO₂ is not yet well understood, the concentration of oxygen vacancies in the lattice required to stabilize the tetragonal phase is found in phases like ZrO_{1.97} and ZrO_{1.98} for tetragonal zirconia doped by rare-earth elements, mainly Cerium (Ce) and Yttrium (Y).

We explored the influence of phase stability of ZrO₂ ceramics following the doping with Ce. The structure of these ceramics and the phase stabilization were investigated by using X-ray and

neutron diffraction, scanning electron microscopy (SEM), as well as microstructure characterization methods using micro-hardness measurements. Moreover, we employed Resonant Ultrasound Spectroscopy (RUS) as a non-destructive evaluation method in order to estimate the presence of low-density regions, state of sintering and the presence and development of small cracks in the structure, by evaluating the complete elasticity matrix. We put in evidence the properties of zirconium-based ceramics for applications in the biomedical field, such as ceramic femoral heads used in hip implant procedures, which are very resistant to scratches resulting from debris caused by accumulation of bone parts, cement or metal that occasionally fall between artificial joint surfaces, but are extremely fragile.

Summary

The substitution of the Zr with Ce in $Zr_{1-x}Ce_xO_2$ leads to a change of the phase composition, a transition from the monoclinic to tetragonal structure. The sample corresponding to $x=0.09$ contains two phases, a monoclinic phase and a tetragonal phase, while the samples with larger Ce concentration contain only a tetragonal phase. The unit cell volume of the tetragonal phase increases with the increase of Ce concentration, for the inner part of the samples. An unknown phase appears at the surface of the samples in connection with a change of chemical composition of the tetragonal phase. A maximum of the average size of coherent blocks and of the microstrain appear for tetragonal phase at $x=0.13$. From the variation of unit cell volume of surface layer we conclude that a decrease of the Ce concentration takes place with the increase of the nominal Ce concentration in the samples.

The resonant ultrasound spectroscopy can be used for quality control of certain ceramic elements of hip prosthesis, such as femoral heads. If the element are incorrectly sinterized, with a density smaller than the prescribed value and the elastic and shear moduli smaller, important modifications appears in the shape of the spectrum and the resonance frequencies.

INFLUENCE OF FE DOPING ON STRUCTURAL AND ELECTRIC PROPERTIES OF MULTIFERROICS $\text{BaTi}_{1-x}\text{Fe}_x\text{O}_3$

Dang N. T.¹, Kozlenko D. P.², Kichanov S. E.², Dang N. V.³, Phan The-Long⁴, Khiem L. H.⁵, Jabarov S. G.^{6,7}, Savenko B. N.²

¹ *Institute of Research and Development, Duy Tan University, 550000 Da Nang, Viet Nam*

² *Frank Laboratory of Neutron Physics, Joint Institute for Nuclear Research, 141980 Dubna, Russia*

³ *Faculty of Physics, College of Science, Thai Nguyen University, 250000 Thai Nguyen, Vietnam*

⁴ *Department of Physics, Chungbuk National University, 361-763 Cheongju, Korea*

⁵ *Advanced Center for Physics, Institute of Physics, Vietnam Academy of Science and Technology, 18 Hoang Quoc Viet, 100000 Hanoi, Viet Nam*

⁶ *Institute of Physics, ANAS, AZ-1143, Baku, Azerbaijan*

⁷ *Bayerisches Geoinstitut, Universitet Bayreuth, D-95440, Bayreuth, Germany*

Among known ferroelectric materials, BaTiO_3 , which has the paraelectric-ferroelectric transition at about 393 K with a very large electric polarization, is the most widely used ferroelectric material. The doping of magnetic transition-metal ions into a ferroelectric material can carry out the fabrication of multiferroic materials. Here, the structural and electrical properties of $\text{BaTi}_{1-x}\text{Fe}_x\text{O}_3$ have been reported.

Polycrystalline $\text{BaTi}_{1-x}\text{Fe}_x\text{O}_3$ ceramics with x values varied in a range of $x = 0 - 0.12$ were synthesized by conventional solid-state reaction. The crystal structures of these samples have been studied by mean of a neutron diffraction. In iron concentration range of $x \leq 0.01$ the compounds has a tetragonal structure with space group $P4mm$, where the ferroelectric state is exist. With further increase of the Fe content the appearance of the new non-polar hexagonal $P6_3/mmc$ phase was observed and above doping level $x \sim 0.07$ the pure hexagonal phase was exist. The dependence of the electric polarization P_s of the tetragonal phase in Fe-doping level was established. In addition, the tetragonal - cubic phase transition have been observed at temperature $T_C = 390$ K in the $\text{BaTi}_{0.9}\text{Fe}_{0.1}\text{O}_3$ sample.

The work has been supported by the RFBR grant № 15-52-54008_viet_a and the Vietnam National Foundation for Science and Technology Development (NAFOSTED) under grant number 103.02-2014.11. This work has been jointly supported by Vietnam Academy of Science and Technology and Russian Academy under project VAST.HTQT.NGA.01/15-16.

CHEMO-VOLTAIC EFFECT IN THE ZrO₂ - NANOPOWDER SYSTEMS

A.S. Doroshkevich^{1,2}, A.I. Lyubchik³, A.V. Shylo², T.Yu. Zelenyak², L.A. Ahkozov²,
T.E. Konstantinova², A.M. Tkachenko², V.A. Turchenko², V.S. Doroshkevich⁴

¹*Joint Institute for Nuclear Research, str. Joliot-Curie, 6, 141980, Dubna, Russia*

²*Donetsk Institute of Physical and engineering NASU Nauki ave, 46, Kiev, Ukraine*

³*Universidade Nova de Lisboa, Portugal, 2829-516 Caparica Ext.: 12201/3/4/5*

⁴*Donetsk National University, str. Schorsa, 17a, Donetsk 83000, Ukraine*

E-mail: doroh.jinr@mail.ru

According to European Renewable Energy Council RE -thinking 2050 report renewable energy should cover 20% of European energy needs in 2020 and 100% in 2050. To achieve this goal development of new efficient alternative energy sources is of key importance.

It was found that exothermic chemical reaction on the semiconductor structure surface lead to the excitons generation. This effect is similar to the photovoltaic mechanism of charge carriers generation was named “chemovoltaic” [1]. However, established effect not found practical application due to the the small yield of free charge carriers.

The goal of this work - to increase the effectiveness of chemovoltaic convertor using as a heterojunction a three-dimensional structure with high chemical surface activity.

Atmospheric humidity was used as the adsorbate whereas the wide band gap ZrO₂ – based dielectric nanoparticle as the adsorbent, and carbon electrodes - as the charge carrier’s collector. The test device with specific surface area of heterojunction $S_{BET} = 128 \text{ m}^2/\text{g}$ at the electrical load of 1 MOhm was produced over 20mkW/m² power density at relative humidity of 90%. According to the results of impedance spectroscopy, voltammetry and thermogravimetry empirical model of observed chemovoltaic effect was developed.

Acknowledgement. This work was supported by project Marie Skłodowska-Curie Actions «HORIZON-2020» Research and Innovation Staff Exchange (Call: H2020-MSCA-RISE-2015).

The results, are shows higher efficiency of used system comparing to known analogues and indirectly demonstrate the possibility of a new renewable energy source creation.

[1]. V.V. Styrov, A.Y. Kabanskii Yu.I. Tyurin // Soviet Technical Physics Letters. 1979, 5, P.343.

STRUCTURAL, MAGNETIC AND VIBRATIONAL PROPERTIES OF MULTIFERROIC GaFeO₃ AT HIGH PRESSURE

N.O. Golosova¹, D.P. Kozlenko¹, S.E. Kichanov¹, E.V. Lukin¹, B.N. Savenko¹, S.G. Jabarov², R.Z. Mehdiyeva², A.I. Mammadov²

¹*Frank Laboratory of Neutron Physics, JINR, 141980 Dubna, Russia*

²*Institute of Physics, ANAS, AZ-1143, Baku, Azerbaijan*

The structural, magnetic and vibrational properties of multiferroic material GaFeO₃ (space group Pc21n) have been studied by means of x-ray (at ambient temperature and pressure up to 30.5 GPa), neutron (at temperature range 10-290 K and pressure up to 6.2 GPa) diffraction and Raman (at ambient temperature and pressure up to 41.8 GPa) spectroscopy.

Pressure dependences of the structural parameters were obtained. The compressibility of GaFeO₃ was found to be anisotropic. The bulk modulus $B_0 = -V(dP/dV)_T$ of GaFeO₃ was 202.8(2.5) GPa. Antisite disorder between Ga₂ and Fe₂ positions was found and as a consequence the magnetic ground state was characterized by the ferrimagnetic arrangement of the magnetic moment of Fe ions. Upon compression up to 6.2 GPa the Néel temperature increased with a pressure coefficient $(1/T_N)dT_N/dP = 0.011(1)$ GPa⁻¹. It indicates the stability of the ground ferrimagnetic state under pressure.

At $P \sim 21.3$ GPa a new structure of orthorhombic perovskite (space group Pbnm) was formed, which accompanied by the volume drop of -7.0%. The complete formation of the Pbnm - phase occurs at 41.8 GPa. It can be assumed from the dramatical changes of the Raman spectrum. Pressure dependences of the observed Raman modes were found. The hardening of phonons was found as pressure increased. It corresponds to strengthening of the spin-phonon coupling upon compression. Pressure dependencies of peak widths for selected Raman modes showed abrupt broadening at $P = 21$ GPa. The coefficients of broadening jumps were close to 2. Such effect may correspond to a new equilibrium position of the GaO₄-tetrahedra or FeO₆-octahedra in GaFeO₃ at pressure of the structural phase transformation.

The work has been supported by RFBR grant 15-02-03248-a.

THE PRESSURE AND TEMPERATURE INDUCED POLYMORPHIC TRANSFORMATIONS IN FLUCONAZOLE

E. Gorkovenko^{1,2}, S. Kichanov², D. Kozlenko², J. Wąsicki³, E. Lukin², B. Savenko²

¹ *Lomonosov Moscow State University, Moscow, Russia*

² *Joint Institute for Nuclear Research, Dubna, Russia*

³ *Faculty of Physics, A.Mickiewicz University, Poznań, Poland*

E-mail: nireta2009@yandex.ru

Reproducible behavior of drug formulations may depend critically on the precise solid form of the drug employed, and the isolation and thorough characterization of the various forms (polymorphs, solvates, complexes) of a given drug are recognized as essential practice in the pharmaceutical industry. The present study relates to the polymorphism of the fluconazole C₁₃H₁₂F₂N₆O.

The crystal structure and vibrational spectra of the fluconazole have been studied by means of X-ray diffraction and Raman spectroscopy at pressures up to 2.5 and 5.5 GPa and in the temperature range from 27 to 150C and 27C, respectively. At a pressure of 0.8 GPa the polymorphic phase transitions between the initial Form I to a new triclinic Form VIII have been observed. At higher pressure P=3.2 GPa the sequence transformation into another polymorphic Form IX have been observed. The lattice parameters, unit cell volumes and vibration modes as functions of pressure have been obtained for the different Forms of the fluconazole. At a pressure of 0.8 GPa the polymorphic phase transitions between the initial Form I to a new triclinic Form VIII have been observed. At higher pressure P=3.2 GPa the sequence transformation into another polymorphic Form IX have been observed. Prior to the melting of fluconazole Form I a transition into a glassy state was found, which is subsequently transformed to a stable polymorphic Form II on heating after cooling. The lattice parameters, unit cell volumes and vibration modes as functions of pressure have been obtained for the different Forms of the fluconazole.

The work has been financed by RFBR Grant N 14-02-00353-a

DEFECT FORMATION ENERGY FOR CHARGE STATES IN TlInS₂

N. Ismayilova

Institute of Physics, ANAS, AZ-1143, Baku, Azerbaijan

In this work, we aimed to examine the formation energy TlInS₂ semiconductors with supercells of 64 and 128 atoms for the various charge states for the Tl vacancy, In vacancy, S vacancy. The calculations are performed within the spin-polarized DFT [1] and the LSDA [2] on double zeta polarized (DZP) basis. Relative stability of defects are determined by their defect formation energy, which is primarily depends on the electronic structure and charge states of the defects. Kinetic properties of defects, such as the mechanism of diffusion and migration energy are strongly depends on the charge states. In addition, chemical reactions involving bond formation and dissociation can also be explained in terms of the defect formation energy, provided that the calculations should be sufficiently accurate. Systematic calculations of the defect formation energy [3-5] given by (1) :

$$E_f(q) = E_d(q) - N\mu + q(E_V + \mu_e) \quad (1)$$

where $E_d(q)$ is the total energy of defect-containing system consisting of N atoms, with atomic chemical potential μ . The reservoir of the electrons is described by their chemical potential μ_e , which is measured relative to the valence band maximum E_V . To calculate the DFE we calculated firstly the energy $E_d(q)$ using first-principles density functional theory, which is widely used for this purpose. Another important physical parameter for the calculation of the defect formation energy is the position of the valence band maximum of (VBM) E_V , which corresponds to the reference energy level for the electron chemical potential. The position of the VBM of the defect-containing supercell is different from that of the defect-free bulk supercell, and the magnitude of this difference depends on the charge state. We used suggestion - the lowest energy level to align the VBM of a defect [6]. We have studied the dependence of defect formation energies on supercell size for charged vacancy as a function of the Fermi energy in TlInS₂.

The calculated transition energy levels for V_S are $(-2/0)=1.5$ eV , $(-1/0)=1.5$ eV. Transition energy levels for V_{In} is $(-2/-1)=1.25$ eV , and for V_{Tl} is $(-2/-1)=1.5$ eV .

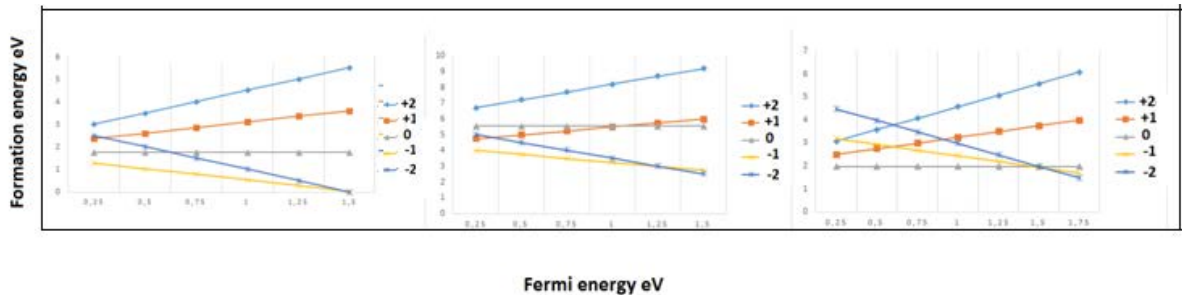


Fig.1 Dependence of DFE V_{Tl} , V_{In} , V_S on charge states as a function of the Fermi energy for TlInS₂ consisting of 63 atoms.

- [1] P. Hohenberg, W. Khon. Inhomogeneous electron gas. Phys. Rev. B 136 B864 –B871. (1964)
- [2] KarasievV., Sjoström T., Dufty J. And Trickey S. Chemical physics, (2014)
- [3] Shim J., Lee E.K., Lee Y. J., Nieminen R. M., Density-functional calculations of defect formation energies using supercell methods: Defects in diamond. Physical Rev. B 71, 0352061-12(2005).
- [4] Jakubas P., Theory of generation of Frenkel pairs in semiconductors: consequences for electric, magnetic, and structural properties. Ph.D, Dissertation, 119 (2009).
- [5] Zunger A., Zhang S.B., Wei S.H., Revisiting the defect physics in CuInSe₂ and CuGaSe₂, Proceeding of: Photovoltaic Specialists Conference, Conference Record of the Twenty-Sixth IEEE, 1-6 (1997).
- [6] M.A. Mehrabova, H.R. Nuriyev, H.S. Orujov ,and Defect formation energy for charge states and electrophysical properties of CdMnTe Vol.9450 (2015).

HIGH PRESSURE STUDY ON CRYSTAL STRUCTURE OF $\text{BaTi}_{0.99}\text{Fe}_{0.01}\text{O}_3$

S. Jabarov¹, D. Ngoc Toan², D. Kozlenko³, S. Kichanov³, N. Dang⁴, P. The-Long⁵, L. Khiem⁶, B. Savenko³, A. Mammadov¹, L. Dubrovinsky⁷

¹ *Institute of Physics, ANAS, AZ-1143, Baku, Azerbaijan*

² *Institute of Research and Development, Duy Tan University*

³ *Joint Institute for Nuclear Research, Dubna, Russia*

⁴ *Faculty of Physics, College of Science, Thai Nguyen University, 250000 Thai Nguyen, Vietnam*

⁵ *Department of Physics, Chungbuk National University, 361-763 Cheongju, Korea*

⁶ *Advanced Center for Physics, Institute of Physics, Vietnam Academy of Science and Technology*

⁷ *Bayerisches Geoinstitut, Universitet Bayreuth, D-95440, Bayreuth, Germany*

E-mail: sakin@jinr.ru

Multiferroic compounds exhibiting the coexistence of magnetic and ferroelectric orders have attracted attention due not only the fundamental importance but also the potential prospects of their practical applications [1]. However, multiferroics with a large polarization and ferromagnetism coexisting close to room temperature have not been identified so far. The doping of magnetic transition-metal ions to a ferroelectric material can carry out the fabrication of these multiferroics. Among known ferroelectric materials, BaTiO_3 , which has the ferroelectric – paraelectric transition at about 393 K with a very large electric polarization, is the most widely used ferroelectric material.

It was shown that the Fe doping into BaTiO_3 strongly affects their physical properties, including structural and magnetic. With increasing Fe doping concentration the structural transformation between the ferroelectric tetragonal $P4mm$ and the non-ferroelectric hexagonal $P63/mmc$ takes place at a threshold Fe doping level of 0.01 [2].

In this study we report the study of crystal structure of polycrystalline $\text{BaTi}_{0.99}\text{Fe}_{0.01}\text{O}_3$ under pressure up to 36 GPa by using neutron, x-ray diffraction and Raman spectroscopy. The neutron diffraction data show the evidence of the tetragonal – cubic phase transition in this compound at temperature $T_C = 390$ K, which is similar to that of undoped BaTiO_3 . Under compression the tetragonal – cubic phase transition also occurs at 18 GPa in $\text{BaTi}_{0.99}\text{Fe}_{0.01}\text{O}_3$, which is significantly higher than that of 2.3 GPa for undoped BaTiO_3 . The structural transition is accompanied by anomalies in pressure behavior of Raman modes.

The work has been supported by the Vietnam National Foundation for Science and Technology Development (NAFOSTED) under grant number 103.02-2014.11 and the RFBR grant № 15-52-54008_viet_a. This work has been jointly supported by Vietnam Academy of Science and Technology and Russian Academy under project VAST.HTQT.NGA.01/15-16.

[1] Prinz G. A. J. Magn. Magn. Mater. 200, 57-68 (1999).

[2] Dang N. V. et al. J. App. Phys. 110, 043914 (2011).

THE MAGNETIC AND STRUCTURAL MODIFICATIONS IN MULTIFERROIC YMn_2O_5 AT HIGH PRESSURE

S. Kichanov¹, D. Kozlenko¹, N. T. Dang², L. Dubrovinsky³, E. Lukin¹, H.-P. Liermann⁴, R. Mekhtieva⁵, B. Savenko¹

¹ *FLNP, Joint Institute for Nuclear Research, 141980 Dubna, Russia*

² *Institute of Research and Development, Duy Tan University, 550000 Da Nang, Viet Nam*

³ *Bayerisches Geoinstitut, Universität Bayreuth, D-95440 Bayreuth, Germany*

⁴ *Photon Sciences, Deutsches Elektronen Synchrotron, D-22607 Hamburg, Germany*

⁵ *Institute of Physics, ANAS, AZ-1143, Baku, Azerbaijan*

E-mail: ekich@nf.jinr.ru

The multiferroic materials, exhibiting simultaneously ferroelectric and magnetic orders, recently have become a subject of extensive scientific research. The RMn_2O_5 compounds are of particular interest since they demonstrate a colossal magnetoelectric effects and complex sequence of magnetic phase transformations, tuning the ferroelectric polarization features. The nature of the magnetoelectric coupling in RMn_2O_5 compounds, arising from the complex interplay of magnetic frustration, spin, lattice and orbital degrees of freedom, is still extensively debated. An important insight into the relationship between the competing factors above and their particular role in formation of magnetoelectric properties of RMn_2O_5 compounds can be given by high pressure studies.

The structural, magnetic and vibrational properties of YMn_2O_5 multiferroic have been studied by means of X-ray, neutron powder diffraction and Raman spectroscopy at pressures up to 30 GPa. Application of high pressure $P > 1$ GPa leads to a gradual suppression of the commensurate and incommensurate antiferromagnetic (AFM) phases with a propagation vector $q = (1/2, 0, q_z \sim 1/4)$ and appearance of the commensurate AFM phase with $q = (1/2, 0, 1/2)$. At $P \sim 16$ GP a structural phase transformation accompanied by anomalies in lattice compression and pressure behaviour of vibrational modes was observed. The observed pressure-induced magnetic transformations in YMn_2O_5 provides clear evidence that q_z component of the propagation vector is controlled by a balance of competing $\text{Mn}^{4+} - \text{Mn}^{4+}$ magnetic interactions in octahedral chains and $\text{Mn}^{4+} - \text{O}_2 - \text{Mn}^{3+}$ interactions linking Mn^{4+}O_6 octahedra and Mn^{3+}O_5 pyramids.

The work has been supported by the RFBR grant 15-02-03248-a.

THE EFFECT OF THERMAL ANNEALING PROCESSES ON STRUCTURAL PROPERTIES OF ZN NANOTUBES

A. Kozlovsky^{1,2}, D. Shlimas¹, K. Kadyrzhanov¹, T. Meyrimova¹; M. Zdorovets^{1,2}

¹ *L.N. Gumilyov Eurasian National*

² *Institute of Nuclear Physics*

E-mail: artem88sddt@mail.ru

In modern electronics for the development of devices and sensors, technical operations of introducing impurities into the semiconductor material are widely used. Particular attention is paid to the creation of ordered arrays of semiconductor nanostructures due to such materials have new optical [1] and electrical [2,3] properties that are important for the creating of optoelectronic [4,5] and thermoelectric [6] devices.

An important factor is the thermal annealing of the semiconductor material to change the electronic states, recovery of the crystal structure and electrical activation of the introduced impurities, although the latter is highly undesirable factor.

In this paper, the results of metallic Zn – nanotubes studies synthesized by electrochemical deposition in the template are presented. As templates, track-etched membranes based on PET with a density of $4.0E+07$, thickness of 12 microns and a pore diameter of 380 nm were used. The structural characteristics of the nanotubes were evaluated by the methods of SEM, EDX and XRD. The effect of thermal annealing on the conductive properties of the nanostructures was carried out. According to the EDX, XRD spectra and resistance-time of annealing diagram, two stages of the change in resistance were observed.

The first stage showed the fall of the resistance before 60 minutes of annealing, at this stage, the formation of zinc oxide (ZnO) phase was observed. The atomic ratio of the elements in this state is $Zn_{91}O_9$.

The second stage showed the sharp increasing in resistance and falling of conductivity at the annealing time from 75 to 150 minutes, at this stage, destruction of Zn - nanotubes associated with the appearance of zinc dioxide phase (ZnO_2) was occurred.

The formation of dioxide and oxide phase in the crystal structure increased the defect structure, which led to sharp increasing of resistance of 15%, and partial destruction of the nanotubes.

Thus, thermal annealing of zinc-based nanotubes, allows us to control the formation of the oxide phase in the nanostructures. The presence of the oxide phase ZnO not more than 10% (wt.) leads to decreasing in resistance and increasing conductivity.

Changing the crystal structure of Zn - nanotubes by thermal annealing opens great opportunity to produce the ordered arrays of n-type semiconductors, which can then be used in nanoelectronics and optics.

[1] R. Asomoza, H. Malodonado, M. D. Olvera [et al.] // J. Mater. Sci. Mater. Electron. –2000. –V.11, № 5. –P. 383.

[2] Li Q. // J. Appl. Polym. Sci. –2006. –V.103, №3. –P.41.

[3] Wienke J. // Thin Solid Films. –2007. –V3. № 4. –P. 5-11.

[4] R. Al-Asmara, G. Ferblantier, F. Maily [et al.] // Thin Solid Films. –2005. –V.473, №1. –P. 49-53

[5] J.O. Williams, L.M. Turton // Trans. Faraday Soc. –1968. –V. 64. –P. 2496-2504.

[6] D.A. Drabold, S.K. Estreicher // Berlin: Springer-Verlag, 2007. –P. 295 .

EXPERIMENTAL (X-RAY, ¹³C CP/MAS NMR, IR, RS, INS, THZ) AND SOLID-STATE DFT STUDY ON (1:1) CO-CRYSTAL OF BROMANILIC ACID AND 2,6-DIMETHYLPYRAZINE

Katarzyna Łuczynska^{ab}, Kacper Druzbicki^{bc}, Krzysztof Lyczko^a and Jan Cz. Dobrowolski^{ad}

^a *Institute of Nuclear Chemistry and Technology, 16 Dorodna Street, 03-195, Warsaw, Poland*

^b *Frank Laboratory of Neutron Physics, Joint Institute for Nuclear Research, 141980, Dubna, Russian Federation*

^c *Department of Radiospectroscopy, Faculty of Physics, Adam Mickiewicz University, Umultowska 85, 61-614, Poznan, Poland*

^d *National Medicines Institute, 30/34 Chelmska Street, 00-725 Warsaw, Poland*

Organic electronic materials including semiconductors, dielectrics and conducting polymers are emerging family of materials with applications similar to their inorganic counterparts, but of much greater potential ease of integration with silicon and other inorganic matrices. One of the most promising organic ferroelectric materials are two-component crystals formed by hydrogen donor and acceptor molecules. The family of bromanilic and chloranilic acid complexes reveals very promising properties which are extensively studied since last decade.

A combined structural, vibrational spectroscopy, and solid-state DFT study of the hydrogen-bonded complex of bromanilic acid with 2,6-dimethylpyrazine will be reported. The crystallographic structure was determined by means of low temperature single-crystal X-ray diffraction, which reveals the molecular units in their native protonation states, forming one dimensional infinite nets of moderate-strength O···H–N hydrogen bonds. The nature of the crystallographic forces, stabilizing the studied structure, has been drawn by employing the noncovalent interactions analysis. It was found that, in addition to the hydrogen bonding, the intermolecular forces are dominated by stacking interactions and C–H···O contacts. The thermal and calorimetric analysis was employed to probe stability of the crystal phase. The structural analysis was further supported by a computationally assisted ¹³C CP/MAS NMR study, providing a complete assignment of the recorded resonances. The vibrational dynamics was explored by combining the optical (IR, Raman, TDs-THz) and inelastic neutron scattering (INS) spectroscopy techniques with the state-of-the-art solid-state density functional theory (DFT) computations. Despite the quasiharmonic approximation assumed throughout the study, an excellent agreement between the theoretical and experimental data was achieved over the entire spectral range, allowing for a deep and possibly thorough understanding of the vibrational characteristics of the system. Particularly, the significant influence of the long-range dipole coupling on the IR spectrum has been revealed. On the basis of a wealth of information gathered, the recent implementation of a dispersion-corrected linear-response scheme has been extensively examined.

This work has been published in:

K. Łuczynska, K. Druzbicki, K. Lyczko, J. Cz. Dobrowolski, *J. Phys. Chem. B.* 2015, 119,6852–6872

СТРУКТУРА СТАБИЛЬНЫХ ГИДРИДОВ ИМС $CeNi_3$

С.А.Лушников, Т.В. Филиппова, И.А. Бобриков

Химический факультет МГУ им. М.В. Ломоносова
Объединенный институт ядерных исследований, Дубна

Интерметаллические соединения (ИМС) состава RT_3 ($R=PЗМ$, $T=Fe, Co, Ni$) являются материалами для компактного и безопасного хранения водорода. Большинство таких соединений кристаллизуются в двух структурных типах $PuNi_3$ (ПГ $R-3m$, № 166) и $CeNi_3$ (ПГ $R6_3/mmc$, № 194). Структурный тип $CeNi_3$ состоит из фрагментов состава RT_2 (структурный тип $MgZn_2$) и RT_5 (структурный тип $CaCu_5$), которые послойно расположены перпендикулярно кристаллографической оси z . В кристаллической решетке ИМС находятся тринадцать типов пустот (двенадцать тетраэдрических и одна октаэдрическая), в которые возможно внедрение водорода [1]. Эти пустоты соответствуют $24l$, $12k$, $4f$, $4e$ (тетраэдрическим) и $6h$ (октаэдрической) кристаллографическим позициям и образуют водородные подрешетки (рис. 1).

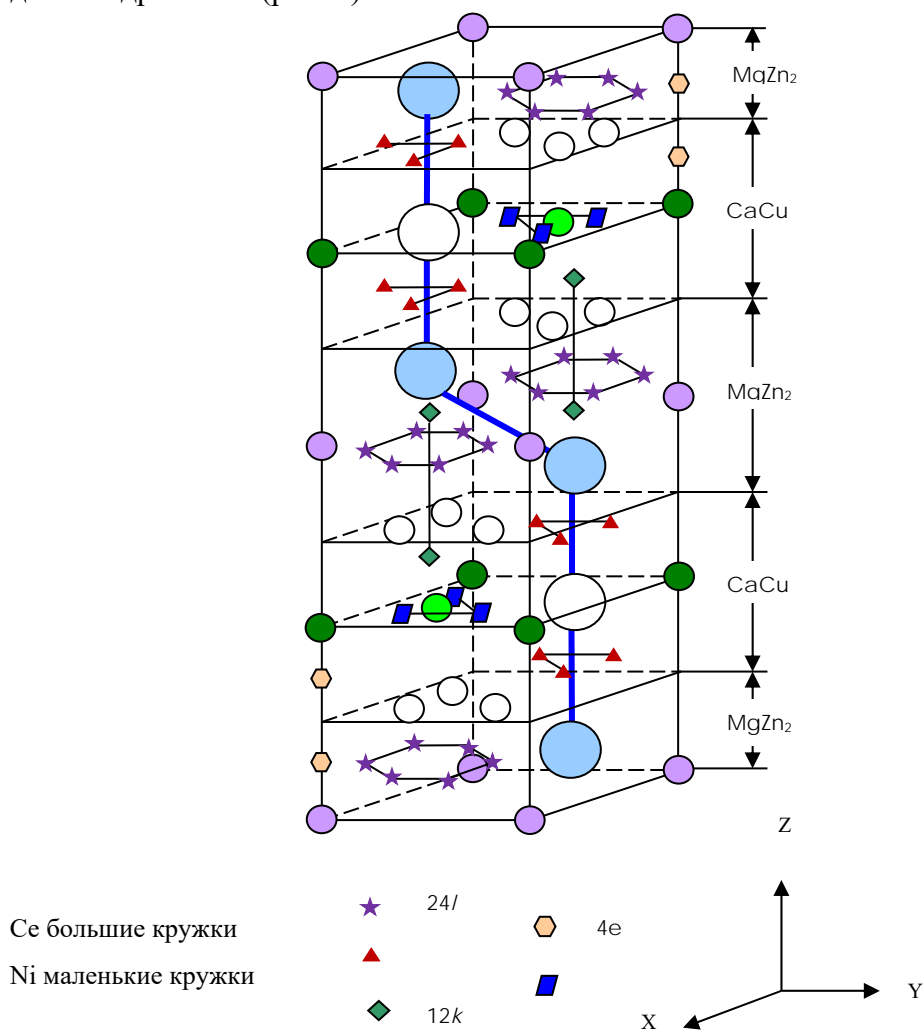


Рис.1. Тетраэдрические ($24l$, $12k$, $4f$, $4e$) и октаэдрические ($6h$) водородные подрешетки в металлической матрице $CeNi_3$ [1].

В работе [2] было обнаружено, что взаимодействие водорода с ИМС CeNi₃ приводит к образованию гидридной фазы состава CeNi₃H_{3.0}. На построенной изотерме абсорбции присутствует плато с равновесным давлением 0.09 бар при температуре 50⁰С. Низкое равновесное давление указывает на высокую стабильность образованной гидридной фазы. При обычных условиях, на воздухе и при комнатной температуре синтезированный образец гидридной фазы CeNi₃H_{3.0}, напротив, очень нестабилен, десорбирует водород и разлагается с образованием исходного интерметаллида. При проведении синтеза гидрида при низкой температуре образуется стабильная гидридная фаза, которая не разлагается на воздухе при комнатной температуре [3]. Таким образом, в зависимости от условий синтеза можно получить стабильные и нестабильные образцы гидридных фаз ИМС CeNi₃. Можно предположить, стабильные и нестабильные образцы гидридов отличаются между собой различным распределением атомов водорода в водородных подрешетках. Для определения позиций атомов водорода в кристаллической решетке гидрида наиболее надежным способом является метод дифракции нейтронов. Структура нестабильных гидридных фаз ИМС CeNi₃ с различным содержанием водорода была определена ранее в работах [4, 5]. Было установлено, что сначала, при низкой концентрации, водород заполняет позиции структурных блоков RT₂. При увеличении концентрации происходит дальнейшее заполнение позиций в блоках RT₅ структуры гидрида. В настоящей работе нейтронографическим методом изучали структуру стабильного гидрида ИМС CeNi₃, синтезированного при низкой температуре. Для снижения некогерентного рассеяния водорода при съемке использовали образцы с дейтерием. Нейтронографические данные были получены на Фурье-дифрактометре высокого разрешения в ОИЯИ г. Дубна. Было установлено, что полученные образцы гидридов состоят из двух фаз. Первая фаза это β-гидрид с анизотропно расширенной вдоль оси z решеткой. Вторая фаза это α-фаза твердого раствора водорода в исходном интерметаллическом соединении. Полученные результаты структурного расчета образцов гидридов ИМС CeNi₃ с высокой стабильностью показали, что дейтерий локализован в междоузлиях обоих блоков RT₂ и RT₅ решетки β-гидридной фазы и в незначительном количестве в α-фазе.

- [1] В.А. Яртысь. Новые аспекты структурной химии гидридов интерметаллических соединений: «изотропные» и «анизотропные» структуры // Координац. химия. т. 18. № 4. (1992) С. 401–408.
- [2] R.H. Van Essen, K.H.J. Bushow, Hydrogen sorption characteristics of Ce-3d and Y-3d intermetallic compounds, J. Less-Common. V.70 (1980) P.189-198.
- [3] С.А. Лушников, Т.В. Филиппова. Гидриды интерметаллического соединения CeNi₃. Неорг. Мат. т.49, №4 (2013) С.1-5.
- [4] V.A. Yartys, O. Isnard, A.B. Raybov, L. G. Akselrud. Unusual effect on hydrogenation: anomalous expansion and volume contraction. J. Alloys Compd. V. 356-357 (2003) P.109-113.
- [5] S.A. Lushnikov, V.N. Verbetsky, V.P. Glaskov, V.A. Somenkov. Structural properties of RT₃ deuterides synthesized under high hydrogen pressure. J. Alloys Compd. V.404-406 (2005) P.103-106.

STRUCTURE OF OPTICAL MATERIALS GeO_2 , In_2O_3 , AND SnO_2 DOPED Eu^{3+} STUDIED BY MEANS OF SMALL ANGLE NEUTRON SCATTERING AND NEUTRON DIFFRACTION

Ch. T. Nguyen^{1,2}, S. Kichanov¹, D. Kozlenko¹, B. Savenko¹

¹ Joint Institute for Nuclear Research, 141980, Dubna, Russia

² Nha Trang Institute of Technology Research & Application, Nhatrang, Vietnam

E-mail: nguyenchithang167@gmail.com

At the present time, one of the topical problems in modern condensed matter physic is produce nanostructure optical materials with the possibility of varying their optical properties at the stage of synthesis. It was observed, that optical properties of these compounds are defined by treatment conditions. In this regard, the application of colloidal chemical methods is most promising for solving this problem, making the distribution of optically active ions more easily doped into the crystal matrix, and most importantly, the possibility of forming complex composite systems with a controllable redistribution of activator ions between the components. The promising materials are simple oxides with doping of optical ions, the oxide systems were doped Eu^{3+} ion (4% at) by sol-gel of the colloid chemical method

Here, we report about structural data of optical compounds $\text{GeO}_2:\text{Eu}^{3+}$, $\text{In}_2\text{O}_3:\text{Eu}^{3+}$ and $\text{SnO}_2:\text{Eu}^{3+}$, which are annealed at different temperature by means of the small angle neutron scattering (SANS).

As result, all of compounds have the formation of stability nanostructures, which was characterized by a fractal dimension corresponding to the scattering of large objects with dimensions of about 30 nm. Further, the annealing nanosystems with different behavior is observed depending on the nature of the oxides: conservation of nanoparticles structure (SANS curves do not change - the samples $\text{GeO}_2:\text{Eu}^{3+}$, $\text{In}_2\text{O}_3:\text{Eu}^{3+}$), or appear the anomalies of new nanoparticles with sizes $\sim 40\text{-}60 \text{ \AA}$ (sample $\text{SnO}_2:\text{Eu}^{3+}$).

The work has been supported by the RFBR and the Ministry of Investment and Innovation of Moscow region under grant № 14-42-03641_r_centr_a.

MOLECULAR ORIENTATION IN AMLODIPINE BESYLATE

T.V. Popiuk^{1,2}, D. Chudoba^{1,3}, L. A. Bulavin², J. Wasicki³, A. Pajzderska³

¹ *Joint Institute for Nuclear Research, Dubna, Russia*

² *Taras Shevchenko National University of Kyiv, Ukraine*

³ *Adam Mickiewicz University, Poznan, Poland*

Amlodipine belongs to a new-generation of drugs. It is known as long-acting dihydropyridine-type calcium channel blockers, inhibits the movement of calcium ions into vascular smooth muscle cells and cardiac muscle cells. Like other medications in this group, amlodipine lowers blood pressure by relaxing the muscles controlling the diameter of blood vessels in the body. Amlodipine is used in the management of hypertension and coronary artery disease. It is on the World Health Organization's List of Essential Medicines, the most important medications needed in a basic health system [1].

Amlodipine is molecular crystal and no phase transitions in the temperature range from 77 K up to the melting point at 450 K have been observed. Nevertheless we cannot exclude a phase transition at lower temperatures. It is known 3 polymorphic forms of amlodipine: besylate, maleate and mesylate.

The aim of the study is to determine the molecular dynamics of the methyl and NH₃ groups in amlodipine besylate as a function of temperature by neutron scattering and NMR methods.

In work has been shown comparison experimental results and calculated by "Monte-Carlo" method.

[1] "WHO Model List of Essential Medicines". World Health Organization. October 2013. Retrieved 22 April 2014.

SUPPRESSION OF THE ANTIFERROMAGNETIC STATE IN $\text{La}_{0.82}\text{Ba}_{0.18}\text{CoO}_3$ COBALTIDE AT HIGH PRESSURE

A.V.Rutkauskas¹, D.P.Kozlenko¹, I.O. Troyanchuk², S.E. Kichanov¹, E.V.Lukin¹, B.N.Savenko¹

¹ *Joint Institute for Nuclear Research, 141980 Dubna, Russia*

² *Scientific and Practical Materials Research Centre of NAS of Belarus, 220072 Minsk, Belarus*

Studies of the $\text{La}_{0.82}\text{Ba}_{0.18}\text{CoO}_3$ compound have been performed by using the neutron diffraction at high pressure up to 4 GPa in the temperature range from 10 K to 290 K. Under normal atmospheric conditions, this compound has a rhombohedral symmetry with space group $R\bar{3}c$. When cooling till the temperature of $T_N = 100$ K there is a non-collinear antiferromagnetic (AFM) phase with propagation vector $\mathbf{k} = (0, -0.5, 0.5)$. This phase is suppressed by high pressure and disappears at $P > 2$ GPa. The degree of instability in the $\text{La}_{0.82}\text{Ba}_{0.18}\text{CoO}_3$ AFM phase in relation to the effects of high pressure is much higher than that of the related compounds with the basic ferromagnetic state. We have analyzed the relationship of the AFM state instability with the electron configuration changes of cobalt ions Co^{3+} in $\text{La}_{0.82}\text{Ba}_{0.18}\text{CoO}_3$ at high pressure.

The work is supported by grants РФФИ #14-02-90051-Бел-а and БРФИ Ф14Р-040.

NEUTRON DIFFRACTION STUDIES OF MOLTEN SALTS IN NONEQUILIBRIUM STATE

O. Shabanov, S. Suleimanov

Dagestan State University, M. Gadzhieva str., 43 a, Makhachkala 367025, Russia

E-mail: s.sagim.i@ya.ru

The vast majority of metals are produced by electrolysis of the molten salt electrolytes. Physicochemical properties of molten salts in equilibrium state have been investigated by modern methods, including the neutron diffraction and spectroscopic methods [1, 2], they lead to the conclusion that the molten salts of many metals are structured. On their radial distribution functions (RDF) are observed sharp and high first and second peaks [1]. Moreover, measurement of their partial structure factors $S_{++}(k)$ show the presence of “pre-peak” in which is believed to long-range polymeric ordering of their basic structural species – complex ions of type $MgCl_4^{2-}$, $AlCl_4^-$ and others [1-3]. An intermediate range ordering appears even for the Li^+ ions in molten mixtures of alkali halides, which is associated with their clustering. This ordering is surprising in view of the simplicity of the interionic interactions in them [4]. The existence of different complex structural units and their characteristic distribution in the equilibrium electrolytes determine observed their physical and chemical properties, the mechanisms and kinetic pathways that decrease current and voltage efficiency in metals electrolyze cells [5, 6].

We have shown [7] that on exposure of the high-voltage microsecond pulsed fields, the molten salts pass into a non-equilibrium state with the disappearance of the characteristic peaks of the Raman spectra and the increased electrical conductivity, which is explained by stimulated dissociation of complex ions. In the course of the structural relaxation of nonequilibrium melts, their Raman spectra and electrical conductivities are restored to the values and features specific to equilibrium systems in over about 10 minutes.

In the literature, there are no experimental RDF, data on the structure and structural parameters of molten salts in a nonequilibrium state. For study in details the structural parameters of molten salts $MgCl_2$, $KAlCl_4$, $ZnCl_2$, $LiCl-KCl$ in non-equilibrium state we propose to perform neutron diffraction at neutron diffractometer DN-2 at 6A-th channel of IBR-2 reactor for their RDF and structural parameters, after playing back their literary RDF in equilibrium state. We would be interested in diffraction study at different temperature in range 600-800 K. We have the anhydrate samples, the high-voltage pulse generator for translation the melts in non-equilibrium state. So, we ask for 4-5 experimental days in total. The results expected for the first time enable a new insight into the structure and properties of the equilibrium and non-equilibrium molten electrolytes and to create a scientific basis for the improvement and intensification of the technological processes.

This work was supported by Russian Foundation for Basic Research, projects № 15-08-00559 and № 14-08-00033-a.

- [1] G.V. Neilson, A.k. Adya. Neutan diffraction studies of liquids// Annu. Rep. Pror. Chem., Sect. C: Phys. Chem.1997. 997.(9)30. 101-146.
- [2] A.-L. Rollet and M. Salanne. Studies of the local structure of molten metal halides//Annu. Rep. Prog. Chem., Sect. C: Phys. Chem. 2011.107. 88-123.
- [3] Pusztai, R.L. McGreevy. The structure of molten $ZnCl_2$ and $MgCl_2$ // J. Phys.: Condens. Matter, 2001. 13 (33) 7213-7222.

- [4] M Salanne, C Simon, P Turq and P A Madden. Intermediate range chemical ordering of cations in simple molten alkali halides// *J. Phys.: Condens. Matte*, 2008. 20 (33)332101
- [5] S.-Y. Yoon., D.R. Sadoway. Spectroscopic and electrochemical studies of molten salts electrolysis of aluminum and magnesium // *Physical Electrochemistry and High Temperature materials Divisions. Proceedings*. 1987. 82-7. 1011-1015.
- [6] Y. Yoon, J.H. Flint, Kipouros, D.R. , D.R. Sadoway. Raman scattering studies of molten salts. Electrolysis of light metals//*In energy reduction Techniques in Metal Electrochemical Processes*, R.G. Bautista and R. Wesely, editors, (Warrendale P.A.: TMS-AIME, 1985) 137.
- [7] O. M. Shabanov, P. T. Kachaev, S. I. Suleymanov. Activation of Solid and Molten Electrolytes and their Relaxation// *Advanced Materials Research*.2013. Volumes Advanced Measurement and Test III 718-720 , pp. 146-150.

ANTIFERROMAGNETIC-FERROMAGNETIC TRANSITION IN ANION DEFICIENT COBALTITES. NEUTRON DIFFRACTION STUDIES

V.V. Sikolenko¹, V.V.Efimov¹, S.A.Tjutjunnikov¹, A.G.Selutin², M.V.Bushinski³, M.Frontzek⁴ and I.O.Troyanchuk³

¹Joint Institute for Nuclear Research, Dubna, JINR

²Institute of Catalysis of Siberian Branch of RAN, Novosibirsk, Russia

³Scientific-Practical Materials Research Center NAN of Belarus, Minsk, Belarus

⁴Paul Scherrer Institute, Villigen, Switzerland

Anion deficient cobaltites $\text{La}_{0.5}\text{Ba}_{0.5}\text{CoO}_{2.8}$ and $\text{Y}_{0.25}\text{Ca}_{0.25}\text{Sr}_{0.5}\text{CoO}_{2.62}$ have been studied as a function of pressure up to 6.5 GPa and temperature 5 - 300 K by neutron powder diffraction. High resolution structural data have been obtained by HRFD diffractometer (IBR-2, FLNP), high pressure experiments with medium resolution have been performed at the DMC (SINQ, PSI) and D20 (HFR, ILL).

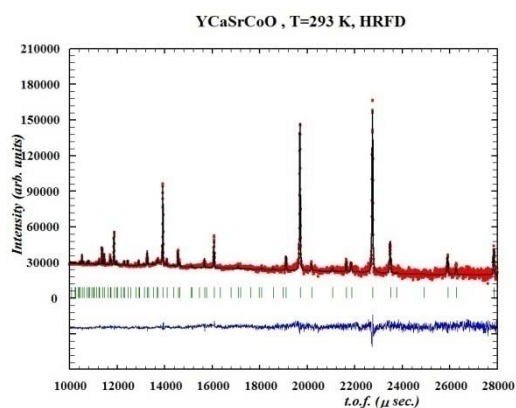


Fig.1 Neutron powder diffraction at ambient pressure (HRFD, Dubna). Experimental data and Rietveld structure refinement is shown

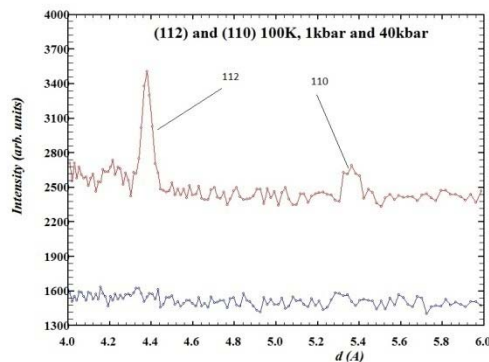


Fig.2. Antiferromagnetic peaks measured at ambient pressure (upper red curve) and at 4 GPa (lower blue curve) at 100K (DMC, PSI)

At ambient pressure both compounds are antiferromagnetic with T_N below 250K. Applied pressure induces in first compound a gradual transition from antiferromagnetic to a ferromagnetic state through a mixed magnetic state, whereas the second compound remains antiferromagnetic in whole pressure range. We suggest that the magnetic ground state depends on unit cell volume and magnetic transition is associated with a spin state crossover of cobalt ions from a mixed high spin/low spin into intermediate spin/low spin states.

NEUTRON DIFFRACTION STUDY OF MAGNETIC AND STRUCTURAL PHASE TRANSITIONS IN NiO AND MnO

S.V. Sumnikov^a, I.A. Bobrikov^a, A.M. Balagurov^a, A. Kuzmin^b, N. Mironova-Ulmane^b

^a*Frank Laboratory of Neutron Physics, Joint Institute for Nuclear Research, RU-141980 Dubna, Russian Federation*

^b*Institute of Solid State Physics, University of Latvia, Kengaraga street 8, LV-1063 Riga, Latvia*

For a better understanding of the correlation between structure and the magnetic properties of simple oxides the magneto-structural phase transitions in NiO and MnO were studied by neutron diffraction technique. Complete separation of nuclear and AFM magnetic diffraction peaks of these oxides makes possible a detailed analysis of the temperature variations of the atomic and magnetic structures during phase transitions.

Experiments were performed in a wide temperature range from 5 to 563 K at the High Resolution Fourier diffractometer (HRFD) at the IBR-2 pulsed reactor (JINR, Dubna). The HRFD resolution function, $R = \Delta d/d$, is determined by the maximum frequency of the fast Fourier chopper. In routine operation ($V_{max} = 4000$ rpm) R is close to 0.001, only slightly depends on d_{hkl} , and improves with increasing d_{hkl} . The experimental data were collected at NiO and MnO powders with large sizes of crystallites. In both oxides the structural transition consists of lowering of the symmetry from cubic to rhombohedral, when during the magnetic transition AFM structure of the Neel type appears.

From diffraction data we were able to obtain temperatures of the structural and magnetic transitions as well as temperature dependences for the rhombohedral distortion and the value of ordered magnetic moment. It was found that in MnO both structural and magnetic transitions occur at the same (within experimental uncertainties) temperature ($T_N = T_c = 123 \pm 3$ K). Contrary, for NiO magnetic transition occurs at 56 ± 9 K higher temperature than structural one ($T_N = 539 \pm 7$ K, $T_c = 483 \pm 5$ K). To our best knowledge, this fact does not yet have an adequate theoretical explanation.

INVESTIGATION OF CRYSTAL AND MAGNETIC STRUCTURES OF BARIUM FERRITES DOPED BY DIAMAGNETIC IONS

¹V.A. Turchenko, ²A.V. Trukhanov, ¹I.A. Bobrikov, ²S.V. Trukhanov

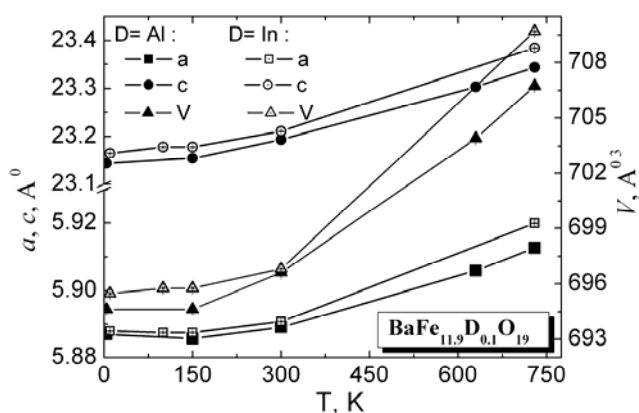
¹ Frank Laboratory of Neutron Physics of Joint Institute for Nuclear Research, Dubna, Russia

²SSPA “Scientific and practical materials research center of NAS of Belarus”, Minsk, Republic of Belarus

E-mail: truhanov86@mail.ru

Barium ferrites with hexagonal structure ($\text{BaFe}_{12}\text{O}_{19}$) are well known by their high electrical and magnetic properties. Their solid solutions doped by Co, Sc, Ti, Nb and etc. [1] display relatively high values of electrical resistance ($\sim 10^5 \div 10^9 \Omega \cdot \text{cm}$) and large magnetization as well as coercive force ($H_c \sim 160 - 55 \text{ kA/m}$) [2, 3] and of the Curie temperature. Furthermore, it is worth to point there excellent chemical stability and corrosion resistivity [4] of these materials that let to use them in corrosive mediums. The recent discovery of considerable ferroelectric polarization in ceramic $\text{BaFe}_{12}\text{O}_{19}$ [5] and $\text{PbFe}_{12}\text{O}_{19}$ [6] with hexagonal structure and collinear ferrimagnetic alignment attract attention of researches and renew the scientific interest for this materials.

In present work, the influence of diamagnetic ions Al and In onto crystal and magnetic structures of solid solution of barium ferrite $\text{BaFe}_{12-x}\text{D}_x\text{O}_{19}$ (D=Al and In; $x = 0.1 - 1.2$) was investigated by neutron diffraction of high resolution in a wide temperature range. Polycrystalline patterns prepared by conventional solid reaction method. Pressured pellets annealed at 1300°C (6 h) in air. The



temperature dependence of lattice parameters for compounds with $x=0.1$ are shown at Fig. The pattern doped by In ions has a little more volume of unit cell unlike pattern doped Al ions. The high resolution of neutron diffractometer allowed carrying out analysis of microstructure parameters, such as sizes of coherent scattering blocks and microstress in crystallites, with temperature changes. The increase of microstress with forming of long-range magnetic order in ferrimagnetic crystal could

have linked with the fact that individual sublattices make different contributions in general deformation. In low temperature range from 150 to 4.2 K the Invar effect (zero thermal expansion coefficient) is observed. Such behavior of lattice parameters of barium ferrites in the range from 150 to 4.2 K explained by a change of the regime of mutual rotations and tilts of the oxygen octahedra.

The financial supports by the Belarusian Republican Foundation for Fundamental Research (Grant no. F15D-003) and Joint Institute for Nuclear Research (Grant no. 04-4-1121-2015/2017).

Reference.

1. Robert C. Pullar // Progress in Materials Science 57. 2012. 1191–1334
2. S. Castro, M. Gayoso, J. Rivas et al. // JMMM 152. 1996. 61-69
3. M.H. Makled, T. Matsui, H. Tsuda et al. // Journal of Materials Processing Technology 160 (2005) 229–233
4. Liu, X., Wang, J., Gan, L.M., Ng, S.C. and Ding, J. // JMMM 184. 1998. 344-354.
5. Xiuna Chen, Guolong Tan // J. Magn. Mater. 2013. V. 327. P. 87.
6. Tan, G. L., Wang, M. // J. Electroceramics. 2011. V. 26. P. 170.

CRITICAL SCATTERING IN SINGLE CRYSTAL OF UNIAXIAL RELAXOR

$\text{Sr}_{0.6}\text{Ba}_{0.4}\text{Nb}_2\text{O}_6$

Vanina P.Yu.¹, Borisov S.A.², Naberezhnov A.A.², Bosak A.A.³,

¹Peter the Great St.Petersburg Polytechnic University, St. Petersburg

²The Ioffe Institute, St. Petersburg

³European Synchrotron Radiation Facility (ESRF), Grenoble, France

E-mail: p.yu.vanina@gmail.com

Crystals of solid solutions $\text{Sr}_{(x)}\text{Ba}_{(1-x)}\text{Nb}_2\text{O}_6$ (SBN $_x$, $0.2 < x < 0.8$, $P4bm$) belong to uniaxial relaxors [1]. At increasing Sr concentration the phase transition temperature decreases [2] with the simultaneous enhancement of relaxor behavior; i.e. the diffuseness of the maximum in the permittivity ϵ becomes more pronounced and the frequency dispersion of $\epsilon(T)$ increases.

In recent years the critical behavior in SBN60–SBN61 crystals is under discussion. We have carried out the study of diffuse scattering near the (002) and (220) sites at zero applied electric field [3]. In vicinity of (002) Bragg peak we have observed an intense scattering, which strongly depended on the temperature and on the applying of the electric field. The analysis of the temperature dependence of the this scattering in SBN60 have shown, that upon cooling in the zero electric field the spatially homogeneous polar state is not formed and the crystal is divided into nanodomains below 320 K. It has been shown that below the Curie temperature the correlation length remains constant and approximately is equal to 27 nm. We also determined the critical exponents $\nu = 0.67(2)$ and $\gamma = 1.33(17)$ and Curie temperature $T_c = 340.5(1.2)$ K.

However, the spatial distribution of diffuse scattering and effect of applied electric field remain practically unclear (fig. 1). We have carried out the study of temperature evolution of diffuse scattering in SBN60 single crystal in two regimes: at zero field and at applied electric field ~ 3 kV/cm. It gives the possibility to obtain the information concerning to spatial organization of the order parameter fluctuations in this crystal near the phase transition temperature. The main idea of these measurements was to determine the effect of applied electric field on critical parameters and to obtain information about spatial organization of the order parameter fluctuations. At present time this information is absent.

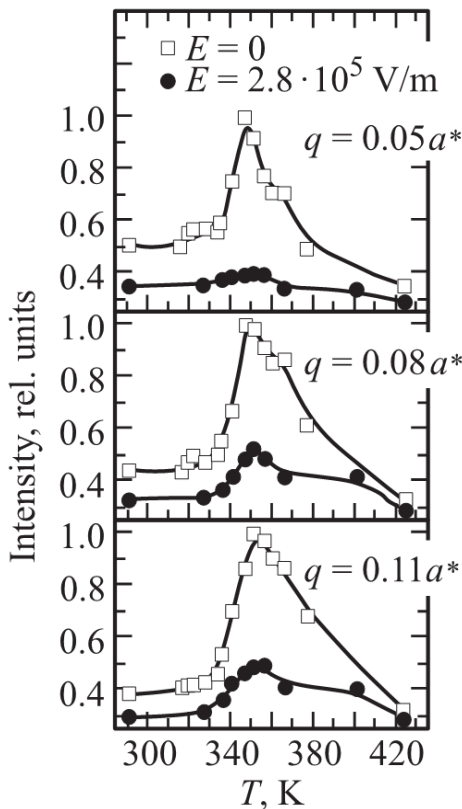


Fig. 1 The experimental data of the temperature dependence of scattering intensity of neutrons in relative terms for several values of the reduced wave vector q near (002) site.

[1] L. Eric Cross, *Ferroelectrics* 76, 241 (1987).

[2] Yu.S. Kuz'minov, *Ferroelectric Crystals for Laser Radiation Control* (Nauka, Moscow, 1982; Adam Hilger, Bristol, 1990).

[3] S.A. Borisov, N.M. Okuneva, S.B. Vakhrushev, A.A. Naberezhnov, T.R. Volk, and A.V. Filimonov *Physics of the Solid State*, 55(2), 334 (2013).

CRYSTAL AND MAGNETIC STRUCTURE OF MANGANITE $\text{La}_{0.7}\text{Sr}_{0.3}\text{Mn}_{0.83}\text{Nb}_{0.17}\text{O}_3$ IN WIDE RANGE OF THE TEMPERATURES AND PRESSURES

M. Th. Vu¹, S. Kichanov¹, E. Lukin¹, B. Savenko¹, D. Kozlenko¹, I. Troyanchuk²

¹ *Joint Institute for Nuclear Research, Dubna, Russia*

² *Scientific and Practical Materials Research Centre, National Academy of Sciences of Belarus*

E-mail: thanhvuminh95@gmail.com

Manganites of perovskite type $\text{R}_{1-x}\text{A}_x\text{MnO}_3$ (R - rare earth, A - alkali earth elements) exhibit rich magnetic and electronic phase diagrams depending on the kind of R, A elements and their ratio. These systems show for particular compositions an extreme sensitivity of magnetic, structural, electronic, transport properties to external fields, and have attracted considerable interest with respect to the recently discovered colossal magnetoresistance (CMR) effect. The properties of manganites depend substantially on a balance between the ferromagnetic (FM) interactions mediated by itinerant charge carriers (double - exchange mechanism) and the superexchange interactions between localized spins of manganese ions, which are usually antiferromagnetic (AFM). A dielectric ferromagnetic state was also detected in the $\text{La}_{0.7}\text{Sr}_{0.3}\text{Mn}_{0.83}\text{Nb}_{0.17}\text{O}_3$ manganite, which has no manganese ions with different valences. To reveal the nature of the ferromagnetic ordering in this manganite, we performed a neutron diffraction at high pressure.

The crystal and magnetic structures of compound $\text{La}_{0.7}\text{Sr}_{0.3}\text{Mn}_{0.83}\text{Nb}_{0.17}\text{O}_3$ have been studied by neutron diffraction at pressure up to 4.5 GPa and temperature range 5-300 K. At ambient pressure, this compound is shown to be a ferromagnetic state FM with $T_C = 150$ K and a magnetic moment of $3.097 \mu_B$ at $T = 4$ K. The crystal structure of which is described by the orthorhombic symmetry with space group Pnma. By applying difference pressures up to 4.5 GPa at varying temperatures, the new antiferromagnetic phase is found. Temperature dependences of magnetic moment at difference pressures, unit cell parameters, atom coordinates, magnetic moments of Mn are also revealed in this work.

The work has been supported by the RFBR grant 14-02-90051_Bel_a and The Joint Project between Vietnam Academy of Science and Technology and the Russian Foundation for Basic Research named VAST.HTQT.NGA.01/15-16.

I N S T R U M E N T S A N D M E T H O D S

SPATIAL DISTRIBUTION OF DIFFRACTED NEUTRON BEAM IN PERFECT AND STRAINED SI CRYSTAL

V.Gavrilovs¹, D.Mjasischev¹, E.Raitman¹, A.Hoser², T.Hoffmann² and P.Mikula³

¹ *Institute of Physical Energetics, Riga, Latvia*

² *Helmholtz-Zentrum, BENSC, Berlin, Germany*

³ *Nuclear Research Institute, Rež, Czech republic*

E-mail: mdmitry@delfi.lv

The spatial distribution of neutron beam Bragg diffracted from Si single crystal undergoing on ultrasound excitation and bending have been measured. The values of ultrasound wave amplitude and uniform strain gradient were determined. For the perfect crystal it was shown that at the same time as the acoustic wave amplitude is increased, the front-face peak position remains unchanged and its value grows linearly. For the strained crystal the spatial distribution of diffracted neutrons inside the profile is analyzed as well as the mechanism of anomalous decrease of diffraction intensity, depending on acoustic waves amplitude and on the value of the uniform strain gradient.

A new types of Pendellösung fringes were observed. These effects observed at the first time, have a different nature in the case of a perfect and deformed crystal. It is supposed that in the perfect crystal this effect may be due to the appearance of the new “sound” extinction length, depending on the amplitude of the ultrasonic wave, thus, it leads to the new interference interactions between neutron wave and ultrasonic phonons. The influence of the crystal bending on the formation of the fringes in Bragg spatial profiles was studied. It is established that within the framework of the dynamical theory of the neutron scattering some asymptotic models valid for the case of Laue geometry can be applied in the case of Bragg geometry also. Good agreement between experimental data and the theory have been obtained.

SAS PROGRAM FOR THE PRELIMINARY DATA TREATMENT FOR THE SMALL ANGLE NEUTRON SCATTERING MULTIDETECTOR SYSTEM ON THE PULSED SOURCE

Soloviev A.G.^a, Solovieva T.M.^a, Ivankov O.I.^{a,b,c,d}, Soloviov D.V.^{a,b,c,d}, Rogachev A.V.^{a,d}, Kovalev Yu.S.^{a,d}, Kuklin A.I.^{a,d}

^a *Joint Institute for Nuclear Research, Dubna, Russia.*

^b *Taras Shevchenko National University of Kyiv, Kyiv, Ukraine*

^c *Institute for Safety Problems of Nuclear Power Plants, Chornobyl, Ukraine*

^d *Moscow Institute of Physics and Technology, Dolgoprudniy, Russia*

The information about the absolute cross sections of small angle scattering is the most important task for small-angle neutrons and X-rays scattering spectrometers. For the pulsed neutron sources and the TOF spectrometers the problem is complicated in case of the whole neutrons wavelengths spectrum using but not the selected wavelength. SAS software is designed for the preliminary data treatment processing of the spectra measured on small-angle spectrometer YuMO (Channel 4 of the IBR-2 reactor). This program allows you to fold the data relating to the same model, to calculate the resolution function for the given experiment conditions, to carry out data correction on dead times of neutron detectors, and to subtract the background from the data detector substrate (in two possible modes of operation of the spectrometer: using a beam chopper neutrons or not), to carry out normalization of the obtained spectrum to an independent (standard) vanadium scatterer, to subtract the data background (s) of the sample (s). SAS works with two ring-wire detectors, but the information about them is directly included to the "raw" data obtained during the experiment, and can operate in multi-detector mode.

ADAPTATION OF THE FSS DIFFRACTOMETER AT THE IBR-2 FAST PULSED REACTOR: CURRENT STATE AND PROSPECTS OF DEVELOPMENT

A. Kruglov¹, G. Bokuchava¹, V. Zhuravlev¹, A. Bulkin², A. Kustov¹, A. Sirotin¹, N. Zernin¹

¹*Frank Laboratory of Neutron Physics, Joint Institute for Nuclear Research, Joliot-Curie str. 6, Dubna, Russia*

²*Petersburg Nuclear Physics Institute, Orlova Roscha, Gatchina, Leningrad district, 188300, Russia*

The Fourier diffractometer FSS on beamline 13 of the IBR-2 reactor is intended for investigations of internal stresses in engineering materials and industrial products using high-resolution neutron diffraction ($\Delta d/d \approx 4 \times 10^{-3}$). In addition to carrying out scientific research, another important direction of scientific and methodological activities on FSS will be further development of the neutron correlation RTOF technique for the analysis of elastic neutron scattering by crystals, as well as development and testing of new detectors, detector electronics and data acquisition electronics. Using FSS it will be possible to probe new ideas in correlation neutron spectrometry, which can be applied further on the European pulsed neutron source ESS. In addition, on the basis of the FSS an educational process will be organized for students, postgraduates and young specialists.

The FSS will be very similar in design to the available IBR-2 diffractometer FSD. The FSS, however, will have a longer flight path between the Fourier chopper and detector, which will allow us to use relatively low rotation speed of the chopper (~ 3000 rpm). In addition, the design of the Fourier chopper on FSS will ensure the minimization of the “collimation effect” of the chopper thus making it possible to reduce distortions of the shape of diffraction peaks. In the course of the implementation of the project major attention will be paid to the enhancement of the detector solid angle, improvement of the resolving power and the solution of the existing technical problems preventing widespread use of this method on pulsed neutron sources.

The FSS diffractometer comprises the following main units: steel conical collimator, neutron Fourier chopper, neutron guide, sample stage and two detectors. The Fourier chopper is between the conical collimator and the neutron guide. The fast Fourier chopper modulates the intensity of the primary neutron beam with the rotation speed of its disk ranging from 0 to 3000 rpm. The neutron guide between the Fourier chopper and the sample is intended to decrease losses in transporting neutrons to the sample. Two detectors comprising 16 ⁶Li-glass scintillation elements each are placed at scattering angles of $\pm 90^\circ$. The radial collimators providing for the effective size of the scattering area of the sample of 1 or 2 mm can be positioned in front of the detectors.

To date, the following works were completed: FSS transportation, The design project for FSS installation, construction of necessary beamline infrastructure, steel collimator tube was manufactured and installed in the beamline channel, neutron guide and Fourier chopper with supporting table were mounted on the beamline, Fourier chopper supply and control system was mounted, Fourier chopper operation modes were tested, the vacuum housing of the neutron guide was adopted for beamline 13, neutron beam parameters were evaluated, the experimental control cabin was installed.

In 2015-2016 it is planned to install and test the 90° -detectors with radial collimators, install electronic systems, make first neutron diffraction measurements and instrument parameters evaluation.

Further development includes replacing of existing mechanical sample table by modern HUBER goniometer, upgrade of neutron beam forming system with adjustable motorized diaphragm for the incident neutron beam, upgrade of FSS DAQ system on the basis of SONIX+ system with List-mode operation mode, automation of experiment control, analysis of the prospects for the use of various type choppers for RTOF techniques, test experiments for residual stress studies with real samples to evaluate main instrument parameters and its performance.

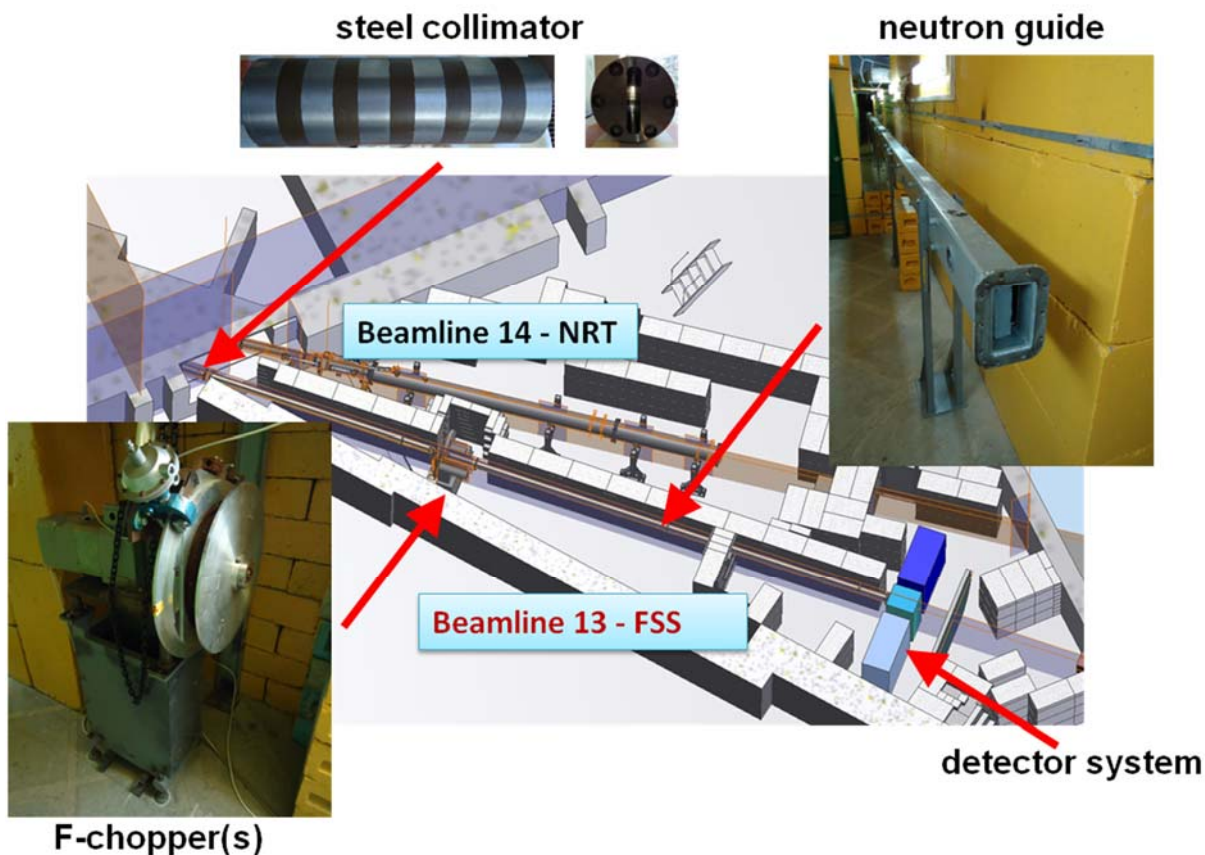


Fig. 1. Layout of the Fourier diffractometer FSS on beamline 13 of the IBR-2 reactor.

Acknowledgements. The work was partially supported by Federal Ministry of Education and Research (BMBF), Germany.

COLD AND THERMAL MODERATOR AT IBR-2 FOR SANS SPECTROMETER: ADVANTAGES AND DISADVANTAGES

A. D. Rogov^a, A. V. Rogachev^a, D. V. Soloviov^{a,b}, O. I. Ivankov^{a,b}, Yu. E. Gorshkova^a,
Yu. S. Kovalev^a, V. I. Gordeliy^{a,c,d} and A. I. Kuklin^a

^a *Joint Institute for Nuclear Research, Dubna, Russia*

^b *Taras Shevchenko National University of Kyiv, Kyiv, Ukraine*

^c *Institute of Structural Biology, Grenoble, France*

^d *Institute of Structural Biology, Juelich, Germany*

E-mail: kuklin@nf.jinr.ru

It is planned that in 2019 new cold moderator to the 4-th beam-line will be installed. The advantage and disadvantage of it is discussed on base of experimental data and calculating by Monte Carlo simulations. Recently, two methane moderators have been tested at the IBR-2 reactor. The measurements of neutron spectra for two methane cold moderators are done for the standard configuration of the SANS instrument. The data from both moderators under different conditions of their operation are compared. The ratio of experimentally determined neutron fluxes of cold and thermal moderators at different wavelength is shown. Monte Carlo simulations are done to determine spectra for cold methane and thermal moderators. The results of the calculations of the ratio of neutron fluxes of cold and thermal moderators at different wavelength are demonstrated.

In addition, the absorption of neutrons in the air gaps on the way from the moderator to the investigated sample is presented. SANS with the protein apoferritin was done in the case of cold methane as well as a thermal moderator and the data were compared. The perspectives for the use of the cold moderator for a SANS spectrometer at the IBR-2 are discussed.

Great losses in the thermal peak region (over 10 times for the maximum and over 4 times for the working wavelength range) with the same reactor power (thus, the background component remains unchanged) cannot be balanced out by the gain at large wavelengths for a spectrometer with the direct sight of the moderator and using the time-of-flight techniques. This conclusion was also confirmed by attempts to derive experimental data not only from the samples described above, but from others as well. So, the advantages of the YuMO spectrometer with the thermal moderator with respect to the tested cold moderator are shown [1].

[1] Kuklin A. I. et al. Analysis of neutron spectra and fluxes obtained with cold and thermal moderators at IBR-2 reactor: Experimental and computer-modeling studies //Physics of Particles and Nuclei Letters. – 2011. – T. 8. – №. 2. – C. 119-128.

NEUTRON IMAGING FACILITY: CURRENT STATE

E. Lukin, S. Kichanov, D. Kozlenko, A. Rutkauskas, B. Savenko

Joint Institute for Nuclear Research, Dubna, Russia

E-mail: lukin@jinr.ru

The development of neutron imaging techniques as a tool for non-destructive analysis of the internal structure, defects and processes in industrial products, functional materials, objects of cultural heritage attracts considerable attention at the present time. The dedicated instruments are available at the many neutron sources. The IBR-2M high flux pulsed reactor is one of the most powerful pulsed neutron sources in the world with the average power 2 MW, power per neutron pulse 1850 MW and neutron flux in pulse of $5 \cdot 10^{15}$ n/cm²/s. However, in Russian Federation there is no dedicated neutron imaging facility for cultural heritage research at the moment. First activities for establishing prospects of neutron imaging development at IBR-2M were made in 2011. Using the experimental setup based on the CCD camera and beamline 12 with mirror neutron guide, it was shown that appropriate quality neutron images can be obtained in rather short time of 10 s with white neutron beam. Following the first successful neutron imaging tests, performed at the beamline 12 of IBR-2, the concept design of the dedicated neutron imaging instrument for installation at the beamline 14 of IBR-2 was developed and its construction was started in 2012. Many various neutron imaging experiments were performed both during construction and finishing of the facility setup. Due to huge empirical work nowadays the neutron imaging facility at the IBR-2M high flux pulsed reactor is available for routine tasks. The main results of such experimental data received during last several years are presented in this work.

ОСОБЕННОСТИ ФОРМИРОВАНИЯ ТОНКОДИСПЕРСНЫХ ПОРОШКОВ $BaI_2:Eu$ ДЛЯ СЦИНТИЛЛЯЦИОННЫХ ДЕТЕКТОРОВ

Т.А. Соломаха, Е.В. Третьяк

НИИ Физико-химических проблем Белгосуниверситета, 220030, г. Минск

E-mail: Tanja_313@mail.ru

В работе предложен оригинальный метод получения тонкодисперсных порошков $BaI_2:Eu$, перспективных в качестве нового сцинтилляционного материала. Определены оптимальные условия формирования указанных порошков, исследовано влияние условий термообработки, концентрации иона-активатора, морфологии частиц прекурсора и др. на их спектрально-люминесцентные свойства.

В настоящее время значительно возрос интерес к сцинтилляционным материалам – это стимулируется растущими потребностями в усовершенствовании радиологических детекторов, используемых в медицине, промышленности и физике высоких энергий. Одним из эффективных материалов в этом направлении может быть йодид бария, активированный ионами Eu^{2+} , поскольку характеризуются достаточно высоким световыходом (до 59000 фотонов/МэВ), умеренной плотностью ($\sim 5,1 \text{ г/см}^3$) и не обладает собственной радиоактивностью. Однако, высокая гигроскопичность и фоточувствительность создает определенные трудности для его широкого использования. Однако, стремительное развитие различных химических подходов синтеза открывает новые возможности в получении таких материалов, особенно в виде керамики, стеклокерамики, а так же ультрадисперсных порошков и различных композитных материалов, что открывает новые возможности для их использования.

В соответствии с вышесказанным целью настоящей работы являлась разработка метода синтеза тонкодисперсного порошка иодида бария, активированного ионами Eu^{2+} , и исследование влияния условий синтеза (режим термообработки, концентрация иона-активатора, морфология частиц прекурсора и др.) на их спектрально-люминесцентные свойства.

Порошки $BaI_2:Eu$ получали термообработкой при 360–400°C прекурсора ($BaCO_3:Eu$) в присутствии иодирующего агента (NH_4I) в инертной атмосфере. $BaCO_3:Eu$ получали обратным осаждением смеси водных растворов $Ba(NO_3)_2$ и $Eu(NO_3)_3$ в раствор гидрокарбоната аммония. СЭМ снимок морфологии получаемых порошков представлен на рисунке 1.

Как видно из рисунка, прекурсор состоит из палочкообразных агрегатов, средний размер которых составляет 2 мкм, собранных в обособленные друг от друга конгломераты округлой формы размером 10.1 ± 0.8 мкм. Строение частиц $BaCO_3:Eu$ позволяет предположить, что они формируются по механизму коллоидной агрегации.

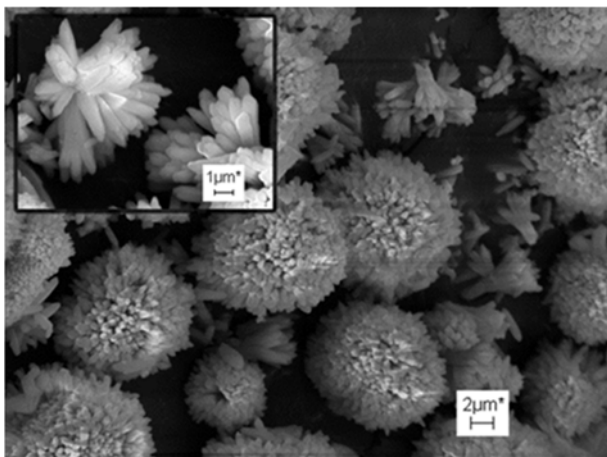


Рис. 1 – СЭМ снимок частиц BaCO₃:Eu

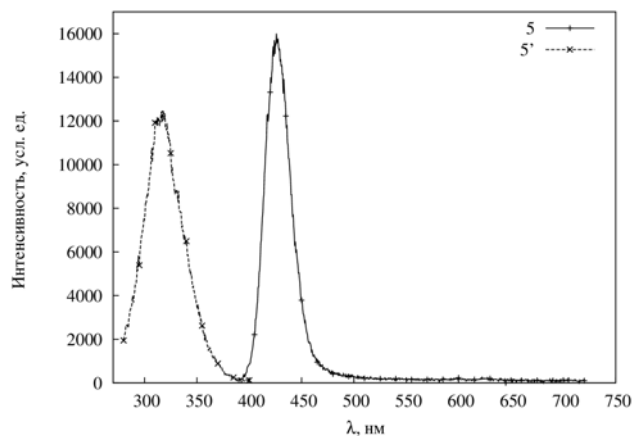
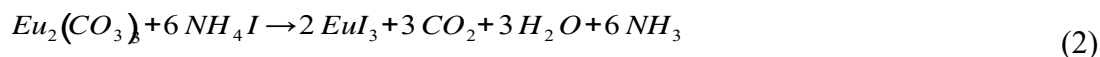
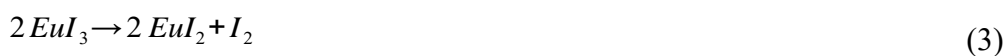


Рис. 2 – Спектр возбуждения люминесценции (5') и люминесценции (5) образца BaI₂:Eu с концентрацией ионов Eu 5 ат. %.

По данным РФА установлено, что формируемые в процессе термообработки BaCO₃:Eu и NH₄I порошки представляют собой кристаллогидрат BaI₂:Eu·2H₂O. Формирование кристаллогидрата связано с выделением воды в соответствии с уравнениями (1) и (2).



Как видно из рисунка 2, спектр возбуждения люминесценции образца BaI₂:Eu·2H₂O симметричен, с максимумом при 316 нм, полоса люминесценции с максимумом при 426 нм симметрична, характерна только для ионов Eu²⁺. Отсутствие полосы люминесценции, характерной для ионов Eu³⁺ по-видимому обусловлено разложением формируемого в процессе термообработки EuI₃ до EuI₂ в соответствии с уравнением 3.



Работы выполнены при поддержке БРФФИ, грант X14M-034.

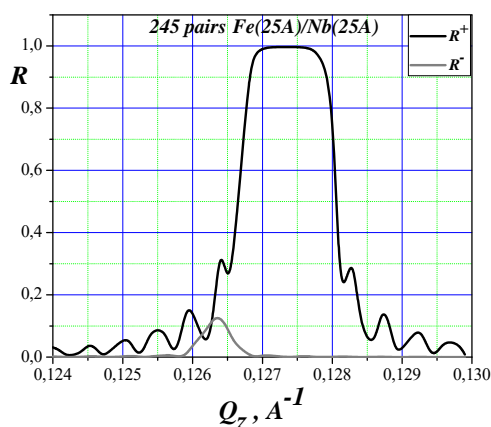
MULTILAYER NEUTRON MONOCHROMATOR-POLARIZER ON THE BASIS OF IRON

Kyaw Zaw Lin¹, V.G. Syromyatnikov^{1,2}

¹ SPSU (Saint Petersburg State University)

² PNPI (Petersburg Nuclear Physics Institute NRC “Kurchatov Institute”)

In this paper the multilayered neutron monochromator polarizer consisting of 490 alternating layers of iron and niobium is offered. Each layer of Fe and Nb has thickness 25 Å. Use of thin layers in the period of structure will allow to receive the reflected Bragg’s peaks with high resolution on wavelength. Existence of identical thickness of layers in the period allows to avoid the Bragg’s peaks of even orders. Parameters of the first Bragg peak for eight model neutron monochromators-polarizers on the basis of iron and cobalt are given in work. Calculated curves show that the first Bragg peak reflected from structure of Fe/Nb has relative half-width of 1.1%, the maximum coefficient of reflection 0.997 and the polarizing efficiency 0.999. Also the first experimental curves of coefficient of reflection of neutrons from structure of Fe/Nb depending on the momentum transfer are given.



A P P L I E D S T U D I E S

HIGH RESOLUTION CORRELATION FOURIER DIFFRACTOMETRY FOR ADVANCED MATERIALS CHARACTERIZATION

G. Bokuchava

Frank Laboratory of Neutron Physics, Joint Institute for Nuclear Research, Dubna, Russia

For the practical applications of many modern high-technological materials, it is vital to control their physical and mechanical properties, which are greatly dependent on the peculiarities of their microstructures. The neutron diffraction has a great potential for the investigation of the microstructural parameters of various constructional materials due to some important advantages of the method: high penetration power of the neutrons, good spatial resolution, applicability for multiphase materials (composites, ceramics, alloys, etc.), non-destructive character of the method, possibility to study materials microstructure and defects (microstrain, coherently scattering crystallite size, dislocation density, etc.). In combination with the time-of-flight (TOF) technique at pulsed neutron sources, this method allows to determine lattice strains along different (hkl) directions simultaneously, i.e. to investigate mechanical anisotropy of crystalline materials on a microscopic scale. In current work several typical examples of materials microstructure studies performed on Fourier Stress Diffractometer (FSD) [1] at the IBR-2 pulsed reactor in FLNP JINR (Dubna, Russia) were given.

The work was supported by Russian Foundation for Basic Research and the Moscow Region Government (project No. 14-42-03585_r_center_a).

[1] G.D. Bokuchava et al., Appl. Phys. A: Mat. Sci. & Proc., 74 [Suppl1], s86-s88 (2002).

[2] G.D. Bokuchava et al., J. of Surf. Inv. X-ray, Synch. & Neutr. Tech., 9(1), 44-52 (2015).

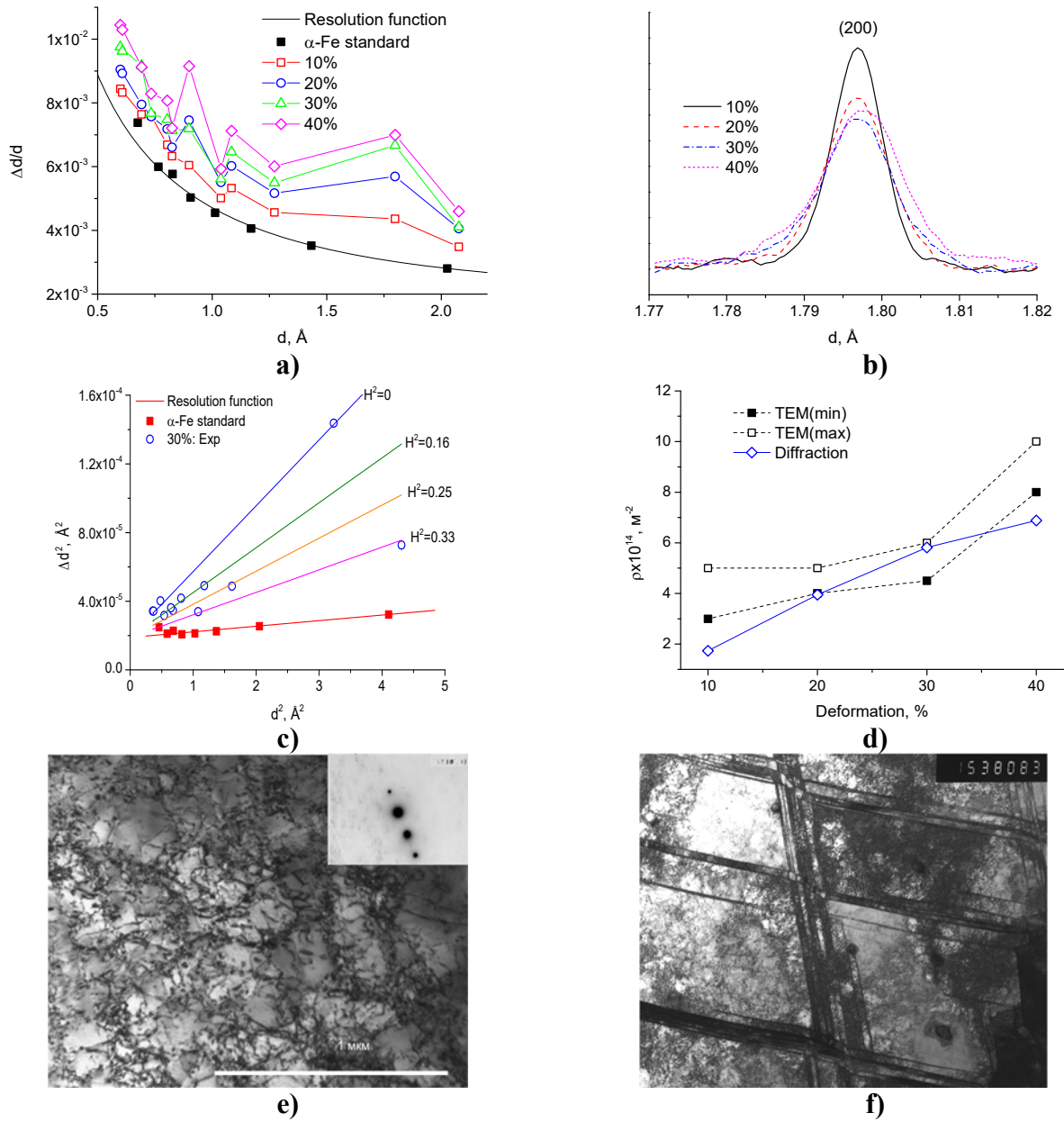


Fig. 1. **a)** Resolution function for 16Cr-15Ni-3Mo-1Ti austenitic steel specimens at different degrees of plastic deformation [2]. **b)** The shape of diffraction peak (200) vs. plastic deformation degree. **c)** Δd^2 vs. d^2 for austenitic steel specimen with 30% of deformation. **d)** Dislocation density estimated from neutron diffraction and TEM data. TEM images of 16Cr-15Ni-3Mo-1Ti steel deformed by 10% **(e)** and 30% **(f)**.

NEUTRON DIFFRACTION CHARACTERIZATION OF RESIDUAL STRESS AND MICROSTRUCTURE IN RECONSTITUTED CHARPY SPECIMENS

Gizo Bokuchava¹, Igor Papushkin¹, Peter Petrov²

¹*Frank Laboratory of Neutron Physics, Joint Institute for Nuclear Research, Dubna, Russia*

²*Institute of Electronics of Bulgarian Academy of Sciences, Sofia, Bulgaria*

One of the pressing problems of modern nuclear power engineering is control of the reactor vessel metal condition during its lifetime and guarantee of the reactor vessel integrity under normal operating conditions, as well as during any design accidents. This is a prerequisite for the safe operation of a shell-type nuclear reactor. Usually the hull steel deteriorates under the neutron irradiation. Therefore, the program of surveillance specimens, which are located at the inner wall of the reactor cavity, is an important source of information about reactor steel properties changes. Typically, surveillance specimens program based on analysis of their mechanical tests results provides verification of the project design characteristics of brittle fracture resistance, evaluation of the reactor vessel functionality, and the material testing maintenance of its operation for the whole project period. However, the surveillance samples test results and radiation exposure monitoring data often indicate the possibility of extending the service life over the project period. At the same time, support of reactor vessel operation beyond the project period usually is not provided within the regular program. In this connection, the problem of surveillance samples reconstitution after mechanical tests using various types of welding techniques (arc stud welding, electron and laser beam welding, etc.) becomes especially important. The purpose of such a reconstruction is to increase the number of irradiated reactor vessel steel samples to obtain representative and reliable data that are used to estimate the radiation embrittlement of reactor vessel material for confirmation or prolongation of its operation life.

It should be noted that the reconstruction technology should not significantly alter the structure and mechanical properties of the material to maintain the representativeness of the data. Therefore, it is necessary to control the level of residual stresses after welding in the reconstituted surveillance specimens. However, during fusion welding residual stresses are definitely generated in almost any welded joints. Usually residual stresses are formed in welded structures as the result of differential contractions, which occur as the weld metal solidifies, and cools down to the ambient temperature. The use of a electron or photon flux in at power densities $\geq 10^6$ W/cm, for electron or laser beam welding, allows one to reduce residual stress level occurring during welding. The use of a lower heat input, e.g. electron or laser beam welding, allows one to reduce residual stress level occurring during welding. At present in the literature there is lack of information about residual stress distribution after electron and laser beam welding.

In order to evaluate feasibility of different welding methods the residual stress level in specimens welded by various techniques should be estimated. Therefore, the main aim of this work was the experimental determination of residual stress distribution and microstructural changes in the test Charpy specimens reconstituted by electron beam (EBW), laser beam (LBW) and arc stud (ASW) welding methods using high resolution neutron diffraction. The experiments were performed on the FSD Fourier diffractometer at the IBR-2 fast pulsed reactor in FLNP JINR (Dubna, Russia). The obtained results confirmed that EBW demonstrates high quality of weld seams and the lowest level of the residual stress as compared to other welding techniques. Apparently, this is due to the small amount of introduced heat at the EBW process (4-5 times lower than, for example, during

ASW), resulting in dramatically reduced deformation of the final product. As expected, for all specimens the residual stress is falling down in regions remote from the weld area. It was found that peak broadening at the centre of a welded joint is often observed due to the change in the material's microstructure during weld process. From the diffraction peak broadening the residual microstrain level was evaluated which directly characterizes the dislocation density in the studied material. As it was expected, the positions of maxima in the microstrain distributions are in good agreement with the positions of the weld centres for all studied specimens. Such microstructural change near weld region is often confirmed by microhardness increase because of martensitic (or martensitic-bainitic) structure forming in weld region and HAZ. Usually this process is followed by increase in dislocation density in material, which in turn affects the diffraction peak broadening effects.

Acknowledgements. The work was supported by RFBR grant No. 15-08-06418_a and Bulgarian Nuclear Regulatory Agency.

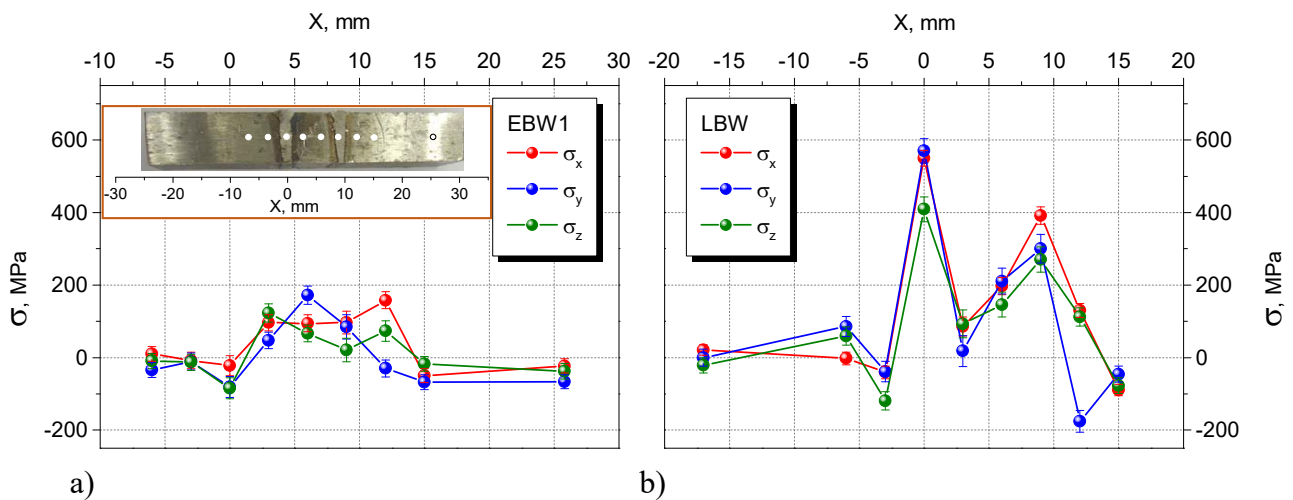


Fig. 2. Residual stress distribution in test Charpy specimens (10x10x55 mm) reconstituted by electron (a) and laser (b) beam welding. Inset: studied Charpy specimen (EBW) with marked scan points.

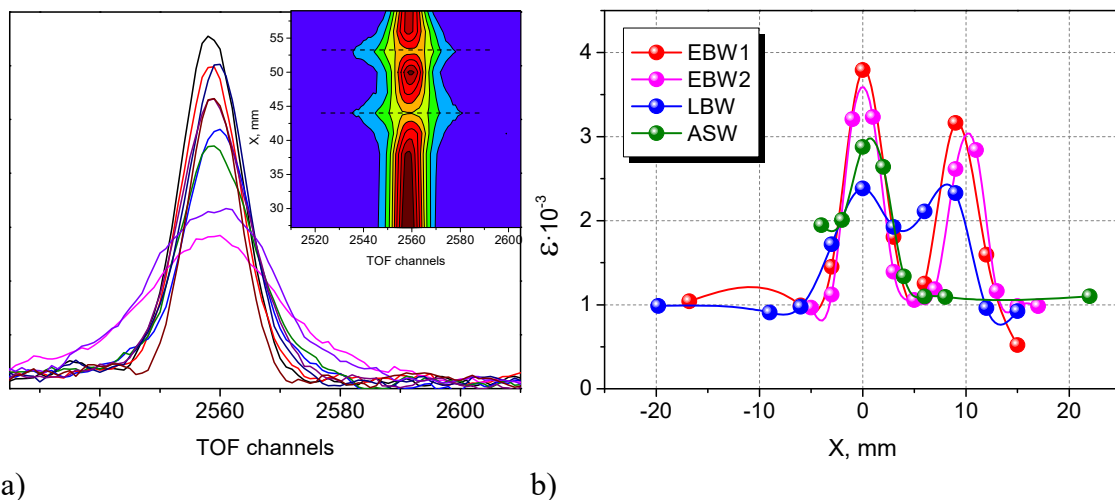


Fig. 3. a) The shape of diffraction peak (110) during scanning across welds. Inset: 3D intensity map of the neutron diffraction pattern near (110) reflection during scan across weld seam. The horizontal dashed lines indicate the positions of the centers of weld seams. b) Residual microstrain distribution in all studied Charpy specimens. The weld seams centers are located at X = 0 mm and X = 10 mm.

INVESTIGATION OF RESIDUAL STRESS IN FORMULA 1 RACING CAR GEARWHEEL WELDED BY ELECTRON BEAM

Igor Papushkin¹, Darina Kaisheva², Gizo Bokuchava¹, Peter Petrov³

¹*Frank Laboratory of Neutron Physics, Joint Institute for Nuclear Research, Joliot-Curie str. 6, Dubna, Russia*

²*South-West University "Neofit Rilski", 66 Ivan Mihailov Str., 2700 Blagoevgrad, Bulgaria*

³*Institute of Electronics of Bulgarian Academy of Sciences, 72 Tzarigradsko Chaussee, 1784 Sofia, Bulgaria*

During manufacturing industrial components and units various technological operations are used in order to improve materials and service properties and lifetime of the detail. One of the important operations is welding which is a potentially beneficial fastening process for many industrial applications as it reduces weight as well as saves cost. However during welding, a substantial residual stress field may develop, as it necessarily involves large temperature gradients from weld metal to bulk material. The welding thermal cycle generates inhomogeneous heating and cooling in the regions near the heat source, thus causing residual stress in the weldment. It is well known that welding residual stresses are detrimental to the integrity and fitness-for-service of welded industrial structures due to their susceptibility to fracture criterion, fatigue, hydrogen-induced cracking and stress-corrosion cracking. Thus, the quantitative measurement of welding residual stress is very important for the safe and economical operation of various industrial structures.

Electron and laser beam welding have a number of advantages over conventional welding techniques. Achieve the high energy density means that narrow welds and heat-affected zones (HAZ) can be obtained [1]. Electron beam welding (EBW) gives high quality welds and it could be taken as a reference welding method. In last years, it was also demonstrated that laser welding with a powerful CO₂ laser system can be successfully applied for various industrial applications. It should be pointed out that all these methods give a satisfactory weld quality and heat affected zone size (HAZ). For example, during the beam welding the temperature of the "to-be-tested" reactor vessel material has to remain below the reactor operating temperature in order to avoid effects of annealing that would induce changes in the material properties. Careful selection of the welding parameters and optimization of the heat input allows reduction of the width of the weld and HAZ and allows one to lower the maximum temperature in the specimens during welding.

In our recent studies [2-4] it was found that EBW demonstrates high quality of weld seams and the lowest level of the residual stress as compared to other welding techniques. Apparently, this is due to the small amount of introduced heat at the EBW process (4-5 times lower than, for example, during arc stud welding), resulting in dramatically reduced deformation of the final product. Therefore, the EBW technique can be widely used for various industrial applications. In order to select suitable welding parameters and, consequently, optimal stress distribution in welded joints the neutron diffraction method is of great importance providing nondestructive and precise residual stress evaluation.



Fig. 4. Photography of the welded gear. Right: photo made during the experiment

In this study, non-destructive neutron diffraction method was used to determine residual stresses in gearwheel car transmission. The sample is a wheel used in the gear box of sport cars. A gear wheel has a protruding shaft. The disk is mounted on the shaft and welded by electron beam welding. Then the weld area is subjected to final heat treatment. Residual strains and stresses occurring during welding process have a strong impact on the performance properties of the detail. Therefore it is necessary to perform post-weld heat treatment to reduce the welding residual stress, or during welding process sequentially put two welds to compensate the stresses. Failure to execute additional conditions lead to appearance of cracks delayed fracture in the weld or heat affected zone. For this reason, knowledge of residual stress level and distribution is very important for electron beam welding process optimization.

Therefore, the main aim of this work was the experimental determination of residual stress distribution and microstructural changes in the gear wheel welded by electron beam using high resolution neutron diffraction. Fig. 1 shows photography of the welded gear. The product is a toothed wheel with a protruding shaft on one side. Disc is put on the shaft adjacent to the gear wheel and welded by electron beam.

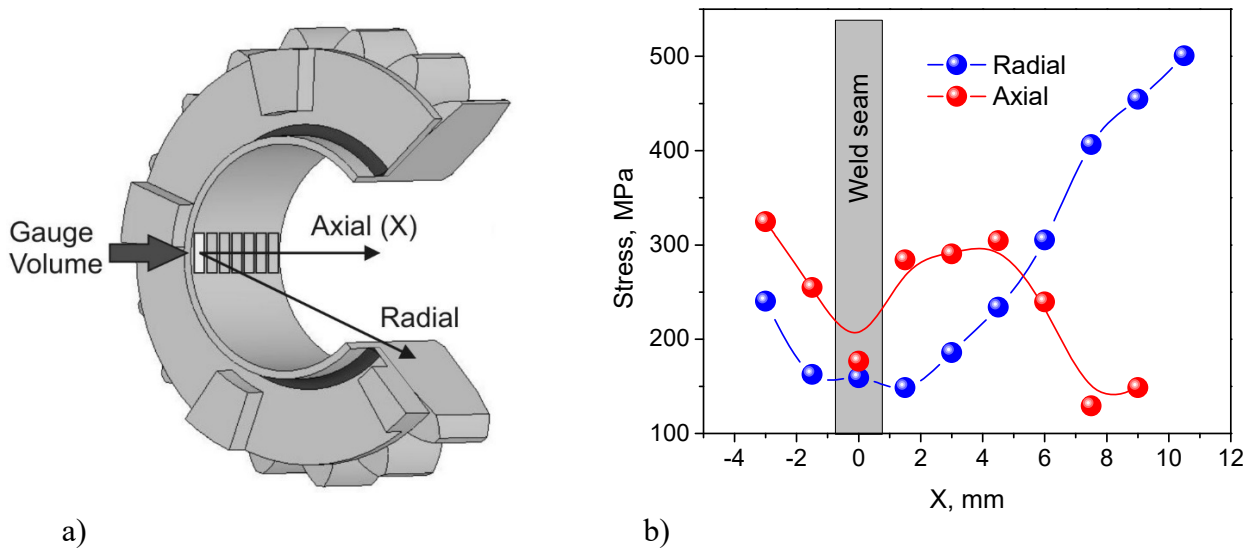


Fig. 5. a) Scheme of residual stress measurement in gear wheel sample. b) Residual stress distribution in the sample.

The neutron diffraction method allowed evaluating the stresses distribution in the radial and axial components of the circularly welded gear. Feature of this study was to carry out experiments to determine the residual stress without destroying the sample. It should be noted that in later this detail will be exploited in the real gearbox of a sports car and, therefore, its structural integrity is very important. Analysis of diffraction peak broadening gives quite low level of residual microstrain, which ensures the absence of cold cracking in the weld zone. The data will be useful for the analysis of the performance of the built-in gear transmission for sports cars.

The experiments were performed on the FSD Fourier diffractometer at the IBR-2 fast pulsed reactor in FLNP JINR (Dubna, Russia). Electron beam welding was carried out in Institute of Electronics of Bulgarian Academy of Sciences (Sofia, Bulgaria).

Acknowledgements. The work was partially supported by RFBR (grant No. 15-08-06418_a) and Bulgarian Nuclear Regulatory Agency.

- [1] Petrov P., “Advanced welding processes for reconstitution Charpy test specimens”, **Welding in the world**, Vol.52, pp. 365-370 (2008).
- [2] Gizo Bokuchava, Igor Papushkin, Andrew Venter, Peter Petrov, “*Residual stress studies in electron beam welding using neutron diffraction*”, **Journal of Materials Science and Technology**, 2014, Vol. 22, No. 1, pp. 3-11. ISSN 0861-9786.
- [3] Gizo Bokuchava, Igor Papushkin, Peter Petrov, “*Residual Stress Study by Neutron Diffraction in the Charpy Specimens Reconstructed by Various Welding Methods*”, **Comptes rendus de l'Académie bulgare des Sciences**, 2014, Vol. 67, Issue No. 6, pp. 763-768. ISSN 1310-1331.

CRYSTALLOGRAPHIC PREFERRED ORIENTATIONS AND ELASTIC ANISOTROPY OF SHEET SILICATE BEARING ROCKS

R. Vasin¹, T. Lokajiček², T. Svitek², H.-R. Wenk³

¹*Joint Institute for Nuclear Research, Dubna, Russia*

²*Institute of Geology of the CAS*

³*UC Berkeley*

E-mail: olddragon@mail.ru

Studies of the elastic anisotropy of rocks are important for understanding the internal structure of the Earth, seismology and earthquake physics, geophysical prospecting. Rocks containing sheet silicates attract most attention. Sheet silicates are characterized by high anisotropy of elastic properties, specific grain morphology and strong preferred orientations of grains. Due to high penetration depth of thermal neutrons, these preferred orientations could be studied in bulk rocks. Data analysis methods, such as that realized in the MAUD software [1] allow to extract from neutron diffraction data preferred orientations of all minerals composing the rock, as well as mineral volume fractions, crystallographic information. With sophisticated self-consistent routines, e.g., GeoMixSelf [2] it is possible to include all the quantitative information on textures and morphological features of rock into the model of its bulk elastic properties. Pores and cracks could also be accounted for. In this contribution, we demonstrate the results of multimineral rock measurements on SKAT texture diffractometer in Frank Laboratory of Neutron Physics (JINR, Dubna) [3]. Obtained data are used in bulk elastic properties modeling that are compared with elastic wave velocities measurements at different pressures [4]. From this comparison, important information on porosity could be derived. It is shown, that the biggest source of discrepancy between the model and ultrasonic experiment are uncertainties in single crystal elastic properties.

[1] Lutterotti L., Matthies S., Wenk H.-R., Schultz A. S., Richardson J.W. Combined texture and structure analysis of deformed limestone from time-of-flight neutron diffraction spectra. *J. Appl. Phys.* (1997) 81, 594-600.

[2] Matthies S. GEO-MIX-SELF calculations of the elastic properties of a textured graphite sample at different hydrostatic pressures. *J. Appl. Cryst.* (2012) 45, 1-16.

[3] Keppler R., Ullemeyer K., Behrmann J.H., Stipp M. Potential of full pattern fit methods for the texture analysis of geological materials: implications from texture measurements at the recently upgraded neutron time-of-flight diffractometer SKAT. *J. Appl. Cryst.* (2014) 47, 1520-1534.

[4] Lokajicek T., Svitek T. Laboratory measurement of elastic anisotropy on spherical rock samples by longitudinal and transverse sounding under confining pressure. *Ultrasonics* (2015) 56, 294-302.

PRECISE DETERMINATION OF MICROSTRUCTURAL CHARACTERISTICS FROM REVERSE TIME-OF-FLIGHT NEUTRON DIFFRACTION DATA

R. Vasin¹, A. Balagurov¹, I. Bobrikov¹, M. Leoni², S. Sumnikov¹

¹*Joint Institute for Nuclear Research, Dubna, Russia*

²*DICAM, University of Trento*

³*UC Berkeley*

E-mail: olddragon@mail.ru

Different microstructural peculiarities of materials – small crystallite size, dislocations, stacking faults, etc. – are reflected in the shapes of diffraction peaks and could be studied with peak profile analysis methods. During time, X-ray and synchrotron diffraction have posed themselves as very good methods for the microstructure analysis due to their high resolution. High-resolution neutron diffraction at both continuous (with monochromatic beam) and pulsed (with TOF technique) sources also can be used for peak profile analysis. Our experience shows that new developments in the correlation Fourier method (RTOF – reverse time of flight with fast Fourier chopper [1]) made possible doing a precise profile analysis of diffraction peaks. Among positive features of this technique are absence of long ‘tails’ of diffraction lines and practically constant $\Delta d/d$ resolution in wide d-spacing range.

In this contribution, we demonstrate the application of WPPM method [2] realized in the PM2K software [3] to the analysis of HRFD (High-Resolution Fourier Diffractometer [1]) data of several powder samples. Main challenges in the adaptation of the method and software to this analysis were proper account for the HRFD resolution function [4] and non-Poisson statistics. Neutron diffraction experiments and data processing in FLNP JINR within the framework of this research are supported by RFBF project 14-29-04091.

[1] Balagurov A. M. High-resolution Fourier diffraction at the IBR-2 reactor. *Neutron News*. (2005) 16, 8–12.

[2] Scardi P., Leoni M. Whole powder pattern modelling. *Acta Cryst.* (2002). A58, 190-200.

[3] Leoni M., Confente T., Scardi P. PM2K: a flexible program implementing Whole Powder Pattern Modelling. *Zeitschrift Für Krist. Suppl.* (2006). 23, 249–254.

[4] Balagurov A.M., Kudryashev V.A. Correlation Fourier diffractometry for long-pulse neutron sources: a new concept. ICANS-XIX conference, Grindelwald, Switzerland (2010).

C A R B O N N A N O S Y S T E M S

EXPERIMENTAL ASPECTS OF INVESTIGATIONS OF FULLERENE SOLUTIONS

J. Narmandakh^{1,2}, T.V. Tropin¹, O.A. Ivankov^{1,4}, R.A. Eremin¹, M.V. Avdeev¹, V. L. Aksenov^{1,3}

¹*Frank Laboratory of Neutron Physics, Joint Institute for Nuclear Research, Dubna, Russia*

²*Institute of Physics and Technology, Mongolian Academy Sciences, Ulaanbaatar, Mongolia*

³*Petersburg Nuclear Physics Institute, National Research Centre “Kurchatov Institute”, Gatchina, Russia*

⁴*Kyiv Taras Shevchenko National University, Kyiv, Ukraine*

Nowadays, the third allotropic carbon compounds, called fullerenes, have been playing the main role in various research areas. Particularly, the investigations of fullerene C₆₀ and C₇₀ in different solvents have grown up intensively due to their unique properties [1, 2]. A large number of effects, such as cluster formation, solvatochromic effects, nonlinear dissolution properties etc., were investigated in the last few years [4-6]. The kinetics of dissolution and cluster formation of fullerene in different solutions by various methods are reported in the present work.

Small-angle neutron scattering is one of the most conventional methods for studying of the nanostructures in fullerene solutions. The investigation of cluster size of fullerene C₇₀ in CS₂ solvent were performed at the YuMO instrument of the IBR-2 reactor. The value of the gyration radius (R_g) was evaluated from SANS data to be in the range of 3.32-5.56 Å, depending on sample preparation procedure. In general, the obtained R_g values are considered to be in close agreement with similar experimental results [7] and theoretical estimates.

The kinetics of dissolution of fullerene in solutions weren't completely explained so far. In our previous work [6], the kinetics of dissolution were investigated for fullerene in non-polar and low polar solvents. In the present work, we investigated kinetics of dissolution processes in C₆₀/NMP solutions of various concentrations at different temperatures and stirring speeds by UV-Vis spectrometry. The modeled absorption peak values give the possibility of definition of kinetics of dissolution. The obtained results will allow one in the future to take account of these effects while modeling the kinetics of slow growth of large clusters in C₆₀/NMP solutions.

[1] Beck M.T., Mandi, G., Fullerene Sci. and Technol., (1997), 5(2), 291-310.

[2] Avdeev, M.V., Khokhryakov, A.A., Tropin, T.V., Andrievsky G.V., et al., Langmuir, (2004), 20, 4363–4368.

[3] Andrievsky, G.V., Klochkov, V.K., Karyakina, E.L., Mchedlov-Petrossyan, N.O., Chem. Phys. Lett., (1999), 300, 392-396.

[4] Kyzyma, O.A., Korobov, M.V., Avdeev, M.V., Garamus, V.M., Petrenko, V.I., Aksenov, V.L., Bulavin, L.A., Fullerenes, Nanotubes and Carbon Nanostructures, (2010), 18, 458-461.

[5] Tropin, T. V., Jargalan, N., Avdeev, M. V., Kyzyma, O. A., Sangaa, D., Aksenov, V. L., Physics of the Solid State, (2014), 56, 148-151.

[6] Jargalan, N., Tropin, T. V., Avdeev, M. V., Aksenov, V. L., Journal of Surface Investigation: X-ray, Synchrotron and Neutron Techniques, (2015), 1, 16-20.

[7] Affholter, K.A., Henderson, S.J., Wignall, et al., J. Chem. Phys., (1993), 99: 9224.

DETONATION NANODIAMONDS IN AQUEOUS SUSPENSIONS BY SANS

O. Tomchuk

Physics Department, National Taras Shevchenko University of Kyiv

E-mai: tomchuk@jinr.ru

A continuous spatial transition from sp³ (bulk) to sp² (surface) carbon structure in detonation nanodiamond (DND) is proposed on the basis of small-angle neutron scattering (SANS) analysis. The SANS contrast variation on DND dispersed in different liquids (water, dimethylsulphoxide) reveals the same shift in the mean scattering length density (SLD) of DND towards the lower value as compared to pure diamond (sp³ state of carbon), which is related to the presence of a non-diamond component in the DND structure. Carbon at the DND surface is characterized by the graphitic sp² state, which means that there should be some spatial transition from sp³ to sp² states within the particle volume. Assuming the ‘core-shell’ structure of quasi-spherical and polydisperse DND particles, which suggests a sharp boundary between the diamond ‘core’ and graphite ‘shell’ (30 vol. % as revealed from the mean SLD shift), and taking into account the experimentally found particle size of 7 nm, one obtains reasonable 0.4 nm for the thickness of the graphite shell. At the same time, the diffusive character of the particle surface is deduced basing on the deviation from the Porod law. This suggests a more complex modulation of the sp³–sp² transition as compared to the ‘core-shell’ representation. As a result, the continuous (without any strict boundary) SLD profile of the power-law type describing the diffusive surface is concluded. Still, a specific feature of the profile at the particle boundary reflects that non-diamond states are concentrated mainly close to the particle surface, which explains quite good precision of the ‘core-shell’ approximation with respect to the mean SLD. The found transition is consistent with the previous data of ab initio computer simulations for diamond nanocrystals (size up to 3.3 nm) which showed that the most stable structures require the existence of sp^{2+x} bonds over the crystalline volume.

C O M P U T A T I O N A L S T U D I E S

STRUCTURAL PROPERTIES OF ELASTOMERIC MEMBRANES BASED ON SILICONE RUBBER USING SMALL-ANGLE NEUTRON SCATTERING

E. Anitas¹, I. Bica¹, R. Erhan¹, M. Bunoiu¹, A. Kuklin¹

¹ *Joint Institute for Nuclear Research, Dubna, Russia*

² *West University of Timisoara, Romania*

E-mail: eanitasro@gmail.com

The morphology of elastomeric membranes based on silicone rubber, at various concentrations of the catalyst (C) is determined by small-angle neutron scattering (SANS) technique. In the investigated q -range, nearly all membranes display a hierarchical organization of crystallites in which ramified mesoscale mass fractals are composed of either mass or surface-like fractals nanoclusters. We use the Beaucage model in order to extract information about the fractal dimensions of the clusters. We show that the fractal dimension of the mesoscale fractal is fixed at and is independent with the addition of C. However, the nanoscale fractals are characterized by a transition from mass to surface-like fractals at high values of C concentrations.

SCATTERING FROM SURFACE FRACTALS

Yu. Cherny^{*}, E. M. Anitas, V. A. Osipov and A. I. Kuklin

Bogoliubov Laboratory of Theoretical Physics

E-mail: cherny@theor.jinr.ru

It is shown that small-angle scattering (SAS) from surface fractals can be explained in terms of the power-law type polydispersity. The power-law decay of the scattering intensity $I(q) \propto q^{D_s-6}$, where $2 < D_s < 3$ is the surface fractal dimension of the system, is realized as a non-coherent superposition of three-dimensional objects obeying a power-law distribution $dN(r) \propto r^{-\tau} dr$, with $D_s = \tau - 1$. The distribution is continuous for random fractals and discrete for deterministic surface fractals, since the deterministic fractals are shown to be constructed as a sum of deterministic mass fractals of subsequent iterations. As an example, the surface fractal is constructed by means of superposition of three-dimensional mass Cantor sets and its fractal scattering properties are studied. We suggest the two-dimensional version of the Cantor surface fractal and of the Koch snowflake. The present analysis allows us to extract additional information from SAS data, such as the edges of the fractal region, the fractal iteration number and the scaling factor. We derive an analytical expression for the radius of gyration of three-dimensional Cantor surface fractal.

TO THE QUESTION OF CONFORMATIONAL EQUILIBRIUM AND POLYMORPH'S STATES IN THE SOLID STATE AND UNDER THE MATRIX CONDITIONS

A. Kwocz,^a D. Chudoba,^{c,d} Ł. Hetmańczyk,^e P. Szklarz,^b A. Filarowski^{a,d}

^a Faculty of Chemistry, University of Wrocław, 14 F. Joliot-Curie st., 50-383 Wrocław, Poland.

^c Faculty of Physics, A. Mickiewicz University, Umultowska 85, 61-614 Poznań, Poland.

^d Frank Laboratory of Neutron Physics, JINR, 141980 Dubna, Russia.

^e Jagiellonian University, Faculty of Chemistry, Ingardena 3, 30-060 Kraków, Poland.

The nitro derivative of ortho-hydroxy acetophenone has been studied by experimental and theoretical methods. Two polymorphic forms of this compound have been obtained by evaporation of polar and non-polar solutions. Both polymorphs have been investigated by Infrared (IR), Raman, Incoherent Inelastic Neutron Scattering (IINS), X-ray, differential scanning calorimetry (DSC) and density functional theory (DFT) methods. In one of the polymorphs the existence of a phase transition has been shown by DSC method. The potential energy curves on rotation and isomerization have been calculated by DFT calculations for estimation of barriers of the conformational change and adjustment. A complete spectral analysis of vibrational spectra has been accomplished. The infrared spectra have been measured in a wide temperature range in order to reveal the spectral bands most sensitive to a phase transition. The dynamics of the nitro group and its affect on the crystal state of the studied compound have been analysed. On the basis of the abovementioned studies the nature of the phase transition has been explained.

L A Y E R E D N A N O S T R U C T U R E S

STRUCTURAL AND PHASE CHARACTERIZATION OF POROUS CO/PD MULTILAYERED THIN FILMS

A. Maximenko^{1,2}, J. Fedotova², M. Marszałek¹, O. Kupreeva³, S. Lazarouk³, A. Zarzycki¹, S. Zavadski³, J. Kasiuk², V. Bayev²

¹*The Henryk Niewodniczanski Institute of Nuclear Physics PAS, Krakow, Poland*

²*National Centre for Particle and High Energy Physics of BSU, Minsk, Belarus*

³*Belarusian State University of Informatics and Radioelectronics, Minsk, Belarus*

The development of information and communication technologies requires increasing the efficiency of data storage. At the moment, one of the main strategies in storage technology is perpendicular magnetic recording utilizing materials with perpendicular magnetic anisotropy (PMA). Due to the growing demand for storage volumes, a continuing trend of reducing the size of the unit cell memory is observed the last few years. However, this approach inevitably faces the problem of so called superparamagnetic limit – undesirable thermally-induced fluctuations of magnetic moment when unit cell size falls below 10 nm. That is why a search of new technologies to overcome this limit is the important research challenge in data storage field nowadays. One of the most promising approaches is when the recording medium is formed not by the separated islands of the magnetic material (bits of information) but by the magnetic domains that are created and localized by perforating continuous exchange-coupled magnetic films with PMA. The orientation of magnetic moments is additionally supported by its pining on defects (holes of a magnetic film). The planar magnetic systems based on this effect are denoted as “antidots” [1, 2].

Our research is focused on study of Co/Pd multilayered antidot arrays with perpendicular magnetic anisotropy of prepared by template-assisted thermal evaporation on porous TiO₂ wafers. Two kinds of porous and continuous Pd_{10 nm}/[Co_{0.3 nm}/Pd_{1 nm}]₁₅/Pd_{2 nm} and Pd_{10 nm}/[Co_{0.3 nm}/Pd_{0.55 nm}]₁₅/Pd_{2 nm} films with 10 nm Pd seed layer and 2 nm Pd protective cap layer were synthesized on porous TiO₂ templates and Si/SiO₂ smooth wafers in order to determine the effect of the porous morphology on magnetic properties. Using various magnetic techniques (SQUID, magnetic resonance spectroscopy, magnetic force microscopy) it was established that both porous and continues Co/Pd MLs possess perpendicular magnetic anisotropy with effective uniaxial anisotropy constant over 1.5×10^5 J/m³ typical for [(Co, Fe) – (Pt, Pd)]_n MLs [1].

Structural and phase characterization were made by scanning electron microscopy (SEM) using HITACHI S-4800 at voltage of 15 kV, X-ray reflectivity (XRR) and X-ray diffraction (XRD) performed with two-circle laboratory diffractometer (Panalytical X'Pert Pro) equipped with PW3050/60 vertical goniometer and PW3383/00 X-ray tube (2.2 kW, $\lambda_{Cu} = 1.54056$ Å).

SEM images of initial TiO₂ template (Fig. 1a) and porous Pd/[Co_{0.3 nm}/Pd_{1 nm}]/Pd (fig. 1b and 1c) multilayers demonstrate tubular structure of anodized TiO₂ and porous structure of Co/Pd ML that reflects nanoporous structure of the template. According to SEM results the inner diameter pores in TiO₂ template was ~ 30 nm while the diameter pores in Pd/[Co_{0.3 nm}/Pd_{1 nm}]/Pd sample is ~ 20 nm. Also the fig. 1c shows fine granular structure of Co/Pd ML.

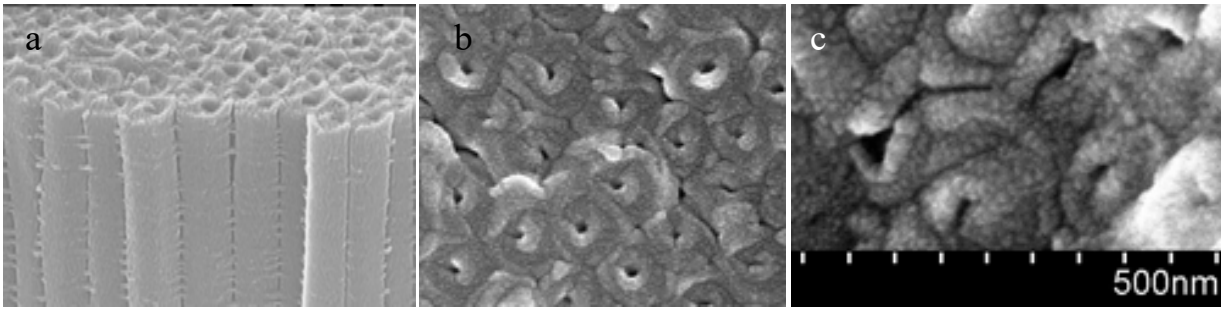


Figure 1 – SEM images of porous TiO₂ template (a), Pd/[Co_{0.3 nm}/Pd_{1 nm}]/Pd film deposited on porous TiO₂ (b) and its high magnification image illustrating granular structure of the multilayer surface (c).

So as XRD patterns of Co/Pd MLs reveal the presence of both Pd and Co_xPd_{100-x} alloy with cubic fcc structure we suppose that Co is diluted in Pd lattice forming a compound structure (quasi-alloy or solid solution) with alternating Co:Pd ratio along the growth direction of MLs. This assumption is confirmed by the XRR results obtained for reference continuous ML films on Si/SiO₂ wafers. The XRR patterns showed typical Kiessig fringes arising from the finite thickness of the multilayers and were fitted by Parrat algorithm [3]. The model based on nominal thicknesses of Pd and Co films showed that the roughness of both interfaces is larger than the nominal thickness of films, most likely due to diffusion of Co atoms into Pd films during the deposition and formation of the CoPd quasi - alloy. Therefore we assumed that the whole stack of Co/Pd films consists of CoPd alloy with thickness equal to the thickness of 15 deposited Co/Pd bilayers.

Thus, present results of structure and phase characterization of porous Co/Pd MLs revealed its compound structure representing CoPd quasi – alloy with alternating metal ratio along the growth direction. Unfortunately X-ray methods are quite uncertain to describe the precise distribution of Co and Pd atoms along the growth direction of MLs playing the decisive role in forming of magnetic properties and specifying perpendicular magnetic anisotropy. We suppose that polarized neutron reflectometry will be able to reveal the peculiarities of local atomic order as well as magnetic moments arrangement in order to improve the technique of preparation of antidot magnetic arrays for perpendicular magnetic recording.

- [1] C. Schulze, M. Faustini, J. Lee, H. Schletter, M. Lutz, P. Krone, M. Gass, K. Sader, A.L. Bleloch, M. Hietschold et.al. // *Nanotechnology*. 2010. V. 21. P. 495701-1.
- [2] M. T. Rahman, N. N. Shams, C. H. Lai, J. Fidler, and D. Suess // *Phys. Rev.* 2010. V. B 81. P. 014418
- [3] L. G. Parratt // *Phys. Rev.* 1954. V. 95. P. 359.

TITANIUM BASED COMPOSITES DEPOSITED BY THERMIONIC VACUUM ARC METHOD INVESTIGATED BY MEANS OF SANS

R. Vladoiu¹, M. Balasoiu^{2,3}, D. Soloviov^{2,4}, A. Mandes¹, V. Dinca¹, A.I. Kuklin²

¹*Department of Plasma Physics, Faculty of Physics, Chemistry, Electronics and Oil Technology, Ovidius University, Mamaia 124, Constanta, 900527, Romania*

²*Joint Institute for Nuclear Research, Dubna, Russia*

³*Horia Hulubei National Institute for Physics and Nuclear Engineering, Bucharest, Romania*

⁴*Taras Shevchenko University, Kiev, Ukraine*

Small-angle neutron scattering (SANS) is a valuable technique for studying nanostructures, which characteristic structural features lies mostly in the interval of 1-100 nm.

In the present paper, for the first time a small-angle neutron scattering (SANS) investigation of the titanium based materials deposited on different substrates and conditions by the TVA method is reported.

Thin film deposition process by thermionic vacuum arc (TVA), an original discharge type in pure vapor plasma, might become one of the most suitable technologies to significantly improve the tribological properties of the surfaces covered with different materials. Due to the deposition in high vacuum conditions and without buffer gas, the films have a high purity, increased adhesion, low friction, low roughness, and a compact nanostructure. Titanium based thin films are envisaged for surface coatings applications requiring low roughness, good smoothness and low friction coefficient.

In Fig.1 the scattering curve from Ti-Ag deposited on a special substrate required by specific industrial applications (OLC 45-stainless steel with 45 percent of carbon inside) is presented.

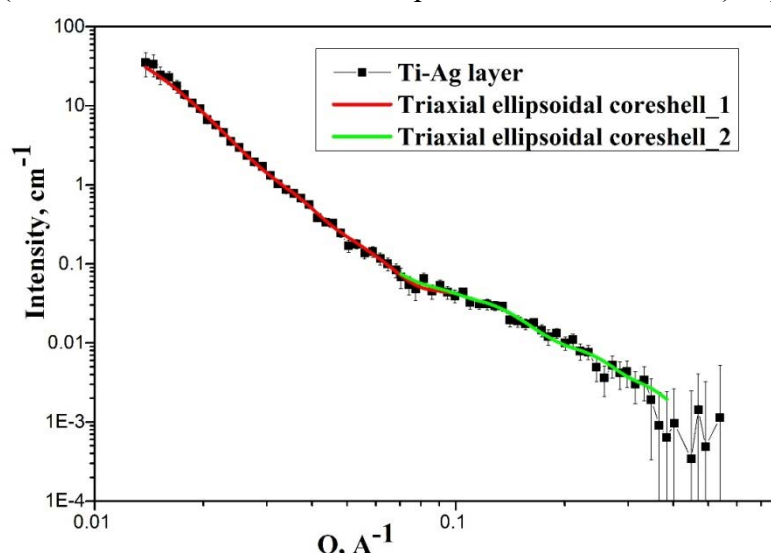


Fig.1 Experimental SANS from Ti-Ag layer and the model curve fittings with FITTER program: (i) experimental data in the range of $0.01 \text{ \AA}^{-1} \leq Q \leq 0.3 \text{ \AA}^{-1}$ (black squares); (ii) triaxial ellipsoidal core-shell fit (red line): another triaxial ellipsoidal core-shell fit (green line)

The preliminary analyzes of the experimental data have shown that the characteristic SANS contribution from the Ti-Ag layer in the range of $0.01 \text{ \AA}^{-1} \leq Q \leq 0.3 \text{ \AA}^{-1}$ reveals different sized nanostructures (see Fig.1). This result indicates promising perspectives for future investigations.

Acknowledgments. This work was supported by the JINR-Romania Scientific Projects Nos. 33/23.01.2015 items 48, 25 and 34/23.01.2015 items 47, 24.

NEUTRON DEPOLARIZATION INVESTIGATIONS OF SPRING EXCHANGE INTERACTION NANOCOMPOSITES

D.Patroi¹, V.D. Zhaketov², Yu.V. Nikitenko², M.M. Codescu¹, E.A. Patroi¹, E. Manta¹

¹*National Institute for R&D in Electrical Engineering, Bucharest, Romania*

²*Joint Institute for Nuclear Research, Dubna, Russia*

E-mail: delia.patroi@icpe-ca.ro

Neutron depolarization of magnetic state of spring exchange interaction nanocomposites based on NdFeB is carried out. It is detected a different behavior for magnetically soft and rigid nanocomposite. Magnetically hard nanocomposite exhibits coercive force equal to field of maximal neutron depolarization and for soft one a maximal depolarization field has value smaller than coercive field. Conclusion is made that it is connected with different magnetization regime and it is important for realization of spring regime. It was carried out also magnetic measurements using vibrating sample magnetometer and X-ray diffraction in order to evaluate the crystallographic phases involved in relationship with the magnetic behavior.

Neutron experiments revealed a ratio between anisotropy field and coercive field of 0.85 which indicates the possibility of the increasing of the magnetic properties by the increasing of the coercive field.

Both, the neutron experiments and classic magnetometry experiments confirmed the existence of the two crystalline phases, evidenced by X-ray diffractometry, being a soft and a hard magnetic phases. The magnetic domains were found to be in order of few microns in relationship with the ratio of 0.85 between the anisotropy and coercive field.

By neutron experiments were evidenced exist islands (with not big volume concentration) with induction 5.2 T, but they not contribute to the global magnetic properties, as it was evidenced by magnetometry experiments. It remains to investigate further, if they are assumed with some particular crystalline phases.

[1] O. Halpern and T. Holstein, On the passage of neutrons through ferromagnets //Phys. Rev. 59 (1941) 960.

[2] M. Rekveldt, Neutron depolarization in magnetic materials //Neutron News, Vol. 4, No. 4 (1993) 15-19.

[3] V.L. Aksenov, E.B. Dokukin, Yu.V. Nikitenko. Neutron depolarization investigations of high-temperature superconductors in the mixed state //Physica B 213&214 (1995) 100-106.

MAGNETIC AND LATTICE EXCITATIONS

TRANSITION FROM SPIN GLASS TO FERROMAGNETIC STATE: INFLUENCE ON TRANSPORT PHENOMENA IN SOME CR DOPED MANGANITES

M.L. Craus, A. Islamov, V. Turchenko, E. Anitas, R. Erhan

Joint Institute for Nuclear Research, Dubna, Russia

E-mail: mihailiviu@yahoo.com

The presence of the multiple electronic states in the magnetoresistive manganites plays an important role in their dependence with the intensity of magnetic field and temperature. Our aim is to establish the correlations between the transition from spin glass to ferromagnetic state on transport phenomena in Cr doped manganites, by using neutron diffraction, small-angle X-ray and neutron scattering (SAXS/SANS). Neutron diffraction has been performed at room temperature, and SAXS and SANS measurements were performed in the range $258 \div 353$ K ($H = 0$). The variation of the molar magnetization and of the resistance with temperature and intensity of the applied magnetic field were determined by using a Foner type magnetometer and, respectively, the four probes method between 77 and 400 K, at $H_{\max} = 1$ T.

We observed a monotonous decrease of the lattice constants and of the unit cell volume with the increase of the Cr concentration. Variation of molar magnetization with temperature at relatively low magnetic fields shows a dependence on the thermal history of the samples, attributed to the transformation from the ferromagnetic to spin glass state. A large variation of the resistance with the magnetic field intensity was observed near room temperature for all investigated manganites.

For samples with $x = 0.05, 0.10, 0.15$ and 0.20 , the SANS data allows us to obtain the volume fraction of the magnetic phase using the Porod invariant. An interesting behavior can be observed for $x = 0.15$ sample, where we obtain the power-law decay scattering exponent $\alpha \approx 2$ for $T = 293$ K, which indicates the formation of 2D disk-like structures. We found that for $x = 0.00, 0.05$ and 0.20 at $T = 343$ K, we have $\alpha = 1$ and show that the magnetic nano-domains have a 1D rod-like shape with the radius in the range $2.5 - 5 \text{ \AA}$ and the height in the range $40 - 60 \text{ \AA}$. For these concentrations the general characteristic is that a decreasing of the temperature determines a slight increasing of the scattering exponent α , which indicates that the rod-like magnetic structures expand to form worm-like structures.

Summary

The $\text{La}_{0.54}\text{Ho}_{0.11}\text{Sr}_{0.35}\text{Mn}_{1-x}\text{Cr}_x\text{O}_3$ manganites were synthesized by sol-gel method and investigated by neutron diffraction, small-angle X-ray and neutron scattering (SAXS/SANS). Magnetic and resistance measurements were performed with a Foner type magnetometer and, respectively, the four probes method.

For all the samples was observed, by using SANS data, a change of the volume of the magnetic phase with the temperature. The samples corresponding to $x=0.00, 0.05$ and 0.20 have a 1D rod-like shape, which expand to a worm-like structure with the decrease of the temperature.

PHASE TRANSITION, STRUCTURAL CHANGES AND H₂O REORIENTATIONAL MOTION IN [Ca(H₂O)₂](ReO₄)₂ STUDIED BY NEUTRON SCATTERING METHODS

J. Hetmanczyk, L. Hetmanczyk

Jagiellonian University, Faculty of Chemistry, Ingardena 3, 30-060 Kraków Poland

Joint Institute for Nuclear Research, Dubna, Russia

E-mail: joanna.hetmanczyk@uj.edu.pl

Diaquacalciumrhenate(VII), with the formula: [Ca(H₂O)₂](ReO₄)₂, is a particularly interesting molecular material, because of the occurrence of reorientational motions of the H₂O ligands. At room temperature, (RT) diaquacalciumrhenate(VII) crystallises in the centrosymmetric monoclinic system (space group C2/c, No. = 15) with the unit cell parameters: $a = 18.8975(2)$ Å, $b = 7.0720(2)$ Å, $c = 14.1910(2)$ Å, $\alpha = \beta = 90^\circ$, $\gamma = 115.38^\circ$ and with eight molecules per unit cell ($Z = 8$) [1,2]. The polymorphism of the mentioned above compound was investigated by us by means of differential scanning calorimetry. One reversible phase transition has been found at: $T_c = 261.6$ K (on heating) and $T_c = 235.5$ K (on cooling). Vibrational–reorientational dynamics of H₂O ligands and ReO₄⁻ anions in the high- and low-temperature phases of [Ca(H₂O)₂](ReO₄)₂ was investigated by Fourier transform middle and far-infrared spectroscopy (FT-MIR and FT-FIR), Raman Spectroscopy (RS) and quasielastic and inelastic incoherent Neutron Scattering (QENS and IINS) methods. FT-IR and FT-RS measurements showed that bands associated with H₂O vibrations modes narrow continuously with temperature decreasing. From the temperature dependence of FWHM of the bands connected with $\nu(\text{HOH})$ in Raman spectra and rocking(H₂O) mode in infrared spectra, we can conclude that the reorientational motions of H₂O ligands do not contribute to the phase transition mechanism. The ligands perform fast ($\tau \gg 10^{-11}$ - 10^{-12} s) stochastic reorientational motions in the high and low temperature phases I and II. The estimated mean value of activation energy for the reorientation of the H₂O ligands is ca. 11.1 kJmol⁻¹ from Raman spectroscopy and 11.6 kJmol⁻¹ from infrared spectroscopy.

The aim of the present study is to find connections between the previously recorded phase transition on one hand and eventual changes in the rate of stochastic reorientational motions of the H₂O ligands, or a change of the crystal structure, on the other, by means of inelastic/quasi-elastic incoherent neutron scattering (IINS/QENS) and neutron powder diffraction (NPD) methods. The incoherent inelastic/quasielastic neutron scattering spectra as well as diffraction patterns were measured using the time-of-flight method on a NERA spectrometer [3] at the high flux pulsed reactor IBR-2 in Dubna (Russia) at temperatures: 5, 200, 250 and 295 K.

The $G(\nu)$ functions was calculated in the one-phonon-approximation from the time-of-flight IINS spectra [4] of [Ca(H₂O)₂](ReO₄)₂. The $G(\nu)$ spectra obtained at 295 K are very diffused, because of a dynamical disorder of H₂O molecules connected with their fast molecular reorientational motions. The $G(\nu)$ spectra obtained for the low temperature phase at temperatures 5 K show some separate peaks characteristic for an ordered phase.

In order to support and compare with experimental data the theoretical spectra were predicted by DFT calculations. The total energy optimization and the frequency calculations were performed basing on the periodic density functional theory (DFT) method implemented in the CASTEP code [5,6]. Exchange and correlation parts were approximated using the generalized gradient

approximation (GGA) at PBE functional. Norm-conserving pseudopotentials were used with a plane wave cut-off energy of 800 eV. The initial unit cell optimized in CASTEP periodic boundary condition calculations for $[\text{Ca}(\text{H}_2\text{O})_2](\text{ReO}_4)_2$ compound, was constructed based on the X-ray single crystal diffraction data [2,3]. The aCLIMAX software [7] was used to determine the intensities of transition obtained from DFT calculations. Next, these intensities (Dirac delta function) were convoluted with a resolution function characteristic for NERA spectrometer and converted to density of states with the help of the RES program [8]. Using three complementary methods (IINS, IR, and RS) all characteristic frequencies of the internal vibrations of H_2O and ReO_4^- and external vibrations were detected. We have obtained good agreement between calculated and experimental spectra.

The neutron scattering (IINS, QENS) studies performed with NERA time of flight spectrometer in the temperature range of 5–295 K did not give the evidence of fast (correlation time $\tau < 10$ -11 s) stochastic reorientational motions of H_2O (180° flips) ligands in high and low temperature phases. The QENS peak, registered at 250 and 200 K, does not show any broadening. However, a very small quasi-elastic broadening is visible in the QENS spectra at 295 K. We suspect that this broadening may be connected with picoseconds reorientational jumps of H_2O molecules around their two fold symmetry axis.

The neutron diffraction pattern NPD (measured simultaneously with the IINS/QENS spectra) at 295 K is nearly exactly the same as that at 250 K, which implies that the phase transition at T_c does not display a structural character. The space group is the same for high and low temperature phases.

Acknowledgements

The research (FT-IR) was carried out with the equipment purchased thanks to the financial support of the European Regional Development Fund in the framework of the Polish Innovation Economy Operational Program (contract no. POIG.02.01.00-12-023/08).

The project was supported by grant of the Polish Plenipotentiary to JINR and JINR Directorate from 25.02.2014, Nr 118 p.7.

- [1] W. H. Baur and D.Kassner; *J. Solid State Chem.* 100 (1992) 166.
- [2] R. G.Matveeva, V.V. Ilyukhin, M. B.Varfolomeev, N. V.Belov; *Soviet Physics – Doklady*, 252 (1980) 92.
- [3] I. Natkaniec, D. Chudoba, Ł. Hetmańczyk, V.Yu. Kazimirov, J. Krawczyk, I.L. Sashin, S. Zalewski, *Journal of Physics: Conference Series*, 554 (2014) 012002.
- [4] S.W. Lovesey, *Theory of Neutron Scattering from Condensed Matter*, Clarendon Press, Oxford, 1984.
- [5] S.J. Clark, M.D. Segall, C.J. Pickard, P.J. Hasnip, M.J. Probert, K. Refson, M.C. Payne, *Z. Kristallogr.* 220 (2005) 567.
- [6] K. Refson, S.J. Clark, P.R. Tulip, *Phys. Rev. B* 73 (2006) 155114.
- [7] A.J. Ramirez-Cuesta, *Comput. Phys. Comm.* 157 (2004) 226.
- [8] W.J. Kazimirov, I. Natkaniec, Programme for Calculation of the Resolution Function of NERA-PR and KDSOG-M Inelastic Neutron Scattering Inverse Geometry spectrometers, Preprint P14-2003-48 JINR, Dubna, 2003.

SPECTROSCOPIC AND THERMAL ANALYSIS OF LITHOCHOLIC ACID

M. Ordon, D. Chudoba

Joint Institute for Nuclear Research, Dubna, Russia

E-mail: meg1988@op.pl

The properties of lithocholic acid (LCA) are reported [1]. This is a natural carboxylic acid which is characterized by the presence of saturated cyclopentanoperhydrophenanthrene ring in rigid core. This compound possesses the 3-position hydroxyl groups of R-configuration.

Phase situation and enthalpies of phase transitions were characterized using differential scanning calorimetry (DSC), polarizing optical microscopy (POM) and transmitted light intensity (TLI). Derivatography method was used to determine the thermal stability of the sterol (Fig.1.) [2].

Neutron characteristic of stability of crystal and glass phases and dynamics of selected functional groups was obtained by incoherent inelastic neutron scattering (IINS) and neutron powder diffraction (ND), by using NERA spectrometer, working at IBR-2 pulsed reactor at Joint Institute for Nuclear Research [3].

It has been proven that the LCA is thermally stable up to 250°C. The liquid phase undergoes cooling down to the metastable glass state of very long relaxation time – more than a year. Infrared spectroscopy studies revealed the differences between the stable (crystal) phase and the glass state.

- [1]. W. Nes, “Analysis of Sterols and Other Biologically Significant Steroids”, ISBN 0323154441, Elsev., 2012.
- [2]. A. Rudzki, M.D. Ossowska-Chruściel, M. Ordon „Thermal analysis and simulation model of natural lithocholic acid”, *J Therm Anal Calorim*, DOI 10.1007/s10973-015-4656-3, 2015.
- [3]. A. Szyzewskia, K. Hołderna-Natkanieca, “Progesterone and testosterone studies by neutron scattering and nuclear magnetic resonance methods and quantum chemistry calculations”, *Journal of Molecular Structure* 693, 2004, pp. 49–71.

PRESSURE EFFECTS ON CRYSTAL STRUCTURE AND VIBRATION SPECTRA OF AN ANTIFERROELECTRIC NaNbO_3

B. Savenko¹, S. Kichanov¹, S. Jabarov^{2,3}, D. Kozlenko¹, E. Lukin¹

¹ *Frank Laboratory of Neutron Physics, Joint Institute for Nuclear Research, 141980 Dubna, Russia*

² *Bayerisches Geoinstitut, University Bayreuth, D-95440 Bayreuth, Germany*

³ *Institute of Physics, Azerbaijan National Academy of Sciences, AZ-1143, Baku, Azerbaijan*

The oxide ferroelectrics has become a subject of extensive scientific research due it shows interesting ferroelectric, pyroelectric, piezoelectric and nonlinear optical properties for an application in various electric devices, such as transducers, actuators, capacitors or ferroelectric random access memory. The polar phase in an oxide ferroelectrics can be changes well by the application of high pressure, which is direct method of controlled variation of physical properties by means of variation of interatomic distances and angles.

The alkaline niobates exhibits an unusually large number of interesting physical phenomena like as ferroelectricity, antiferroelectricity or relaxor properties, complex sequence of temperature and pressure driven structural phase transitions and as result the rich contented phase diagrams. In comparison with conventional ferroelectrics, pressure behavior of a NaNbO_3 remains poorly explored. In order to study in detail the high pressure effects on the crystal structure and vibrational properties of antiferroelectric NaNbO_3 , we have performed the powder X-ray, neutron diffraction, and Raman spectroscopy experiments in the 0 – 30 GPa pressure range.

The antiferroelectric NaNbO_3 has an orthorhombic structure with $Pbcm$ symmetry. Our results demonstrate the application of high pressure leads to successive structural phase transitions in sodium niobate, accompanied by anomalies in pressure behavior of lattice parameters and different vibrational modes.

The work has been supported by the RFBR grant №14-02-00948-a.

DYNAMICS OF $(\text{NH}_4)_2\text{MeO}_2\text{F}_4$ (ME=W, MO) COMPOUNDS BY THE INELASTIC INCOHERENT NEUTRON SCATTERING

L.S.Smironov¹, I.Natkaniec², I.L.Sashin², S.Zalewski², V.G.Simkin², E.V.Bogdanov³, I.N.Florov³

¹NIC "KI" FSBI SSC RF Institute for Theoretical and Experimental Physics, Moscow, Russia

²Joint Institute for Nuclear Research, Dubna, Russia

³FSBIS L.V.Kirenskii's Institute of Physics SD RAS, Krasnoyarsk, Russia

The acentric building blocks of metal oxide fluoride anions $(\text{MeO}_2\text{F}_4)^{2-}$ give the possibility to prepare functional materials with important physical properties as ferroelectricity, ferroelasticity, piezoelectricity, second order non-linear optical behavior, etc. The aforementioned physical properties can be realized in initial phase, or they can appear as the result of phase transitions, that is important for many practical aims [1].

$(\text{NH}_4)_2\text{WO}_2\text{F}_4$ has phase transitions $G_0 \rightarrow G_1 \rightarrow G_2$ at temperatures $T_{c1}=201$ K ($G_0 \rightarrow G_1$) and $T_{c2}=160$ K ($G_1 \rightarrow G_2$) [2,3]. Crystal structure of G_0 phase is known as orthorhombic with sp. gr. *Cmcm*, $Z=4$ and lattice parameters $a=5.9292(3)$, $b=14.3940(7)$, $c=7.1351(3)$ Å [3,4]. The crystal structure of $(\text{NH}_4)_2\text{WO}_2\text{F}_4$ at 133 K in G_2 phase has triclinic unit cell with sp.gr *P-1*, $Z=4$ and lattice parameters $a=5.9013(4)$, $b=14.1993(9)$, $c=7.7162(5)$, $\alpha=90.022(2)$, $\beta=112.466(2)$, $\gamma=89.999(2)^\circ$ [4]. Atomic positions, except hydrogen, were determined by single crystal x-ray diffraction at 238 K, and the structure has two crystallographically independent ammonium groups [3].

$(\text{NH}_4)_2\text{MoO}_2\text{F}_4$ undergoes phase transitions $G_0 \rightarrow G_1 \rightarrow G_2$ but at temperatures $T_{c1}=270$ K ($G_0 \rightarrow G_1$) and $T_{c2} \approx 180$ K ($G_1 \rightarrow G_2$) [6]. $(\text{NH}_4)_2\text{MoO}_2\text{F}_4$ has at room temperature the crystal structure for phase G_0 similar to that of $(\text{NH}_4)_2\text{WO}_2\text{F}_4$: sp. gr. *Cmcm*, $Z=4$ and lattice parameters $a=5.9592(5)$, $b=14.467(1)$, $c=7.0992(5)$ Å [7]. Crystal structure of $(\text{NH}_4)_2\text{MoO}_2\text{F}_4$ in phase G_1 determined at $T=233$ K is suited to sp.gr. *Pnma*, $Z=4$ with lattice parameters $a=7.1374(6)$, $b=5.9090(5)$, $c=14.292(1)$ Å [8]. Thus ionic radii of Mo (0.6 Å) and W (0.59 Å) are closed but physical properties have significant difference. Crystal structures of these compounds at room temperatures are similar, have two crystallographically independent ammonium groups N1 and N2 with the environment ten and eight O(F) atoms, respectively. Thus each ammonium ion, N1H_4 or N2H_4 , occupies individual potential well and has individual librational energy. The influence of metal atom, W or Mo, on librational energies of ammonium ions could be observed by means of inelastic incoherent neutron scattering (IINS).

Earlier the study of oxyfluoride $(\text{NH}_4)_2\text{WO}_2\text{F}_4$ by the IINS was carried out on HRMECS spectrometer, ANL (USA), for the investigation of peculiarities of phase transitions from 10 to 300 K at normal pressure [9]. The report contains results of obtained values of ammonium libration energies for both compounds, which can explain difference in T_{c1} and T_{c2} transition temperatures for $(\text{NH}_4)_2\text{WO}_2\text{F}_4$ and $(\text{NH}_4)_2\text{MoO}_2\text{F}_4$ respectively.

[1] R.L.Withers, F.J.Brink, Y.Liu, L.Noren. *Polyhedron*, 26 (2007) 290.

[2] S.V.Mel'nikova, V.D.Fokina, N.M.Laptash, *FTT*, 48 (2006) 110.

[3] I.N.Flyorov, V.D.Fokina, M.V.Gorev et al. *FTT*, 48 (2006) 711.

[4] A.A.Udovenko, N.M.Laptash, *Acta Cryst. B*64 (2008) 645.

[5] I.N.Flyorov, V.D.Fokina, M.V.Gorev et al. *FTT*, 49 (2007) 1093.

[6] S.V.Mel'nikova, N.M.Laptash. *FTT*, 50 (2008) 493.

[7] A.D.Vasiliev, N.M,Laptash. Report P-11 Report.

[8] S.V.Mel'nikova, A.D.Vasil'ev, N.M.Laptash, Report.

[9] L.S.Smironov, A.I.Kolesnikov, I.N.Flyorov et al. *FTT*, 51 (2009) 2224.

M A G N E T I C C O L L O I D N A N O S Y S T E M S

STRUCTURAL COMPARISON OF SEVERAL WATER BASED FERROFLUIDS BY MEANS OF TEM AND SANS METHODS

M. Balasoiu^{1,2}, A.-M. Balasoiu-Gaina^{1,3,4}, D. Soloviov^{1,5}, O. Ivankov^{1,5}, I. Malaescu⁴, N. Lupu⁶

¹*Frank Laboratory of Neutron Physics, Joint Institute of Nuclear Research, Dubna, Russia*

²*Horia Hulubei National Institute of Physics and Nuclear Engineering, Bucharest, Romania*

³*CMCF, Moscow State University, Moscow, Russia*

⁴*West University of Timisoara, Department of Physics, Romania*

⁵*Taras Shevchenko University, Kiev, Ukraine*

⁶*National Institute of Research & Development for Technical Physics, Iasi, Romania*

E-mail: balas@jinr.ru ; alexandra@balasoiu.com

Ferrofluids, ultrastable dispersions of magnetic nanoparticles in liquids, find a wide range of applications in many technical and industrial fields, as well as in medicine and biotechnology.

Nowadays researches on developing ferrofluids with new types of particles, new synthesis methods, increased particle concentration, using different stabilization methods and compounds are in progress [1]. Water-based ferrofluids present the most complex microstructural behavior and their properties improvement represents an important challenge in this field.

The knowledge about the microstructure of ferrofluids is very important to understand and control the mechanisms of their stabilization. The non-ionic ferrofluids in contrast to the ionic ones, often show the presence of aggregates in their structure even at low particle concentration and in the absence of the magnetic field. These factors diminish the long-term stability of the ferrofluids.

In the present paper results on the structure investigation of several water based ferrofluid samples by means of small angle neutron scattering (SANS) and transmission electron microscopy (TEM) are presented and discussed.

[1] M. Balasoiu, O.I. Ivankov, D.V. Soloviov, S.N. Lysenko, R.M. Yakushev, A.-M. Balasoiu-Gaina, N. Lupu, J. Optoelectron. Adv. Mater. **17**(7-8), 1114-1121 (2015).

ON THE SILICONE RUBBER ELASTOMER MICROSTRUCTURE BY MEANS OF SANS

M. Balasoiu^{1,2}, I. Bica³, D. V. Soloviov^{1,4}, M. Bunoiu³

¹Frank Laboratory of Neutron Physics, Joint Institute of Nuclear Research, Dubna, Russia

²Horia Hulubei National Institute of Physics and Nuclear Engineering, Bucharest, Romania

³West University of Timisoara, Department of Physics, Romania

³Taras Shevchenko University, Kiev, Ukraine

Magnetic elastomers (ME's) are specific classes of smart substances composed from elastomer matrices filled with ferromagnetic nanoparticles responding in a complex way to the changes of external conditions.

The synthesis and the study of structure and physical properties of these advanced materials combining the functional properties of highly elastic polymers and ferromagnetic substances should be considered as a perspective way to provide the understanding on the construction principles of a wide class of materials for electronics, electrical engineering, medicine, aero and cosmic industries.

Earlier investigations have analyzed, by means of small-angle neutron scattering method, subtle structural features of the polymeric matrix and the ensemble of embedded ferroparticles as resulting from the conditions of preparation of ferroelastomers by the variation of ferroparticle concentration and the strength of a transversal external magnetic field applied during polymerization [1,2,3].

A detailed analysis of q -dependencies of scattering intensity for matrix enabled us to built a two-level model structure and related scattering function:

$$I(q) = I_{01} \exp[-(qR_g)^2 / 3] + I_{02} [1 + (qR_c)^2]^{-2} \quad (1)$$

Here the first Guinier – term describes the large scale inhomogeneities (domains, radius gyration R_G), and the second Debye-term is related to the smaller globular objects (domains) with correlation radius R_C . The coefficients I_{01} and I_{02} are proportional to the squared contrast factors, volume contents and characteristic volumes of corresponding objects. This model function approximates the data for matrix satisfactory (Fig.1) with parameters given in Table 1.

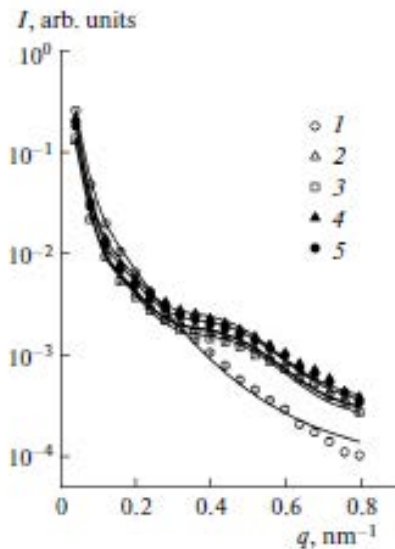


Fig.1. Scattering intensities $I(q)$ vs. momentum transfer q for matrix P1 (1) and ferroelastomers P12-P15 (2-5) with high content of magnetite (synthesis in magnetic field perpendicular to the plane of polymer film). The beam is orthogonal to the plane of sample. Lines are the approximation functions for matrix (1) and ferroelastomers.

Table 1. Parameters of functions (1) for elastomer matrix.

№ of sample	B, Gauss	I ₀₁ , arb.un.	R _G , nm	I ₀₂ ·10 ⁵ , arb.un.	R _C , nm
P ₁	0	0.487±0.002	39.3±0.1	4590 ±60	6.37±0.04

Due to the increasing of the scattering intensity for the matrix with the decrease of q , effects of the structural arrangements of the particle assemblies inside the matrix are not evident at momentum transfer smaller than 0.4 nm^{-1} . To try to decrease the scattering intensity for the elastomer matrix, synthesis procedure was changed.

In the present paper results on the microstructure properties of several elastomeric matrices investigated by means of SANS are discussed.

[1] M. Balasoiu, V.T. Lebedev, D.N. Orlova, I. Bica, *Crystallography Reports* **56(7)**, 93-96 (2011).

[2] M. Balasoiu, I. Bica, Yu.L. Raikher, E.B. Dokukin, L. Almasy, B. Vatzulik, A.I. Kuklin, *Optoelectronics and Advanced Materials – Rapid Communications*, **5(5)**, 523-526 (2011).

[3] M. Balasoiu, V.T. Lebedev, I. Bica, Yu.L. Raikher, in „Actual problems of condensed matter physics”, Ed. Yu.M. Raikher, ISBN 978-5-7691-2418-1, Perm, 106-115 (2015) (Russ.)

HYDROPHILIC VERSUS HYDROPHOBIC OLEATE COATED MAGNETIC PARTICLES

E. Puscasu¹, L. Sacarescu², A. Domocos¹, R. Turcu³, C. Leostean³, D. Creanga¹, M. Balasoiu^{4,5}

¹ "Alexandru Ioan Cuza" University, Physics Faculty, Iasi, Romania

² "Petru Poni" Institute of Macromolecular Chemistry, Iasi, Romania

³ National Institute of Research and Development of Isotopic and Molecular Technology, Cluj, Romania

⁴ Institute of Nuclear Research, Dubna, Russian Federation

⁵ Horia Hulubei National Institute for Physics and Nuclear Engineering, Bucharest, Romania

Magnetic nanoparticles (MNPs) in colloidal suspensions were prepared using ferric and ferrous salt precursors according to classical chemical route of co-precipitation in alkali reaction media [1]. Oleate ion from oleic acid was used to develop hydrophobic coating shell for ferrophase stabilization

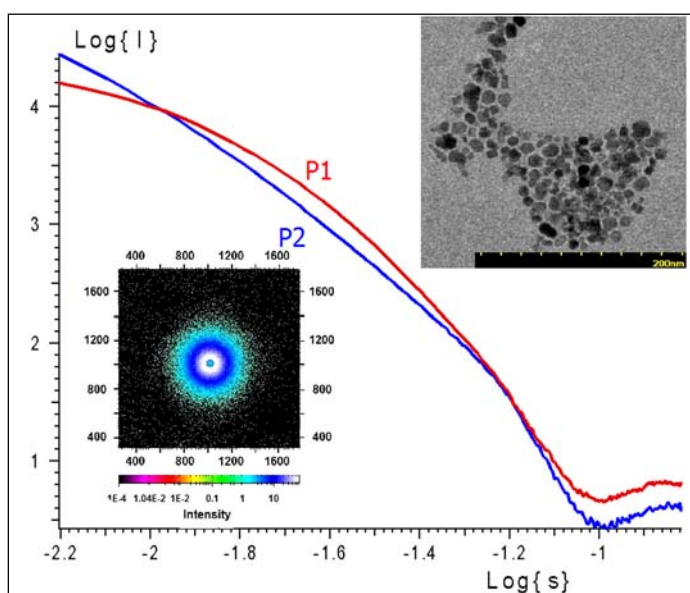


Fig. 1. Microstructural investigation on MNP samples

in hydrophobic medium (P1); sodium oleate was used to yield hydrophilic coating of MNPs in colloidal aqueous suspension (P2). XRD analysis revealed typical spinel structures in both samples with all characteristic peaks while VSM shown dominant superparamagnetic properties. Polydispersed but fine granulated iron oxide with rather symmetrical particle shape resulted from TEM data for P1 while some asymmetrical structures appeared in P2. SAXS investigation of the two diluted suspensions (Fig. 1) evidenced average values of about 7 nm (P1) and respectively 10 nm (P2) in good agreement with TEM measurements and ensuring good stability in suspension. The interpretation of different particle symmetry was based on coating shell arrangement differences, i.e. single oleate layer in hydrophobic colloidal MNPs compared to double oleate layer in hydrophilic MNP sample. In this latter case coated particle interaction seems to be favored resulting in some clusters with character of mass fractals (2.4 fractal dimension) as shown from SAXS data analysis. Various applications in technical and biomedical field could be designed based on the MNP samples stabilized with oleate since its biocompatibility was demonstrated in literature [2].

Acknowledgement: this research was supported by the JINR-UAIC Scientific Projects Nos. 33/23.01.2015 items 57,58 and 34/23.01.2015 items 56, 57.

[1] Massart, R. (1981). Preparation of aqueous magnetic liquids in alkaline and acidic media, IEEE Trans. Magn., 17 (2): 1247-1248.

[2] Sun J, Zhou S, Hou P, Yang Y, Weng J, Li X, Li M (2007). Synthesis and characterization of biocompatible Fe₃O₄ nanoparticles. J. Biomed. Mater., Res. A., 80(2):333-341.2.

STRUCTURE OF MAGNETOFERRITIN IN AQUEOUS SOLUTION

L.Melnikova¹, P.Kopcansky¹, Z. Mitróová¹, V.I.Petrenko^{2,3}, O.I.Ivankov^{2,3}, M.V.Avdeev², V.M. Garamus⁴, L. Almasy⁵

¹ Institute of Experimental Physics, SAS, Watsonova 47, 040 01 Kosice, Slovakia

² Joint Institute for Nuclear Research, Joliot-Curie 6, 141980 Dubna, Moscow region, Russia

³ Kyiv Taras Shevchenko National University, Volodymyrska Street 64, Kyiv, 01033 Ukraine

⁴ Helmholtz-Zentrum Geesthacht: Centre for Materials and Coastal Research, Max-Planck-Street 1, 21502 Geesthacht, Germany

⁵ Wigner Research Centre for Physics, HAS, H-1525 Budapest, POB 49, Hungary

The protein cage of ferritin, iron storage protein with external diameter of 12 nm, has been shown to be a suitable environment for magnetite (Fe₃O₄), or maghemite (γ-Fe₂O₃) controlled synthesis, enabling formation of magnetoferritin bio-complex. The structure of magnetoferritin in aqueous solution was investigated by powerful small-angle X-rays (SAXS) and neutrons (SANS) scattering for different loading factors (average number of iron atoms per complex). The magnetoferritin shell with loading factor higher than 160 has exhibited partial destruction as compared to the native hollow state of apoferritin [1,2]. These changes were followed by the increase of size and structural polydispersity and the change of match points in the SANS contrast variation with the loading factor growth [3]. It could be expected that the structure and stability of the magnetoferritin package was changed due to the specific effect of iron oxides in the core. Magnetoferritin was able also to reduce the size and amount of lysozyme amyloid fibrils that was confirmed using SAXS method and fluorescence spectroscopy [4]. Detailed structural research of magnetoferritin aqueous solution with superparamagnetic behavior is important due to the high possibility of applications in the biomedical field of science (e.g. a contrast agent in radiology, a drug carrier in the targeted transport, or a standard in diagnostics of various diseases).

Acknowledgements

This work was supported within the project PHYSNET, VEGA 045 and APVV 0171-10.

- [1] Melníková, L. - Mitróová, Z. - Timko, M. - Kováč, J. - Avdeev, M. V. - Petrenko, V. I. - Garamus, V. M. - Almásy, L. - Kopčanský, P. Structural characterization of magnetoferritin. In *Mendeleev commun.* 2014, vol. 24, no. 2, p. 80-81
- [2] Melníková, L. - Petrenko, V. I. - Avdeev, M. V. - Garamus, V. M. - Almásy, L. - Ivankov, O.I. - Bulavin, L. A. - Mitróová, Z. - Kopčanský, P. Effect of iron oxide loading on magnetoferritin structure in solution as revealed by SAXS and SANS. In *Colloids Surf. B.* 2014, vol. 123, p. 82-88
- [3] Melnikova, L. - Petrenko, V. I. - Avdeev, M. V. - Ivankov, O. I. - Bulavin, L. A. - Garamus, V. M. - Almásy, L. - Mitroova, Z. – Kopcansky, P. SANS contrast variation study of magnetoferritin structure at various iron loading. In *J. Magn. Magn. Mater.* 2015, vol. 377, p. 77-80
- [4] Kopcansky, P. - Siposova, K. - Melnikova, L. - Bednarikova, Z. - Timko, M. - Mitroova, Z. - Antosova, A. - Garamus, V. M. - Petrenko, V. I. - Avdeev, M. V. – Gazova, Z. Destroying activity of magnetoferritin on lysozyme amyloid fibrils. In *J. Magn. Magn. Mater.* 2015, vol. 377, p. 267-271

STRUCTURE OF MAGNETIC FLUIDS AT INTERFACE WITH SILICON INVESTIGATED BY NEUTRON AND X-RAY REFLECTOMETRY

I.V.Gapon¹, P.Kopcansky², O.Soltwedel, M.V.Avdeev³, L.A.Bulavin¹, V.I.Petrenko^{1,3}

¹ *Kyiv Taras Shevchenko National University, Volodymyrska Street 64, Kyiv, 01033 Ukraine*

² *Institute of Experimental Physics, SAS, Watsonova 47, 040 01 Kosice, Slovakia*

³ *Joint Institute for Nuclear Research, Joliot-Curie 6, 141980 Dubna, Moscow region, Russia*

Ferrofluids (FF) are colloidal system of magnetic nanoparticles with solvents of different polarity. In such systems layers of surfactants are frequently used for stabilization of magnetic nanoparticles. Great interest to these systems is related with possibility of their use for controlled drug delivery, diagnostics and treatment of various diseases, for example cancer. For the moment, synthesis of stable biocompatible FF with pre-defined properties is quite big problem. Therefore, the study of biocompatible FF is of great interest. At the same time behavior of magnetic nanoparticles in the bulk and at interfaces can be very different due to specific adsorption properties, which should be considered in a variety of applications. It also remains an open question regarding to the possible differences in the stability of magnetic fluids in bulk and at interfaces.

The main aim of this work was to obtain structural parameters of biocompatible ferrofluids and to study of FF stability in the bulk and at the interface. Information about the structure of FF in bulk was obtained from small-angle neutron scattering experiments. Neutron reflectometry experiments were done to investigate behavior of magnetic fluids with different solvents (polar and non-polar) at the interface with silicon. It was shown that only single magnetic nanoparticles, coated by surfactant molecules, are adsorbed to the surface of the silicon from bulk of ferrofluids for both solvent type. Impact magnetic field parallel to interface is not detected. It was checked of influence of gravity on the adsorption properties of magnetic particles. X-ray reflectometry makes it possible to study free liquid surfaces or interfaces air/FF. Some additional particles organizations were observed at air/MFs interface only for low concentrated fluids. It was found that structural organization of nanoparticles at the interface air/ MFs dependent on concentration of magnetite in initial MF. The biggest effect on additional particles organization near surface is observed for perpendicular magnetic field.

MATERIALS FOR ENERGY APPLICATIONS

STRUCTURAL AND ELECTROCHEMICAL PROPERTIES OF DOPED 5 V SPINEL CATHODE MATERIALS $\text{LiNi}_{0.5-x}\text{Mn}_{1.5-y}\text{M}_{x+y}\text{O}_4$ ($\text{M} = \text{CO, CR, TI; } X+Y=0.05$) PREPARED BY MECHANOCHEMICAL WAY

N.V. Kosova¹, I.A. Bobrikov², O.A. Podgornova¹, E.T. Devyatkina¹, A.M. Balagurov², A.K. Gutakovskii^{3,4}

¹*Institute of Solid State Chemistry and Mechanochemistry SB RAS, Novosibirsk, Russia*

²*Joint Institute for Nuclear Research, Dubna, Russia*

³*Rzhanov Institute of Semiconductor Physics SB RAS, Novosibirsk, Russia*

⁴*Novosibirsk State University, 2 Pirogova, 630090 Novosibirsk, Russia*

Pure $\text{LiNi}_{0.5}\text{Mn}_{1.5}\text{O}_4$ and doped spinel cathode materials $\text{LiNi}_{0.5-x}\text{Mn}_{1.5-y}\text{M}_{x+y}\text{O}_4$ ($\text{M} = \text{Co, Cr, Ti; } x+y=0.05$) were prepared by mechanochemically assisted solid state synthesis using a high-energy AGO-2 planetary mill followed by annealing at 700 and 800 °C. The samples were characterized by X-ray and high resolution neutron powder diffraction with Rietveld refinement, high-resolution transmission electron microscopy and electron microdiffraction, Fourier transform infrared spectroscopy, galvanostatic cycling, and galvanostatic intermittent titration technique. Neutron diffraction experiments have been made on the High Resolution Fourier Diffractometer (HRFD) at the IBR-2 pulsed reactor in JINR (Dubna). According to the neutron diffraction results the structure of samples-800 °C is well refined with the single $Fd-3m$ spinel. On the contrary, the structure of samples-700 °C can be described by 1) two-phase materials with the 5-10% fraction of the $P4_332$ spinel depending on the substitution ion 2) one phase $P4_332$ spinel structure with considerable redistribution of Ni and Mn between cation positions. It has been found that the substitution ions preferably substitute Ni ions, which correlates with the appearance of $\text{Li}_y\text{Ni}_{1-y}\text{O}$ by-product (3-8%). The average crystal size of pure spinel is less than 100 nm, while the crystal size of the doped spinels is 110-140 nm for samples-800 °C and 60-110 nm for samples-700 °C. Crystalline microstrains change in opposite way. Besides, the surface phase, coherently conjugated with the crystal bulk, was observed for samples-700 °C and assigned to the intermediate appeared due to the reconstruction of the disordered to the ordered spinel. Results of transmission electron microscopy and electron microdiffraction experiments are in good line with the neutron diffraction results but indicate two phase condition ($Fd-3m + P4_332$) for doped samples-700 °C. The electrochemical performance of the doped spinels depends on the annealing temperature. For all doped samples, two pairs of redox peaks are observed on the dQ/dV vs. voltage plots revealing the prevalence of disordered spinel phase. However, the separation between them increases for samples-800 °C due to disappearance of the ordered phase, resulting in better charge-discharge performance. Pure spinels show a significant deterioration upon cycling because of side reactions of their nanoparticles with electrolyte. Lithium diffusion coefficient (D_{Li^+}) of the doped spinels-800 °C is two orders of magnitude higher as compared with that of the undoped spinel. The highest rate capability is observed for the Ti-doped spinel-800 °C due to larger lattice parameter.

The neutron diffraction investigations were financially supported by Russian Foundation for Basic Research (project #14-02-31506). Transmission electron microscopy studies were performed using the equipment of CCU "Nanostructures". The part of the work was carried out with the support of the Ministry of Education and Science of the Russian Federation (project ID RFMEFI62114X0004) and RSCF (project No 14-22-00143).

INVESTIGATION OF ELECTROCHEMICALLY STIMULATED STRUCTURAL TRANSFORMATIONS IN $\text{Li}_3\text{V}_2(\text{PO}_4)_3$ ELECTRODE USING NEUTRON DIFFRACTION METHOD

A.V. Ivanishchev¹, A.V. Churikov¹, I.A. Bobrikov², O.Yu. Ivanshina², A.V. Ushakov¹

¹ *Institute of Chemistry, Saratov State University named after N.G. Chernyshevsky, Astrakhanskaya str. 83, 410012, Saratov, Russian Federation*

² *Frank Laboratory of Neutron Physics, Joint Institute for Nuclear Research, Joliot-Curie str. 6, Dubna, Moscow reg., Russia, 141980*

E-mail: ivanischevav@inbox.ru

Currently, lithium-ion batteries (LIB) are considered as the most promising among autonomous power sources. Search for new and improvement of existing LIB's materials and components is aimed at increasing energy density and capacity, safety and working life of batteries. Lithium-vanadium phosphate $\text{Li}_3\text{V}_2(\text{PO}_4)_3$ is considered as a promising cathode material for several reasons: high operating voltage (3.6-4.7 V) and specific capacity (197 mAh/g), as well as high chemical and thermal stability inherent to lithium intercalated phosphates of transition metals. A feature of $\text{Li}_3\text{V}_2(\text{PO}_4)_3$ structure is the ability to maintain rapid transport of lithium ions, so a joint study of structural and electrochemical characteristics of the material is of considerable interest.

As an instrument of structural analysis in the present work, the method of neutron diffraction was used. Due to the peculiarities of the interaction of neutrons with atoms of different elements, it allows to define the content of each type of atoms in different crystallographic positions, in contrast to the X-ray diffraction method, where the presence of each element can only be evaluated indirectly by the deviation of the lattice parameters from the standard values. Thus, using the Rietveld method the atomic coordinates and occupancy of crystallographic positions were refined in the crystal structure of $\text{Li}_3\text{V}_2(\text{PO}_4)_3$. The results of neutron diffraction data processing are shown in Table 1.

Table 1. Atomic coordinates and population of crystallographic positions of $\text{Li}_3\text{V}_2(\text{PO}_4)_3$ according to the method of neutron diffraction

Atom	x	y	z	B	occ.
V1	0.2517	0.4711	-0.1101	0.5	1
V1	-0.2481	0.9618	-0.1104	0.5	1
P1	0.09551	0.10283	-0.13216	0.65	1
P2	-0.10889	0.60803	-0.16188	0.65	1
P3	-0.00113	0.26587	-0.48327	0.65	1
O1	0.41065	0.09297	-0.34643	0.8	1
O2	-0.40831	0.60362	-0.32643	0.8	1
O3	0.30075	0.49118	-0.26495	0.8	1
O4	-0.36612	0.98539	-0.27868	0.8	1
O5	0.14193	0.09045	-0.03404	0.8	1
O6	-0.1769	0.54369	-0.04757	0.8	1
O7	0.43881	0.31633	-0.11494	0.8	1
O8	-0.44687	0.86495	-0.07742	0.8	1
O9	0.13552	0.13409	-0.429	0.8	1

O10	-0.16604	0.66723	-0.44458	0.8	1
O11	0.13984	0.26826	-0.18538	0.8	1
O12	-0.17142	0.81033	-0.17034	0.8	1
Li1	0.06043	0.33501	-0.30615	1	1
Li2	-0.36414	0.73424	-0.33903	1	1
Li3	0.47283	0.38036	-0.24584	1	1

To determine the parameters of the lithium transport in $\text{Li}_3\text{V}_2(\text{PO}_4)_3$ -electrode a combination of electrochemical methods was used: galvanostatic charge-discharge, cyclic voltammetry (CV), pulsed chronoampero- and chronopotentiometry (PITT and GITT, relatively), electrode impedance spectroscopy (EIS). Analysis of electrochemical data was performed according to previously obtained theoretical solutions [1,2]. Joint measurements by neutron diffraction and CV allowed to correlate changes in the structural parameters and form of cyclic voltammogram of $\text{Li}_3\text{V}_2(\text{PO}_4)_3$ -electrode (Fig.1a). i, t -transients of $\text{Li}_3\text{V}_2(\text{PO}_4)_3$ -electrode (Fig.1b) are of a stepped shape and are the result of superposition of two diffusion processes with different time and kinetic constants which are in good agreement with the same parameters, found in the GITT and EIS methods. The calculated values of diffusion coefficients for the maximally lithiated and delithiated phases of intercalation material were determined as 10^{-12} cm^2/s for the transfer in a thin surface layer, and 10^{-9} and $3 \cdot 10^{-10}$ cm^2/s , respectively, for transfer in the bulk of material's particle.

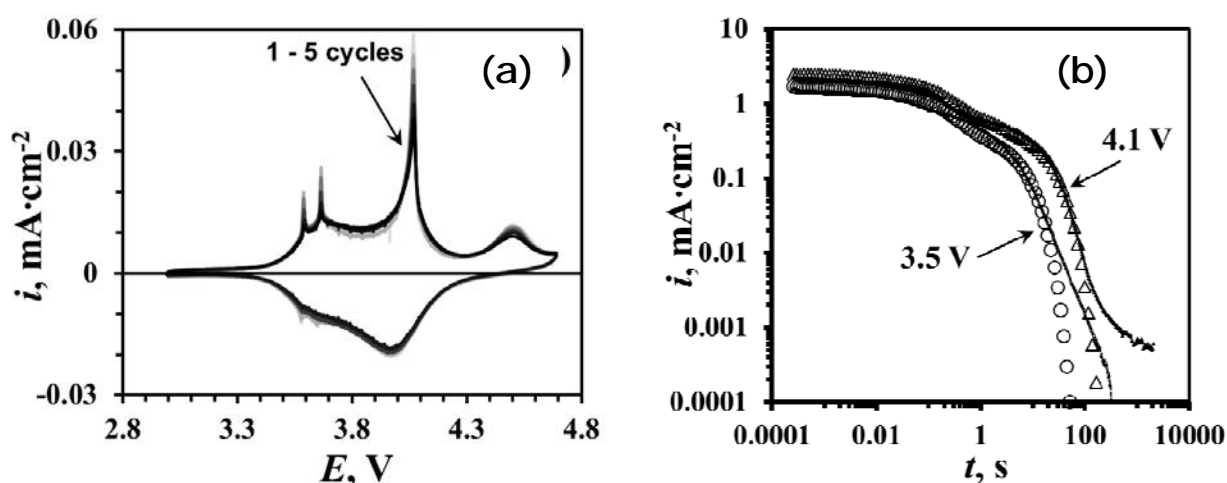


Fig.1. Cyclic voltammograms measured at potential scan rate of $0.05 \text{ mV} \cdot \text{s}^{-1}$ (a) and i, t -transients (b) of $\text{Li}_3\text{V}_2(\text{PO}_4)_3$ -electrode: experimental (filled markers) and calculated (empty markers) data.

Neutron diffraction study of $\text{Li}_3\text{V}_2(\text{PO}_4)_3$ is supported by Russian Science Foundation (project 15-13-10006), synthesis and electrochemical study of $\text{Li}_3\text{V}_2(\text{PO}_4)_3$ is supported by Russian Foundation for Basic Research (project 14-29-04005).

[1] A.V. Ivanishchev, A.V. Churikov, A.V. Ushakov, *Electrochim. Acta.* 2014 (122) 187.

[2] A.V. Churikov, A.V. Ivanishchev, A.V. Ushakov, V.O. Romanova, *J. Solid State Electrochem.* 18 (2014) 1425.

HYDRO- AND SOLVOTHERMAL SYNTHESIS OF COMPLEX LITHIUM AND D-METALS PHOSPHATES AS CATHODE MATERIALS FOR LI-ION BATTERIES

V.D. Sumanov¹, O.A. Drozhzhin¹, A.N. Baranov¹, E.V. Antipov¹

¹ *Lomonosov MSU, Chemical Department, Russia*

E-mail: wertuals@mail.ru

At the moment, olivine-structured complex phosphates of lithium and transitional metals are considered as one of most promising cathode materials for li-ion batteries; LiFePO₄ is actually most studied. Besides advantages, such as high theoretical capacity, low cost and excellent cyclability, LiFePO₄ has serious drawbacks. One of them – low working potential in comparison with other materials (3.4V vs. Li/Li⁺). In other side, materials with higher potential such as LiCoPO₄, LiMnPO₄, LiNiPO₄ cannot be used in li-ion batteries at the moment, because of low achievable capacity and poor cycle life. Usage of solid solution from the specified materials, for example LiFe_{1-x}M_xPO₄, gives opportunity to combine high working potential, structure stability and good cyclability. For the perfect electrochemical performance and cycle life it is important to obtain material with definite morphology and size of particles. In this work were performed different types of solvothermal synthesis and reaction mechanism study of LiMn_{0.5}Fe_{0.5}PO₄ cathode material.

All samples of LiMn_{0.5}Fe_{0.5}PO₄ were synthesized via hydrothermal and solvothermal route. For solvothermal synthesis as solvents ethanol, ethylene glycol, polyethylene glycol were used. Mechanism of phase nucleation and crystal growth in hydro- and solvothermal conditions were investigated. Particles obtained using by hydrothermal and solvothermal methods have plate-like morphology with 50-200 nm thickness. Samples were studied by X-ray diffraction, scanning electronic microscopy (SEM), elemental analysis (EDX).

Electrochemical properties of the specified materials are evaluated by galvanostatic and potentiostatic methods. Values of reversible capacity for all materials are 140-150 mAh/g at C/20 discharge rate.

The work was supported with the RFBR grants (14-03-31473, 14-29-04064).

HYDROTHERMAL SYNTHESIS OF SODIUM AND TRANSITION METALS FLUOROPHOSPHATES AS CATHODE MATERIALS FOR LITHIUM- AND SODIUM- ION BATTERIES

I. Tereshchenko, G. Skorupsky, O. Drozhzhin, N. Khasanova, E. Antipov

Lomonosov Moscow State University, Department of Chemistry

E-mail: ivteresh@gmail.com

Sodium and transition metals fluorophosphates with formula $\text{Na}_2\text{MPO}_4\text{F}$ ($\text{M} = \text{Fe}, \text{Co}, \text{Mn}$) represent a perspective type of compounds for use in cathode materials of lithium- and sodium-ion batteries because of two reasons: the theoretical possibility to extract more than one alkaline ion per formula unit (with corresponding oxidation of d-cation up to +4 oxidation state) and rather high operating voltages in the case of $\text{M}=\text{Co}$ and Mn [1]. As a result, rather high theoretical energy density may be achieved, in the case of average voltage 4.5 V it amounts 550 W·h/kg per one alkaline metal ion. $\text{Na}_2\text{MPO}_4\text{F}$ ($\text{M}=\text{Fe}, \text{Co}$) consists of alternating layers of sodium ions and layers of interconnected FeO_4F_2 and PO_4 polyhedra, while $\text{Na}_2\text{MnPO}_4\text{F}$ has a framework type of structure which has not good intrinsic sodium diffusion characteristics of layered structure but may be more stable.

In the present work the main attention is given to the hydrothermal synthesis of the $\text{Na}_2\text{MPO}_4\text{F}$ ($\text{M}=\text{Co}, \text{Fe}$) and investigation of its morphology and electrochemical properties depending on synthetic conditions. Crystal structure study of $\text{Na}_{2-x}\text{CoPO}_4\text{F}$ with different amount of deintercalated sodium ions is also performed using in-situ and ex-situ x-ray powder diffraction and EDX analysis. Cathode materials based on obtained $\text{Na}_2\text{CoPO}_4\text{F}$ samples demonstrate more than 50% of theoretical discharge capacity for one alkaline metal ion in spite of strong amorphization during cycling. $\text{Na}_2\text{FePO}_4\text{F}$ shows more than 80% of theoretical capacity for one alkaline metal ion. Also the possibility of obtaining $\text{Na}_2\text{MnPO}_4\text{F}$ and solid solutions with compositions $\text{Na}_2\text{Co}_{1-x}\text{Mn}_x\text{PO}_4\text{F}$ ($x=0.2, 0.4, 0.6, 0.8$) and $\text{Na}_2\text{Mn}_{1-x}\text{Fe}_x\text{PO}_4\text{F}$ ($x=0.2, 0.4, 0.6$) using hydrothermal route is established. It is shown that compositions $\text{Na}_2\text{Co}_{1-x}\text{Mn}_x\text{PO}_4\text{F}$ ($x=0.2, 0.4$) are isostructural to $\text{Na}_2\text{CoPO}_4\text{F}$. At the moment cathode materials based on hydrothermally obtained $\text{Na}_2\text{MnPO}_4\text{F}$ and $\text{Na}_2\text{Mn}_{0.6}\text{Fe}_{0.4}\text{PO}_4\text{F}$ demonstrate discharge capacity of 5% and 10% per one alkaline ion respectively. Weak electrochemical activity of the manganese-containing compounds can be attributed to the strong Jahn-Teller distortion of Mn^{+3} and slow diffusion of alkaline ions. The latter problem could be mitigated due to the small size of hydrothermally obtained $\text{Na}_2\text{MnPO}_4\text{F}$ particles that was about 100 nm.

Acknowledgements. The work was supported with the RFBR grants (14-03-31473, 14-29-04064).

[1] Khasanova, N.R., et al. New Form of $\text{Li}_2\text{FePO}_4\text{F}$ as Cathode Material for Li-Ion Batteries // *Chemistry of materials*, 2012. **24**(22): p. 4271-4273.

NEUTRON DIFFRACTION AND ELECTROCHEMICAL STUDY OF LITHIUM INTERCALATION IN THE SYSTEM $\text{Li}_4\text{Ti}_5\text{O}_{12}$ - $\text{Li}_7\text{Ti}_5\text{O}_{12}$

A.V. Ushakov¹, A.V. Ivanishchev¹, A.V. Churikov¹, I.A. Bobrikov², O.Yu. Ivanshina²

¹ *Institute of Chemistry, Saratov State University named after N.G. Chernyshevsky, Astrakhanskaya str. 83, Saratov, Russian Federation, 410012*

² *Frank Laboratory of Neutron Physics, Joint Institute for Nuclear Research, Joliot-Curie str. 6, Dubna, Moscow reg., Russia, 141980*

E-mail: arsenivushakov@ya.ru

Lithium titanate $\text{Li}_4\text{Ti}_5\text{O}_{12}$ with the partially inverted spinel structure is the material that can be used as anode in safe large scale lithium-ion battery. Lithium intercalation in this material occurs at the potential of 1.55 V vs. $\text{Li}|\text{Li}^+$ via two-phase reaction to form $\text{Li}_7\text{Ti}_5\text{O}_{12}$ with rock salt structure. It is interesting to study the relationship of change of structural and electrochemical characteristics of the material in this process.

Lithium titanate was prepared by solid-phase synthesis method with preliminary mechanochemical activation. [1]. The starting materials were Li_2CO_3 and TiO_2 (rutile). Heat treatment was carried out in a tubular furnace. The composition of the final product was controlled by the XRD-analysis (Fig.1a). As an instrument of structural analysis in the present work the method of neutron diffraction was used. The measurements were performed using HRFD-diffractometer at high resolution. The exposure time was 12 hours for each sample. The neutron diffraction pattern of $\text{Li}_4\text{Ti}_5\text{O}_{12}$ is shown in Fig.1b. Due to the peculiarities of the interaction of neutrons with atoms of different elements, it allows to define the content of each type of atoms in different crystallographic positions, in contrast to the X-ray diffraction method, where the presence of each element can only be evaluated indirectly by the deviation of the lattice parameters from the standard values. Thus, using the Rietveld method the atomic coordinates and occupancy of crystallographic positions were refined in the crystal structure of $\text{Li}_4\text{Ti}_5\text{O}_{12}$. The results of neutron diffraction data processing are shown in Table 1.

Approaches based on the methods of cyclic voltammetry (CV), potentiostatic intermittent titration (PITT) and electrochemical impedance spectroscopy (EIS) were used to determine the diffusion coefficient of lithium in $\text{Li}_4\text{Ti}_5\text{O}_{12}$ - $\text{Li}_7\text{Ti}_5\text{O}_{12}$ system [2,3]. The figure 2 shows cyclic voltammograms measured at different temperatures. The calculated values of diffusion coefficients were defined as: $0.6 \cdot 10^{-12}$ and $0.3 \cdot 10^{-12}$ for anodic and cathodic processes, respectively, at 5 °C, $12 \cdot 10^{-12}$ and $5 \cdot 10^{-12}$ for anodic and cathodic processes, respectively, at 40 °C.

Neutron diffraction study of $\text{Li}_4\text{Ti}_5\text{O}_{12}$ is supported by Russian Science Foundation (project 15-13-10006), synthesis and electrochemical study of $\text{Li}_4\text{Ti}_5\text{O}_{12}$ is supported by Russian Foundation for Basic Research (project 13 03 00492).

[1] Kosova N. V., Devyatkina E. T., *Rus. J. Electrochem.* 48 (2014) 320.

[2] Ivanishchev A.V., Churikov A.V., Ushakov A.V., *Electrochim. Acta.* 122 (2014) 187.

[3] Churikov A.V., Ivanishchev A.V., Ushakov A.V., Romanova V.O., *J. Solid State Electrochem.* 18 (2014) 1425.

S O F T M A T T E R

INFLUENCE OF TETRASODIUM ETHYLENEDIAMINETETRAACETATE ON BINDING CAPACITY OF HUMAN LACTOFERRIN

L. Anghel¹, R. V. Erhan^{2,3}, G. Duca¹

¹ *Institute of Chemistry of the Academy of Sciences of Moldova, 3, Academiei Street, MD-2028, Chisinau, Republic of Moldova*

² *Horia Hulubei National Institute for R&D in Physics and Nuclear Engineering, 30 Reactorului Street, P.O.BOX MG-6, Bucharest - Magurele, Romania*

³ *Frank Laboratory of Neutron Physics, Joint Institute for Nuclear Research, 141980, Dubna, 6 Joliot-Curie Street, Russia*

Human lactoferrin is a protein that belongs to transferrin family. This protein also known as lactotransferrin, originally was isolated from milk and later it was found in biological fluids such as blood plasma, tears, saliva, pancreatic juice, bile. In blood plasma lactoferrin derives from specific granules of neutrophils but there are evidences that it might be produced by other cells and even microorganisms [1].

Lactoferrin shares similar polypeptide topology with the other proteins members of transferrin family. The number of amino acids in the protein structure varies depending on the origin of the molecule. The structure of a lactoferrin molecule is composed of α -helix and β -sheets. The protein structure is divided in two lobes, referred as N- and C- lobes which are connected by a 3-turn-helix. Both protein lobes share a degree of similarity of about 40 % [2]. Each lobe contains an iron-binding site consisting, where the coordination of a ferric ion is produced via one carboxylate oxygen, two phenolate oxygens and one imidazole nitrogen from one aspartate, two tyrosines and one histidine, respectively. Ferric ion is stabilized in the protein binding site through two oxygens from carbonate ion.

Lactoferrin molecules reversibly bind ferric ions and therefore they can be found in the iron-free open form (apolactoferrin) and associated with iron ions, the closed form (hololactoferrin). Apolactoferrin has an open conformation whilst hololactoferrin has a closed conformation (Fig. 1).

The high affinity of lactoferrin for iron determines a great part of its biochemical properties. We are particularly interested in investigating the mechanism that triggers iron release from the lactoferrin structure at physiological pH. Using UV-vis spectrophotometric titration method we have identified that the presence of tetrasodium ethylenediaminetetraacetate initiates the process of iron release from lactoferrin structure and the opening of its domains. In order to examine the effect of tetrasodium ethylenediaminetetraacetate on binding properties of lactoferrin we have undertaken the present work.

The small-angle neutron scattering experiment will provide us a direct estimation for the molecular size and conformation of lactoferrin under physiological conditions in the presence and absence of tetrasodium ethylenediaminetetraacetate. Results of this study will help gain a better understanding about the mechanism that triggers iron release from lactoferrin structure in biological systems.

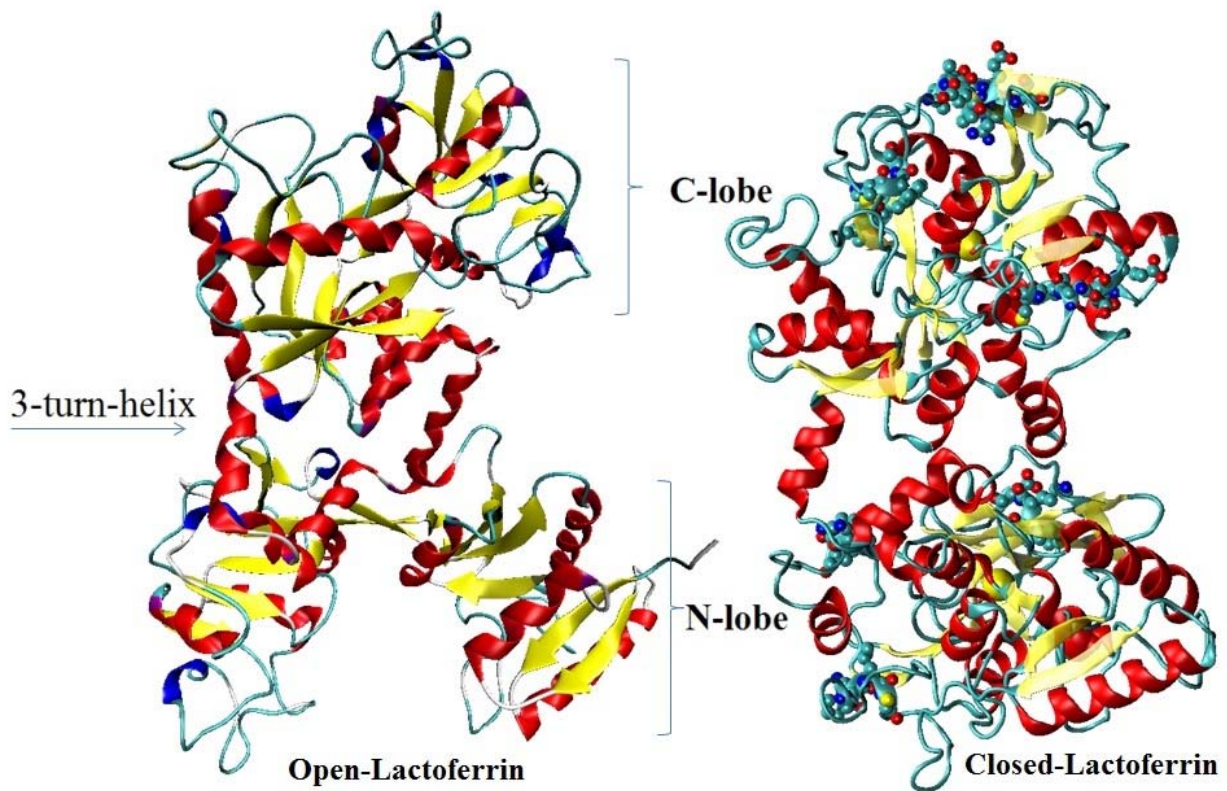


Figure 1. Graphical representation of the open (PDB entry 1LFH.pdb) and closed (PDB entry 1B0L.pdb) form of human lactoferrin.

- [1] Levay, P.F.; Viljoen, M. Lactoferrin: a general review. *Haematologica*, 1995, 80, pp. 252-267.
- [2] Baker, E.N.; Baker, H.M. Molecular structure, binding properties and dynamics of lactoferrin. *Cellular and Molecular Life Sciences*, 2005, 62, pp. 2531-2539.

COMBINED SURFACE TENSION AND SMALL-ANGLE NEUTRON SCATTERING INVESTIGATIONS OF AQUEOUS MICELLE SOLUTIONS OF DODECYLBENZENE SULFONIC ACID

O. Artykulnyi^{1,2}, V. Petrenko^{1,2}, L. Bulavin¹, L. Rosta³, M. Avdeev²

¹ Taras Shevchenko National University of Kyiv, Physics Department, Kyiv, Ukraine

² Joint Institute for Nuclear Research, Frank Laboratory of Neutron Physics, Dubna, Russia

³ Wigner Research Centre for Physics, Hungarian Academy of Sciences, Budapest, Hungary

Surfactants are compounds that reduce surface tension and frequently used in various applications. Thus, substances with surfactant properties are used as a stabilizer of particles in colloidal liquid systems like magnetic liquids. One of the most effective surfactant for stabilization of magnetic nanoparticles in aqueous medium is dodecylbenzene sulfonic acid (DBSA), $C_{12}H_{25}C_6H_4SO_3H$. It should be mentioned that pure DBSA aqueous solutions are poorly studied.

The given work is dedicated to investigation of the structure and interaction parameters of DBSA micelles in a heavy water according to small-angle neutron scattering (SANS) data. SANS results were supplemented by surface tension experiments. The value of critical micelle concentration, area per molecule and free energy were obtained from the analysis of surface tension vs DBSA concentration in water. The mentioned above parameters are necessary for fitting of SANS data for aqueous DBSA micelles solutions. Aggregation number of micelle, degree of ionization, form and size of micelle, micelles surface potential were obtained from SANS-data approximation. The obtained parameters were used for estimation of free (non-adsorbed) surfactant concentration in water-based ferrofluids stabilized with DBSA.

It is found that in the system water – magnetite (1.3% volume fraction)–dodecylbenzenesulfonate acid (2.2% volume fraction), 95% of dodecylbenzenesulfonate acid are adsorbed on the surface of magnetite, 4% are in a state of micelles, 1% is in a state of monomers. This result may be the estimation of stability of the magnetic fluidic system.

SMALL ANGLE NEUTRON INVESTIGATION OF THE LITHOCHOLIC ACID DERIVATIVE IN THE DIMETHYL SULFOXIDE PRESENCE: MORPHOLOGY AND PHASE TRANSITIONS

Yu. Gorshkova¹, M. Ordon^{1,2}

¹ Joint Institute for Nuclear Research, Frank Laboratory of Neutron Physics, Dubna, Russia

² Siedlce University of Natural Sciences and Humanities, Institute of Chemistry, Siedlce, Poland

e-mail: gorshk@nf.jinr.ru

In recent years an interest in supramolecular gels based on LMOG's (low molecular mass organic gelators) has been increasing, because they can be an alternative biomaterial to polymer gels. Potential applications of LMOG's arise from the fact that they are sensitive to physical stimuli such as temperature, light, ultrasound or chemical stimuli: metal ions or anions [1]. They are widely used in drug delivery, three-dimensional cell culture [2], tissue engineering and regenerative medicine or photoelectronic [3].

It is known that molecule of lithocholic acid (LCA) easy forms hydrogen bonds with proton donor-acceptor solvents. From this point of view the dimethyl sulfoxide (DMSO) is an ideal solvent. It has the ability to form hydrogen bonds by the presence of the carbonyl oxygen and acidic protons in methyl group. Moreover, in small concentration it is non-toxic to cells [4].

Small angle neutron scattering method (SANS) was used to determine morphology and phase behavior of the new derivative of LCA, 4-heptyloxyphenyloxy lithocholic acid ether (7OPhOLCA) as organogelator dissolved in deuterated dimethyl sulfoxide (DMSO-*d*₆). It was found that the substance forms a stable gel with fractal structure spherulite which consists from the lamellas at room temperature. The morphology strongly depends on the temperature in Gel phase (Fig.1.).

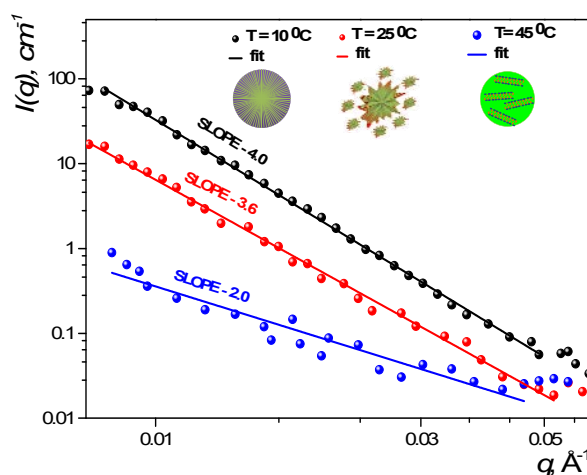


Fig.1. SANS curves for 7OPhOLCA in DMSO-*d*₆ with $C = 0.015\text{g/ml}$ at $T = 10, 25$ and 45°C .

Future increase in temperature makes the system flow and form a Sol phase again. It turns out that the temperature of the Gel-Sol transition changes significantly with concentration of the 7OPhOLCA: $T = 52^\circ\text{C}$ for $C = 0.015\text{g/ml}$ and $T = 35^\circ\text{C}$ for $C = 0.025\text{g/ml}$. The SANS results are in a good agreement with data obtained by DSC and pointed out on the reversible behavior of the Gel-Sol transition with hysteresis on the temperature during heating and cooling (Fig.2.).

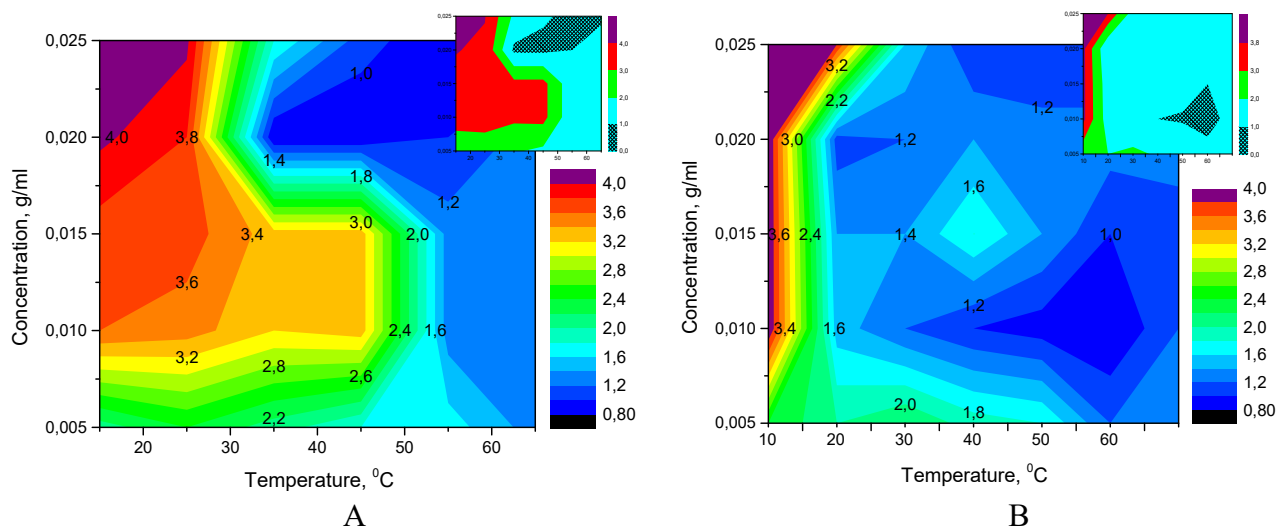


Fig. 2. Diagram of the Sol – Gel transition in depends on the temperature and sample concentration for (A) heating and (B) cooling

It is clear from Fig. 2 that the Sol – Gel transition can be observed only between lamellar organization (green area) and disordered state (blue area). Sum up all mentioned above we propose the Gel – Sol transition scheme (Fig. 3).

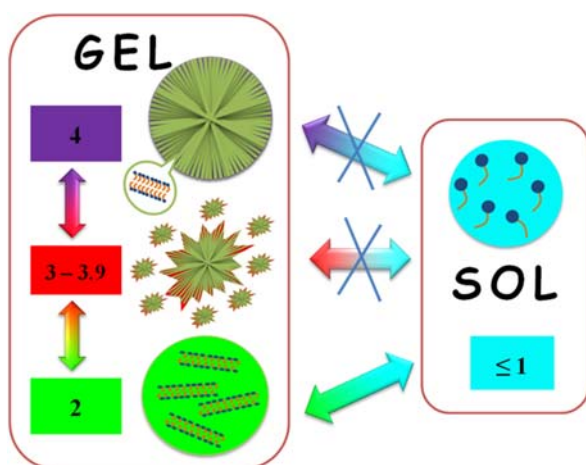


Fig. 3. Proposed Sol – Gel transition scheme for the 7OPhOLCA in DMSO- d_6 determined by SANS. The values 4.3 - 3.9, 2 and 1 correspond to the objects with a smooth surface, surface fractal, lamellas in solution and disordered state, respectively

Thus, we can conclude that increasing as well as decreasing of the temperature induce the morphology and phase transitions. At present work we observed Gel-Sol transition and 3 morphology states in the Gel phase (G1, G2 and G3). The G1 correspond to the objects with a smooth surface, G2 – surface fractal and G3 – lamellas in solution.

Acknowledgement. This work was supported by the Polish Government Plenipotentiary for JINR in Dubna (Grant No.: 45, p. 12 from 27.01.2015).

- [1]. Yu G., Yan X., et all, “Characterization of supramolecular gels”, *Chem. Soc. Rev.*, 2013, **42**, 6697.
- [2]. Mahler M. Reches, M. Rechter, S. Cohen and E. Gazit, *Adv. Mater.*, 2006, 18, 1365.
- [3]. Yu C., Xue M. ”Terthiphenes derivatives of cholesterol-based molecular gels and their sensing applications”, *Langmuir*, 2014, 30, (5), 1257-65.
- [4]. Violante G.D., et all, “Evaluation of the Cytotoxicity Effect of Dimethyl Sulfoxide (DMSO) on Caco2/TC7 Colon Tumor Cell Cultures”, *Biol. Pharm. Bull.*, 2002, 25 (12) 1600—1603.

EFFECT OF IONS AND POLAR SOLVENTS ON THE STRUCTURE AND PHASE TRANSITIONS OF PHOSPHOLIPID MEMBRANES

Yu. Gorshkova

Joint Institute for Nuclear Research, Dubna, Russia

e-mail: gorshk@nf.jinr.ru

The lipid bilayer is the raft for all cell membranes, which play an important role in life. They separate the cell from the surrounding environment and control the penetration of them inside the cell. On the other hand the ions and polar solvents also affect on the structure, conformation and intermembrane interaction of the phospholipid membranes as well as temperature, pressure and pH. For example, anesthetics, short alcohols and carbohydrates reduce the temperature of the phase transition, in contrary, the extension of non-polar lipids chains, external pressure, calcium ions, long alcohols and hydrocarbons increase it [1].

The structure and phase transitions of the fully hydrated unilamellar vesicles (ULVs) and multilamellar vesicles (MLVs) DMPC in the Ca^{2+} ions, dimethyl sulfoxide (DMSO) and diethyl sulfoxide (DESO) presence were investigated by small angle neutron scattering (SANS). SANS experiments have been performed on the YuMO spectrometer at the IBR-2 pulsed reactor in FLNP JINR (Dubna, Russia).

It was shown that MLVs DMPC prepared in $\text{D}_2\text{O}/\text{Ca}^{2+}$ mixture transform to the ULVs spontaneously with increasing of the Ca^{2+} concentration (Fig.1, left).

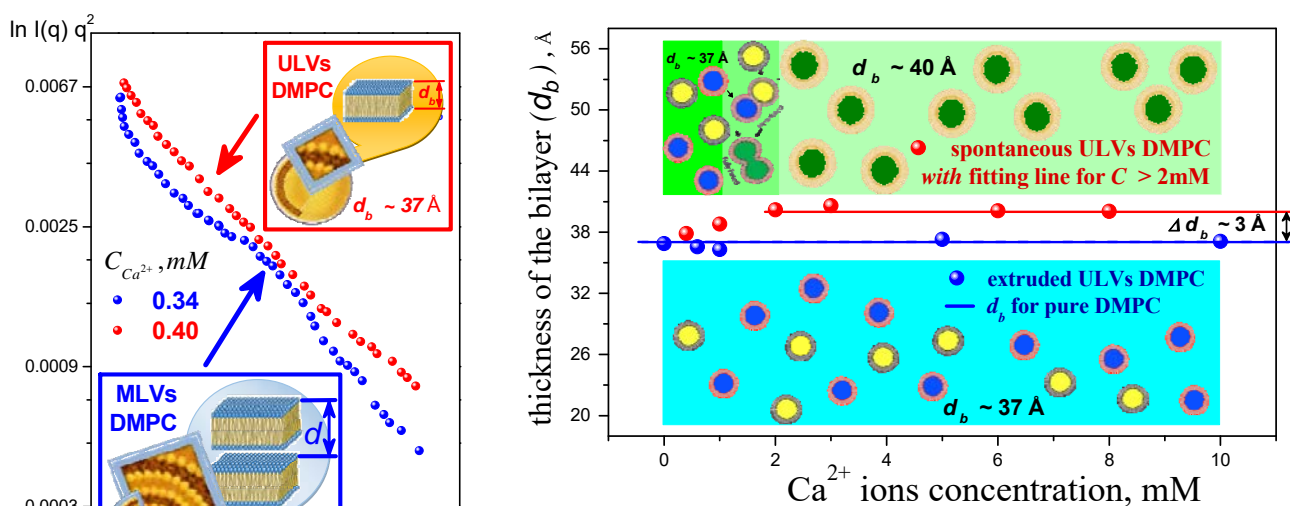


Fig.1. The influence of the Ca^{2+} ions concentration on the spontaneous transition MLVs to ULVs (left) and on the thickness of the lipid bilayer (right) in liquid-crystal phase.

Fusion of the ULVs DMPC in the presence of the divalent cations Ca^{2+} (Fig.1, right) and sulfoxides (Fig.2) was observed. It turned out that the ULVs fusion in the presence of the polar solvents is caused by two factors: time and increasing of the DMSO and DESO concentration. The current work confirms the hypothesis about a crucial role of the hydrophobic interactions in the intermembrane interaction in the presence of sulfoxides. However, it should be noted that these

hydrophobic interactions are stronger in the presence of DESO. At first, DESO causes the fusion of the ULVs about 1/2 hour after samples preparation, while this process occurs in an hour in the presence of DMSO. At the second, the investigation in short-term time scale shown that formation of the MLVs take place at $X_{DESO} = 0.3$ and $X_{DMSO} = 0.4$ [2].

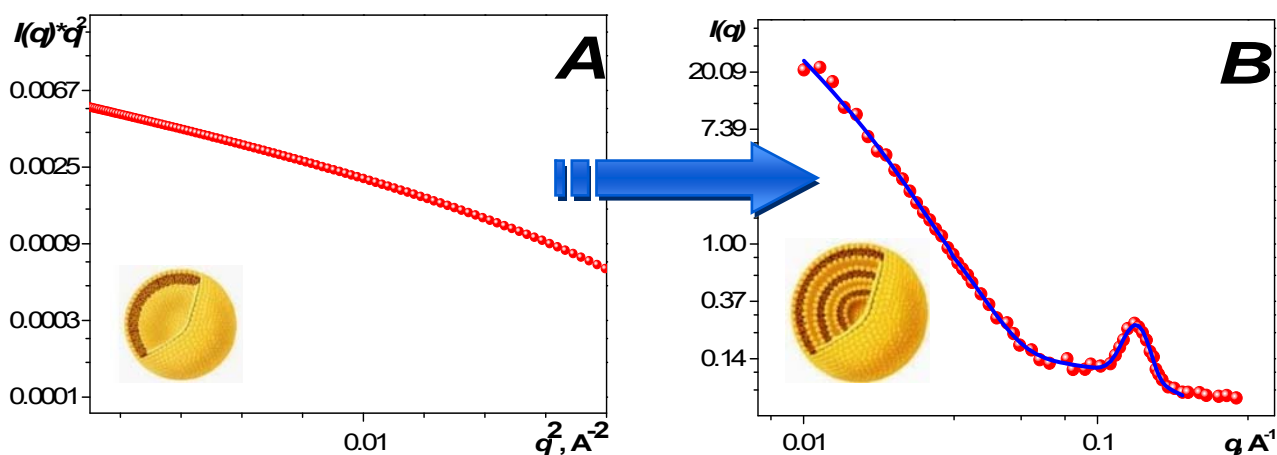


Fig.2. SANS curves on ULVs DMPC (2 wt %) in DMSO/D₂O mixture at $X_{DMSO} = 0.2$ in liquid-crystalline phase at $T = 55$ °C after preparation (A) and 1 hour later (B).

The phase transitions of the spontaneous MLVs DMPC in the DMSO and DESO presence was investigated in wide temperature range (Fig.3). The temperatures of the main phase transition are 35.2°C at the presence of the DMSO ($X_{DMSO} = 0.2$) and 33.6°C at the presence of the DESO ($X_{DESO} = 0.2$). The character of the phase transitions are discussed.

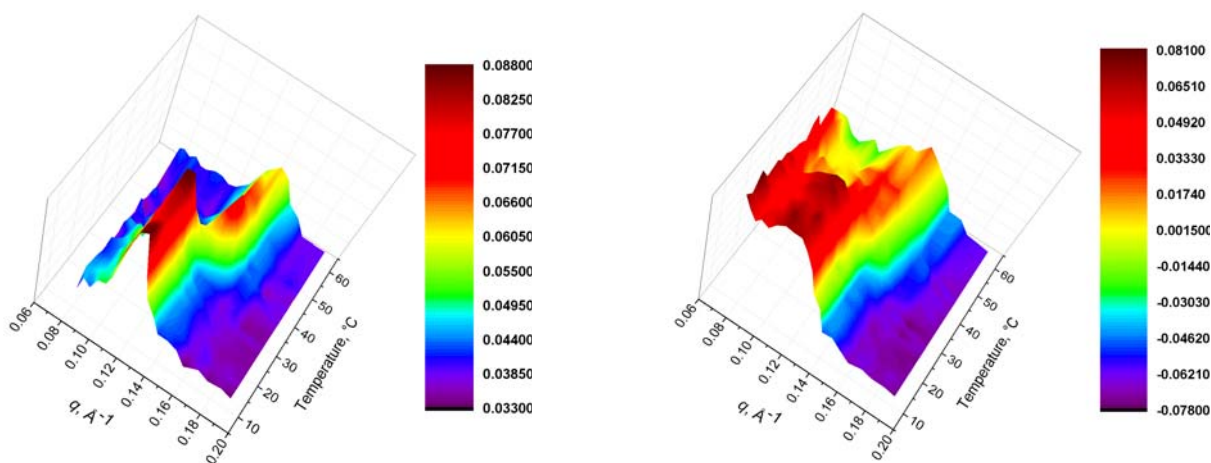


Fig.3. Phase diagrams of the spontaneous MLVs DMPC (2 wt %) in DMSO/D₂O mixture at $X_{DMSO} = 0.2$ (left) and in DESO/D₂O mixture at $X_{DESO} = 0.2$.

Acknowledgement. This research was supported by the JINR-UAIC Scientific Projects No. 33/23.01.2015 items 56.

- [1] D.P. Kharakoz, Success of biological chemistry (RUS). 2001, Vol. 41, PP. 333-364.
- [2] Yu. Gorshkova, Journal of optoelectronics and advanced materials. 2015 (in press)

STRUCTURE OF MIXED MICELLAR SOLUTIONS STUDY BY SMALL ANGLE NEUTRON SCATTERING METHOD

Aldona Rajewska^{1,2}, A. H. Islamov²

¹*National Center for Nuclear Research, 05-400 Swierk-Otwock, A. Soltana str.7, Poland*

²*Joint Institute for Nuclear Research, Laboratory of Neutron Physics, 141980 Dubna, Moscow region, Russia*

The mixed systems of nonionic classic surfactant TX-100 (p-(1,1,3,3-tetramethyl) poly (oxyethylene) and C₁₆TAB (hexadecyltrimethylammonium bromide) cationic classic surfactant in heavy water solutions was investigated for 3 concentrations at various mixing ratios (1:1,2:1,3:1) at temperatures $t = 30^{\circ}\text{C}, 50^{\circ}\text{C}, 70^{\circ}\text{C}$ with two methods - tensiometric and small-angle neutron scattering (SANS) on SANS spectrometer ("YuMO") of the IBR-2 on pulsed neutron source at FLNP, JINR in Dubna (Russia). Measurements have covered Q range from 7×10^{-3} to 0.4 \AA^{-1} . The micellar solutions were prepared in D₂O since the contrast between the micelles and the solvent in neutron experiments is better with D₂O than with H₂O. It was obtained as the result that the shape of micelles changes depending on surfactant concentration at temperature constant. At lower concentrations micelles are spherical but at higher concentrations and are rather ellipsoidal. For calculation and approximation results from SANS experiment was used program PCG 2.0 of Glatter O. and co-workers from University of Graz (Austria).

INVESTIGATION OF PHASE TRANSITION IN NANODISCS BY SMALL-ANGLE SCATTERING METHOD

Yu. Ryzhykau¹, A. Kuklin^{1,2}, M. Nikolaev^{1,3}, D. Soloviov^{1,2}, O. Ivankov^{1,2}, Yu. Kovalev^{1,2}, T. Murugova^{1,2}, E. Zinovev¹, A. Vlasov¹, A. Rogachev^{1,2}, V. Borshchevskiy^{1,2}, V. Gordeliy^{1,2,3,4}

¹ *MIPT, Dolgoprudnyi, Russia*

² *Joint Institute for Nuclear Research, Dubna, Russia*

³ *ICS-6*

⁴ *Institut de Biologie Structurale J.-P. Ebel*

E-mail: rizhikov1@mail.ru

The phase of lipids influence significantly on the living cell functions, providing stability, penetration and the other membrane properties. In fact, phase transitions could lead to the change of membrane proteins mobility in lipidic bilayer.

This paper shows the results of studying of lipidic phase transition in membrane mimicking systems: multilamellar vesicles (MLV), unilamellar vesicles (ULV) and nanodiscs (ND), which were prepared from phospholipids (DMPC and DPPC) and membrane scaffold proteins (MSP1 and MSP1E3D1) [1].

The temperature dependence of ND geometric size, ULV thickness and MLV lattice parameters were measured by small-angle X-Ray scattering (SAXS) and the scattering of neutrons (SANS). SANS curves were obtained on the SANS spectrometer YuMO, Dubna, Russia [2, 3]. SAXS measurements were done on the installation Rigaku, MIPT, Dolgoprudny, Russia.

The ND parameters that were tracked for different temperature were the following: the radius of inertia, the intensity at zero angle – they have been calculated from SAS curves using Guinier approximation and indirect Fourier transform [4]. A method for obtaining the bilayer thickness of ULV is described in [4] and [5]. The lipidic bilayer thickness in ULV and the lattice parameter in MLV were found to change at 23.5 ± 1.0 °C and 42.0 ± 1.0 °C for DMPC and DPPC respectively, which corresponds the literature [6, 7].

Firstly, in works [8] and [9] the SANS curves have been investigated for changes in the temperature range 22 – 26 °C for ND made of DMPC and MSP1E3D1 in H₂O/D₂O mixture with the volume ratio of 42% for heavy water. Such ratio corresponds the protein scattering length density and allows one to annihilate an account for MSP scattering [4, 10]. There have not been any changes above the statistic errors for the radius of inertia. This was an indirect proof of results [11], according to which the temperature of the phase transition for lipids in ND is higher than in a large lipidic bilayer and lies outside of the temperature range 22 – 26 °C.

In this work the temperature range was extended at 22 – 35 °C for DMPC ND and for DPPC ND the SAS curves were obtained at 38 – 50 °C. The temperature changes of ND structure were found, consequently the phase transition takes place. It is discovered that the phase transition of lipids in ND occurs at temperature higher than the phase transition temperature for a bilayer in vesicles. The obtained results are being under discussion.

We greatly acknowledge support of this work by the Russian Foundation for Basic Research (projects 13-04-91320 and 13-02-01460) and by the Russian program “5Top100” of the Ministry of Education and Science of the Russian Federation.

- [1] Ritchie T.K., Grinkova Y.V., Bayburt T.H., Denisov I.G., Zolnerciks J.K., Atkins W.M., Sligar S.G. Reconstitution of membrane proteins in phospholipid bilayer nanodiscs. – *Methods in Enzymology*. – 2009, P. 211–231.
- [2] Kuklin A.I., Islamov A. Kh., Gordeliy V.I. Scientific Reviews: Two-Detector System for Small-Angle Neutron Scattering Instrument. – *Neutron News*. – 2005. – P. 16-18.
- [3] Kuklin A.I. et al., Optimization two-detector system small-angle neutron spectrometer YuMO for nanoobject investigation. – *Journal of Surface Investigations, X-ray, Synchrotron and Neutron Techniques* – 2006. – №6, P.74-83.
- [4] Svergun D.I., Feigin L.A. *Structure Analysis by Small-angle X-ray and Neutron Scattering*. ISBN 0-306-42629-3. New York/London: Plenum Press 1987. XIII, 335 p.
- [5] V.I. Gordeliy, V. Cherezov, J. Teixeira. Strength of thermal undulations of phospholipid membranes. *Phys. Rev. E: Stat., Nonlinear, Soft Matter Phys.*, 2005, 72(6), 061913.
- [6] D.V. Soloviov, Y.E. Gorshkova, O.I. Ivankov, A.N. Zhigunov, L.A. Bulavin, V.I. Gordeliy, A.I. Kuklin. Ripple Phase Behavior in Mixtures of DPPC/POPC lipids: SAXS and SANS Studies *J. Phys. Conf. Ser.* 351, 012010 (2012).
- [7] Mabrey, S., Sturtevant, J. M. Investigation of phase transitions of lipids and lipid mixtures by high sensitivity differential scanning calorimetry. *Proc. Natl. Acad. Sci. U. S. A.* 1976, V. 73, 3862–3866.
- [8] Ryzhykau Yu.L., Nikolaev M.Yu., Kuklin A.I., Kovalev Yu.S., Borshchevskiy V.I., Gordeliy V.I. & Bueldt G. Complex studies of nanodiscs structural changes near the phase transition temperature. *Proceedings of the 57th Conference of MIPT, General and Applied Physics* – 2014. – P. 37-39. (In Russian)
- [9] Kuklin A.I., Rizhikov Yu.L., Nikolaev M.Yu., Vlasov A., Solovov D.V., Ivankov A.I., Rogachev A.V., Borshchevskiy V.I., Gordeliy V.I. Does the phase transition of lipidic membranes in nanodiscs exist? // *COMPLEX AND MAGNETIC SOFT MATTER SYSTEMS: PHYSICO-MECHANICAL PROPERTIES AND STRUCTURE*, Book of Abstracts of 2nd Intern. Summer School and Workshop. 29 Sept. - 3 Oct. 2014. ISBN 978-5-9530-0396-4. Dubna, Russia, 2014. - P. 68.
- [10] Ostanevich Yu.M., Serdyuk I.N. Neutron diffraction studies of the structure of biological macromolecules. – *Usp. Fiz. Nauk.* – 1982. – V. 137. – P. 85-116. (In Russian)
- [11] Denisov G., McLean M.A., Shaw A.W., Grinkova Y.V., Sligar S.G. Thermotropic phase transition in soluble nanoscale lipid bilayers. – *J. Phys. B.* – 2005. – P. 15580-15588.

BICELLES: NEW NANOSYSTEM FOR STUDYING MITOCHONDRIAL MEMBRANE PROTEINS

A. Musatov^a, K. Siposova^a, M. Kubovcikova^b, V. Lysakova^{a,c}, R. Varhac^c

^a *Department of Biophysics,*

^b *Department of Magnetism, Institute of Experimental Physics, Slovak Academy of Science, Kosice, Slovakia*

^c *Department of Biochemistry, P. J. Safarik University in Kosice, Slovakia*

One feature that most directly impacts structural and functional studies of membrane multisubunit protein-lipid complexes *in vitro* is their high hydrophobicity. Although detergents are capable of effectively solubilizing such complexes, they cannot mimic the interactions between proteins and lipid membranes, one of the essential features of cell operation. Bicelles are nanostructures formed by a long- and a short-chain phospholipid dispersed in aqueous solution, have been widely used as model membranes in biological studies [1]. However, to date, there has been no demonstration of structural and functional viability for the fundamental mitochondrial electron transport complexes reconstituted into or interacting with bicelles. In the present work, isolated from bovine heart, cytochrome *c* oxidase was successfully incorporated into bicelles that were formed from the mixture of long- and short-chain phospholipids, specifically 14:0 and 6:0 phosphatidylcholines (1,2-dimyristoyl-*sn*-glycero-3-phosphocholine, (DMPC) and 1,2-dihexanoyl-*sn*-glycero-3-phosphocholine, (DHPC)). Cytochrome *c* oxidase (EC 1.9.3.1; CcO) is mitochondrial multisubunit complex localized in inner mitochondrial membrane. The enzyme catalyzes the transfer of electrons from ferrocyanide to oxygen, a reaction coupled to proton translocation across the inner mitochondrial membrane [2]. Bicelles and CcO incorporated into bicelles (“proteobicelles”) were characterized by absorption spectroscopy, dynamic light scattering, atomic force microscopy, sedimentation velocity, and differential scanning calorimetry. It was demonstrated that at total concentration of phospholipids $C_L = 24$ mM and the molar ratio (“q”) of long-chain DMPC over short-chain DHPC equal to ~ 0.5 the size of bicelles is pH dependent, but overall is in the range of 30-140 nm with the thickness of bicelles of about 4 nm (Figure 1). CcO in bicelles was fully reducible by artificial donors of electrons, exhibited “normal” reaction with external ligands, and was fully active. Both, temperature-induced denaturation and sedimentation velocity analysis indicated that enzyme in bicelles is monomeric. We concluded that CcO in bicelles maintains its structural and functional integrity, and that bicelles can be used for more comprehensive investigation of CcO and most likely other mitochondrial electron transfer complexes. We also believe that more complete investigation of bicelles and proteobicelles regarding the morphology, typical bilayer widths, and aggregate sizes or size distributions using SANS analysis is needed.

Acknowledgment. This work was supported by the research grants from the Slovak Grant Agency VEGA No. 2/0062/14 and ESF 26110230097.

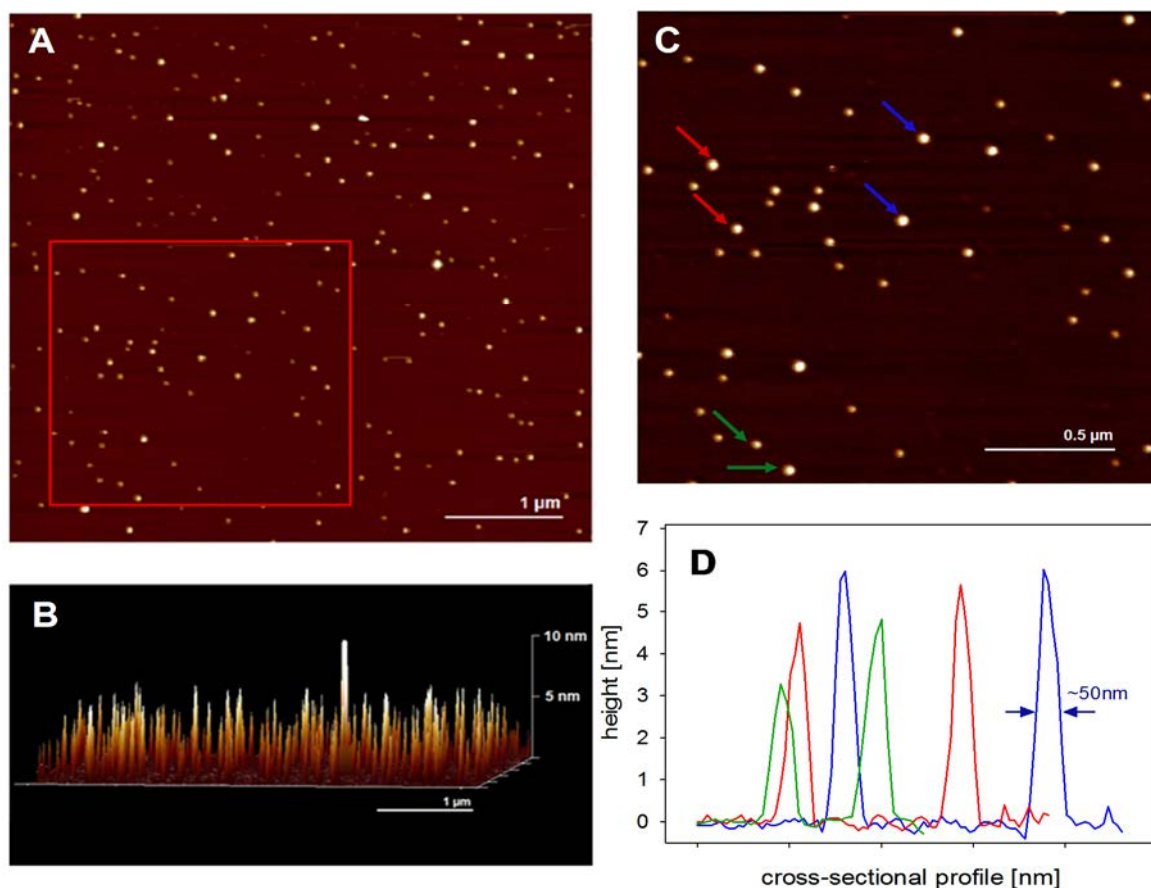


Figure 1. Atomic force microscopy. (A) Overall AFM imaging of bicelles prepared from 17 mM DHPC and 7 mM DMPC in 20 mM phosphate buffer, pH 7.4. The xy scale is $5 \times 5 \mu\text{m}$. (B) Bicelles heights determination. The panel is perpendicular to the scanning plane view of the upper image. (C) Zoomed $2.5 \times 2.5 \mu\text{m}$ area selected and marked by red square in image A. (D) Representative data of determination of bicelles diameter and height. Surface profiling (or cross-section) lines were drawn across the part of the AFM image between two bicelles marked by arrows with the same color. Data demonstrate the diameter ($\sim 50 \text{ nm}$) and height ($4 \pm 1 \text{ nm}$) of the most abundant bicelles. The data analyses were performed using NanoScope Analysis 1.20 software.

- [1] Dürr, U.H.N., Soong, R., Ramamoorthy, A. (2013) *Prog. Nucl. Magn. Reson. Spectrosc.* 69, 1-
- [2] Yoshikawa, S., Tera, T., Takahashi, Y., Tsukihara, T., and Caughey, W. S. (1988) *Proc. Natl. Acad. Sci. U.S.A.* 85, 1354-1358

MULTI-METHODICAL INVESTIGATION AND SAXS/SANS DATA ANALYSIS OF APOFERRITIN BEHAVIOR IN WATER SOLUTIONS

A. Vlasov¹, T. Murugova^{1,2}, O. Ivankov^{1,2}, A. Rogachev^{1,2}, D. Soloviov^{1,2}, A. Zhigunov³, Yu. Kovalev^{1,2}, Yu. Ryzhykau¹, E. Zinovev¹, A. Round⁴, V. Gordeliy^{1,2,5,6}, A. Kuklin^{1,2}

¹ *MIPT, Dolgoprudnyi, Russia*

² *JINR, Dubna, Russia*

³ *Institute of Macromolecular Chemistry CAS, Prague, Czech Republic*

⁴ *EMBL, 6 Jules Horowitz, F-38042 Grenoble, France*

⁵ *Institute of Complex Systems (ICS), ICS-5: Molecular Biophysics, Research Centre Juelich, 52425, Juelich, Germany*

⁶ *Institute of Structural Biology J.P.Ebel, Grenoble, France*

E-mail: vavplanet@mail.ru

In this work we continue applying recent SAS approaches to low resolution studies of the protein complexes mentioned above with a particular goal – to compare SAXS and SANS structures obtained in such way [1].

We present the results of small angle scattering investigation of protein apoferritin via approximation to zero concentration value. We compare the sizes and shapes, including those determined by indirect Fourier transform method, obtained on different instruments: YuMO spectrometer (Dubna, Moscow region, Russia [2]), BM29 beamline (ESRF, Grenoble, France [3]) and Rigaku instrument (MIPT, Dolgoprudny, Moscow region, Russia). The pair-distance distribution function for both small-angle neutron (SANS) and X-ray scattering (SAXS) is computed. It is shown that SANS and SAXS methods give similar form factor (spherical shell with holes) of apoferritin. At the same time, fits of experimental data for SAXS and SANS curves give a little different sizes and volumes of the molecule. The reasons for these discrepancies are discussed.

[1] Kuklin, A. I., et al. "Comparative study on low resolution structures of apoferritin via SANS and SAXS." *Journal of Physics: Conference Series*. Vol. 351. No. 1. IOP Publishing, 2012.

[2] Kuklin, A. I., A. Kh Islamov, and V. I. Gordeliy. "Scientific Reviews: Two-Detector System for Small-Angle Neutron Scattering Instrument." *Neutron News* 16.3 (2005): 16-18.

[3] Roessle, Manfred W., et al. "Upgrade of the small-angle X-ray scattering beamline X33 at the European Molecular Biology Laboratory, Hamburg." *Journal of Applied Crystallography* 40.s1 (2007): 190-194.

MICROMECHANICAL PROPERTIES OF A AL/SiC_p METAL MATRIX COMPOSITE DETERMINED USING TOF NEUTRON DIFFRACTION USING *IN SITU* TENSILE TEST

Gadalińska E.¹, Baczmański A.², Wróbel M.³, Scheffzük Ch.^{4,5}, Wroński S.², Lodini A.⁶, Klosek V.⁷

¹ *Institute of Aviation, CBMK, al. Krakowska 110/114, 02-256 Warszawa, Poland*

² *AGH University of Science and Technology, Faculty of Physics and Applied Computer Science, al. Mickiewicza 30, 30-059 Kraków, Poland*

³ *AGH University of Science and Technology, Faculty of Metals Engineering and Industrial Computer Science, al. Mickiewicza 30, 30-059 Kraków, Poland*

⁴ *Karlsruhe Institute of Technology, Adenauerring 20b, 76131 Karlsruhe, Germany*

⁵ *Frank Laboratory of Neutron Physics, JINR Dubna, 141980 Dubna, Russia*

⁶ *LISM, Université de Reims Champagne-Ardenne, BP 1039, 51687 Reims Cedex2, France*

⁷ *CEA, Laboratoire Léon Brillouin, 91191 Gif-sur-Yvette Cedex, France*

elzbieta.gadalinska@ilot.edu.pl, andrzej.baczmanski@fis.agh.edu.pl, mwrobel@agh.edu.pl, christian.scheffzuek@kit.edu, sebastian.wronski@fis.agh.edu.pl, alain.lodini@univ-reims.fr, vincent.klosek@cea.fr

The metal matrix composites (MMCs) with a ceramic particles reinforcement combine increased strength with ductility sufficient for many structural applications. A significant residual stresses between the matrix and reinforcement can be developed during MMCs heat treatment. As the stress can significantly affect a construction lifetime, their evaluation has the paramount importance [1-4].

In the present work result of the lattice strains measured *in situ* during elastoplastic deformation (i.e., uniaxial tension) of Al/SiC_p metal–matrix composite are presented. The strains were determined for both phases in directions parallel and perpendicular to the applied load. The neutron time-of-flight (TOF) diffraction method allowed the measurement of the lattice strains for Bragg reflections of both phases were used. The measurements were done using neutron diffraction at the EPSILON strain diffractometer of the IBR-2 pulsed reactor at the Frank Laboratory of Neutron Physics, Dubna, Russia and were compared with the neutron diffraction results obtained on the monochromatic neutron beam G5.2 in Laboratoire Leon Brillouin (LLB), Saclay, France. The results obtained in both laboratories, were very similar, despite the fact that in LLB only the Al-(111) and SiC-(111) reflection were used.

Finally, an elastoplastic self-consistent model calibrated by experimental results was applied for calculation of the critical resolved shear stress and hardening parameter of the composite phases. The model correctly predicts stresses in SiC, while the one in Al were slightly overestimated due to the initial thermal stresses created in the material during thermal treatment.

References

- [1] Fitzpatrick ME, Withers PJ, Baczmanski A, Hutchings MT, Levy R, Ceretti M, Lodini A. *Acta Mater* 2002;50:1031.
- [2] Fitzpatrick ME, Hutchings MT, Withers PJ. *Acta Mater.* 1997;45:4867.
- [3] Levy-Tubiana R, Baczmanski A, Lodini A. *Mater Sci Eng A* 2002;341:74.
- [4] Baczmański A., Levy-Tubiana R., Fitzpatrick M.E. and Lodini A., *Acta Mater.* 2004; 52: 1565.

THE NEUTRON TIME-OF-FLIGHT DIFFRACTOMETER EPSILON FOR STRAIN ANALYSIS ON GEOLOGICAL SAMPLES UNDER UNIAXIAL AND TRIAXIAL LOAD CONDITIONS

Ch. Scheffzueck^{1,2}, B.I.R. Mueller¹; B. Altangere² & F.R. Schilling¹

¹ Karlsruhe Institute of Technology, Institute of Applied Geosciences, Karlsruhe, Germany

² Frank Laboratory of Neutron Physics, JINR Dubna, Moscow Region, Russia

The investigation of strain in geological samples with conventional methods, like overcoring and grain size anisotropy, is limited. To detect the intracrystalline strain, diffraction methods can be applied. Because of the large variety of the grain size in geological samples, neutron diffraction is the preferred method. The application of neutron time-of-flight diffraction allows the determination of intracrystalline strain for all the Bragg diffraction lines in the range of the used wavelength (up to $\lambda_{\max} = 7.2 \text{ \AA}$, e.g. $d_{\max} = 5.1 \text{ \AA}$, using a wavelength chopper: $\lambda_{\max} = 14.4 \text{ \AA}$, e.g. $d_{\max} = 10.2 \text{ \AA}$). Therefore, the method is advantageous for multiphase materials with phases of lower crystal symmetries, like polycrystalline geological samples.

The neutron TOF strain diffractometer EPSILON is operated at beam line 7A-1 at the pulsed neutron source IBR-2M, JINR Dubna. The diffractometer has been designed especially for the investigation of rock samples: because of the long flight path of about 107 m the resolution is about $4 \cdot 10^{-3}$ for $d = 2 \text{ \AA}$. The diffractometer, equipped with 9 detector banks at $2\theta = 90^\circ$ is designed in three triplets at radial angles of: -21° , 0° , 21° , 69° , 90° , 111° , 159° , 180° , and 201° , which provides the potential of strain tensor determination. Each detector bank contains nine ^3He detectors. Using the time focusing method the neutron diffraction pattern of the nine detectors at one bank can be stacked. This enables to compensate the low neutron intensity at sample position reasoned by the very long flight path.

Behind the neutron guide with dimensions of $H \times B = 95 \times 50 \text{ mm}^2$ the incident slip system is installed. It consists of two horizontal-vertical diaphragms in a distance of 1,160 mm to select the sample gauge volume. A uniaxial pressure device ($F = 100 \text{ kN}$, $p = 150 \text{ MPa}$) is designed for sample dimensions of 30 mm in diameter and 60 mm in length. The apparatus can be orientated in 45° to the incident neutron beam and allows the simultaneous investigation of strain in direction of σ_1 and σ_3 . The pressure device allows the sample rotation under external load to determine oriented rock properties at different load states. In addition, an acoustic emission sensor system with 12 channels is installed to detect acoustic signals of micro cracks during in situ deformation experiments.

Научное издание

Condensed Matter Research at IBR-2 Reactor
Book of Abstracts of the International Conference

Исследования конденсированных сред на реакторе ИБР-2
Сборник аннотаций международной конференции

D3-2015-82

Сборник отпечатан методом прямого репродуцирования
с оригиналов, предоставленных оргкомитетом.

Ответственная за подготовку сборника к печати *Ю. Е. Горшкова.*

Подписано в печать 22.09.2015.

Формат 60 × 90/16. Бумага офсетная. Печать офсетная.
Усл. печ. л. 9,13. Уч.-изд. л. 16,17. Тираж 165. Заказ 58631.

Издательский отдел Объединенного института ядерных исследований
141980, г. Дубна, Московская обл., ул. Жолио-Кюри, 6.
E-mail: publish@jinr.ru
www.jinr.ru/publish/